REPUBLIQUE DU CAMEROUN
Paix – Travail – Patrie
****
UNIVERSITE DE YAOUNDE I
FACULTE DES SCIENCES
DEPARTEMENT DE PHYSIQUE
****
CENTRE DE RECHERCHE ET DE FORMATION
DOCTORALE EN SCIENCES, TECHNOLOGIES
ET GEOSCIENCES
LABORATOIRE DE MÉCANIQUE, MATÉRIAUX ET STRUCTURES

REPUBLIC OF CAMEROUN
Peace – Work – Fatherland
****
UNIVERSITY OF YAOUNDE I
FACULTY OF SCIENCE
DEPARTMENT OF PHYSICS
****
POSTGRADUATE SCHOOL OF SCIENCES, TECHNOLOGY AND GEOSCIENCES
LABORATORY OF MECHANICS, MATERIALS AND STRUCTURES

ON THE DYNAMICS OF BRIDGES SUBJECTED TO SERVICE LOADS: ROADS TRAFFIC, TRAIN TRAFFIC AND WIND ACTIONS

A thesis
submitted to the postgraduate school of sciences, technology and geosciences of the University of Yaoundé I in partial fulfillment of the requirements for the degree of Doctorat/ PhD in Physics

Par : **ANAGUE TABEJIEU Lionel Merveil**
Master's in Physics

Sous la direction de
NANA NBENDJO Blaise Roméo
Associate Professor
University of Yaoundé I, Cameroon
FILATRELLA Giovanni
Associate Professor
University of Sannio, Italy

Année Académique : 2018

UNIVERSITÉ DE YAOUNDÉ I
UNIVERSITY OF YAOUNDE I

FACULTÉ DES SCIENCES
FACULTY OF SCIENCE

DÉPARTEMENT DE PHYSIQUE
DEPARTMENT OF PHYSICS

ATTESTATION DE CORRECTION DE LA THÈSE DE DOCTORAT/Ph.D

Nous, Professeur **TCHAWOUA Clément** et Professeur **WOAFO Paul**, respectivement Examinateur et Président du jury de la Thèse de Doctorat/Ph.D de Monsieur **ANAGUE TABEJIEU Lionel Merveil**, Matricule **08W0025**, préparée sous la supervision des Professeurs **NANA NBENDJO Blaise Roméo et FILATRELLA Giovanni,** intitulée : «**ON THE DYNAMICS OF BRIDGES SUBJECTED TO SERVICE LOADS : ROADS TRAFFIC, TRAIN TRAFFIC AND WIND ACTIONS**», soutenue le **Mercredi, 19 Septembre 2018**, en vue de l'obtention du grade de Docteur/Ph.D en Physique, Spécialité **Mécanique, Matériaux et Structures,** Option **Mécanique Fondamentale et Systèmes Complexes,** attestons que toutes les corrections demandées par le jury de soutenance ont été effectuées.

En foi de quoi, la présente attestation lui est délivrée pour servir et valoir ce que de droit.

Fait à Yaoundé le ..... 27 SEPT 2018 .....

Examinateur

Prof. TCHAWOUA Clément

Le Chef de Département de Physique

UNIVERSITE DE YAOUNDE I * FACULTE DES SCIENCES * DEPARTEMENT DE PHYSIQUE
Le Chef de Département de Physique

Prof. NDJAKA Jean-Marie Bienvenue

Le Président du jury

Prof. WOAFO Paul

Dedications

- In loving memory of my late father Mr. **NAGUEU Jean (1954 - 2006)** named **FOMESSING**. For the job you've done and the nature deprive you to enjoy the fruits. Your life is still for us an inexhaustible source of inspiration. May the **Almighty God** keep an eye on your courageous children who you left behind you and may your soul rest in Peace!

- To my mother, born Mrs. **ZABKENG Rosalie** who has given all her love to me, encouraged and supported me unconditionally all the time.

- To my brothers and sisters: Mr. **ANAGUE Achille, Daryl, Farel** and Mrs. **ANAGUE Mireille, Armelle, Henriette, July, Fabiola**. Thanks for your encouragement, support, sincere kindness and prayers. For the youngest, may this work constitutes a constructive mirror for your future.

Acknowledgements

This thesis was carried out in the Laboratory of Modelling and Simulation in Engineering, Biomimetics and Prototypes (LaMSEBP), at the University of Yaoundé I (UYI) between January 2014 and September 2017. I am indebted to many people who both directly and indirectly contributed to this thesis, and during my long period of education.

- First of all, I thank the **Almighty God**, the most Merciful and most Gracious, for this achievement.

- I would like to express my deep gratitude and appreciation to my first supervisor, Professor **NANA NBENDJO Blaise Roméo** at the UYI, Cameroon, for giving me the opportunity to work with him. His serious attitude towards research really fascinated me and he helped me to believe on me. His advices and guidance have tremendous influence on my professional and personal growth. He provided a very helpful research environment that allowed me to work on several research projects and collaborate with other professors. He also gave me the freedom to pursue projects of my own choosing, which contributed greatly to my academic independence. My dream is to follow my advisor career for the rest of my life.

- Special thanks to my second supervisor, Professor **FILATRELLA Giovanni** at the University of Sannio, Italy, for his insightful guidance, a good and inspirational cooperation during my study. I will never forget his entire disponibility and implication for this work. I have learnt a lot from him about the analysis of stochastic systems.

- Besides my supervisors, I would like to pay particularly my gratefulness to Professor **WOAFO Paul**, who cordially admitted me in his laboratory, for always providing me with new prospectives in the field of my research and for contributing to my work with beneficial discussion and fruitful collaboration.

- Special thanks also go out to Professor **KOFANE Timoléon Crépin**, pioneer of the nonlinear physics in Cameroon, Head of the Department of Physics, Faculty of Science, University of Yaoundé I and the teaching staff of his Department for their valuable teachings and their fruitful advices.

- I would like to thank Professor **TCHAWOUA Clément** who introduced me in the Structural Engineering Problems via his courses namely: Elasticity and Plasticity, quite beneficial in my research.

- I wish to express my acknowledgments to all the members of the public defence jury who have accepted to discuss and appreciate the results of this thesis, in spite of their numerous duties. Special thank to Professor **SIEWE SIEWE Martin** and Professor **MOUKAM KAKMENI François-Marie** who have agreed to evaluate the results of this thesis.

- During the period of my PhD work, I had the opportunity to meet and collaborate with Professor. Dr. Ing. **DORKA Uwe** from the University of Kassel, Germany, on the horseshoes chaos detection in a cable-stayed bridge structure subjected to randomly moving loads, of whom I would like to thank for his help and his fruitful collaboration. I hope that we will continue to collaborate on this topic in the future.

- I would like to thank all my lab elders and mates whose their various questions during my seminars presentations helped me to improve the quality of this document. Once more thank you Dr. **NANA Bonaventure**, Dr. **TCHEUTCHOUA Omer**, the late Dr. **MBOUSSI Aïssatou**, Dr. **TALLA MBE Jimmy**, Dr. **TAKOUGANG Sifeu**, Dr. **SIMO Hervé**, Dr. **NDOUKOUO Ahoudou**, Dr. **NANHA Armand**, Dr. **ABOBDA Lejuste**, Dr. **NGUEUTEU Serge**, Dr. **DJORWE Philippe**, Dr. **GOUNE Geraud**, Dr. **TALLA Alain**, Dr. **METSEBO Jules**, Dr. **NDEMANOU Buris**, Dr. **NWAGOUM Peguy**, Mr. **CHAMGOUE André**, Mr. **NOTUE Arnaud**, Mr. **OUMBE Gabin**, Mr. **TOKOUE Dianoré**, Mr. **SONFACK Hervé**, Mr. **MBA Steve**, Mr. **DONGMO Eric**, Mrs. **TCHAKUI Murielle**, Mrs. **MAKOUO Lucienne**, Mrs. **FANKEM Raïssa**, Mr. **KEMAJOU Issac**, Mr. **THEPI Raoul**.

- Most importantly, I would like to thank my "father" Mr. **TAZOVAP Jean Louis** for the love of an exemplary father, the advices, encouragements, assistance and education he has brought to me since my secondary high school studies. May you find in this work the achievement of some of your dreams and a real reason of satisfaction.

- Thank a lot to my great family **FODIEU** for their unvaluable support. Your efforts are not vein. Finally, some of your dreams to have a Philosophy Doctor in the family is little by little realized.

- I would like to sincerely and wholeheartedly thank his Majesty **ZEUFACK II Joseph**, Chief of the FONAKEUKEU village for his encouragements and his wise advices. Thanks a lot Majesty, may this work constitute a source of inspiration for the entire populations of the FONAKEUKEU village.

- Special thank to my "mothers" Mrs. **MAFOLEPE FOUEGO Edith Claire**, **AOUNTSA Zoé** and **LOWE WAFFO Chantal**, for their love and all their multifaceted support during my long period of education.

- I am grateful to my uncle Mr. **DONFACK Gabriel** named "**MAGUISSI**" who believed in me and always supported me in this PhD project. I imagine his joy today. Thank a lot dear uncle.

- Special thanks to the families: **TANEKEU, NANGMO, AZEMKOUO, KEUMO, FAHA, CHAMEGUEU, TAMBA** for their unvaluable support.

- Thank a lot to Mr. & Mrs. **MOUKAM** for their love and unvaluable support during the past three years. May this work constitute a constructive mirror for your lovely children.

- Special thank to Mrs. **DJIO Vanessa**, Mr. **NDJOMATCHOUA Frank**, Mr. **NTIECHE Zounedou**, Mr. **GNINZANLONG Carlos**, Mrs. **TCHANGBWA Dorcas**, Mrs. **TAMTO Linda**, Mrs. **NGUIADEM Maéva**, Mr. **MENJOH Roland**, Mr. **NGA OWONO Freddy**, Mr. **KAPALE Serge** for their encouragements and for sharing with me so many good moments.

- All those whose names have not been mentioned here, but who have contributed in one way or the other to the success of this work should hereby receive my sincere gratitude.

≪Safe transportation of goods through the bridges is of practical importance in structural engineering, but in the practical problem it is also embedded a nice part of the physics of random oscillations.≫

Contents

List of Abbreviations

VBI: **V**ehicle-**B**ridge **I**nteraction
TMD: **T**unned **M**ass **D**amper
DAF: **D**anymic **A**mplification **F**actors
DOF: **D**egrees **O**f **F**reedom
PDE: **P**artial **D**ifferential **E**quation
ODE(s): **O**rdinary **D**ifferential **E**quation(s)
SRK4: **S**tochastic Fourth-Order **R**unge-**K**utta
SDE(s): **S**tochastic **D**ifferential **E**quation(s)
RK4: Fourth-Order **R**unge-**K**utta
A-B-M: **A**dams-**B**ashforth-**M**oulton
FDEs: **F**ractional **D**ifferential **E**quation(s)
F-K-P: **F**okker-**P**lanck-**K**olmogorov
PDF: **P**robability **D**ensity **F**unction

List of Figures

List of Tables

Abstract

This dissertation studies the vibratory, including chaotic dynamics analysis of bridges including girder, railway, slab and cable-stayed bridges under the action of moving vehicles, trains and stochastic wind loads. Each moving vehicle is idealised as a point force of constant or random amplitude moving along the bridge deck with stochastic velocity. A train is modelled as a series of point forces of constant amplitudes and intervals moving along the bridge deck in the same direction with constant velocity. After the description of various excited bridge models, Rayleigh theory of beams and thin rectangular plate used to establish their governing equations. Thereafter, appropriated computational tools are used to characterize the dynamical states. The following main results have been obtained:

The dissertation extends the existing deterministic vehicle-bridge system to the case of multiple vehicles moving with stochastic velocities and analyses the vibration of girder, slab and cable-stayed bridges. We demonstrate that the effect of the load random velocities is highly nonlinear, leading to a nonmonotonic behavior of the mean amplitude of the bridge deck versus the intensity of the stochastic term and of the load weight. The intensity of the random component of the loads velocity also constitutes to the enlargement of the possible chaotic domain of the system, and or increase the chances to have a regular behavior of the system. A study on the role of the presence of stay cables in a model of cable-stayed bridge system is investigated. It is shown that these stay cables can increase the degree of safety, but can also paradoxically contribute to destabilization. In the same perspective, a modelling of the plate-vehicles system is presented to simulate the interaction between a rectangular slab bridge and the moving vehicles. The effects of the arrival rate and of the standard deviation of the stochastic velocity on the expected value and variance of the bridge deck deflection response have been investigated.

A study of the role of the track structure and of the bearings on the dynamics of railway and girder bridges, respectively, are included in the thesis. It is assumed that the track structure and bearings can be constituted by viscoelastic materials (such as elastomer) characterized by the so-called *memory effect* modelled by fractional derivatives. We demonstrate that the installation of these type of devices (viscoelastic track structure and bearings) on the bridge deck can effectively contribute to the reduction of the vibration. Also, a proper selection of the material used to build the track structure can contribute to the suppression of chaos in a bridge deck system. Surprisingly, the wind turbulence can initially contribute to decrease the chance for the bridge deck to reach the resonance of the amplitude oscillations.

Keywords: Bridges, vehicles, stochastic wind load, beams, plates, moving loads, stochastic velocities, fractional order derivative, random chaos, amplitude of vibration.

Résumé

Cette thèse décrit l'analyse vibratoire, incluant la dynamique chaotique des ponts poutres, les ponts ferroviaires, des ponts dalles et des ponts à câbles sous l'action des véhicules en mouvement, des trains et/ou des vents turbulents. Chaque véhicule en mouvement est modélisé comme une force ponctuelle d'amplitude constante ou non se déplaçant le long du tablier avec une vitesse aléatoire. Le train est modélisé comme une série de forces ponctuelles d'amplitudes et d'intervalles constants se déplaçant à vitesse constante le long de la piste de chemin de fer. Après la description des différents types de ponts sous excitations mobiles étudiés, le théorie des poutres de Rayleigh et celle des plaques sont appliquées pour établir les équations décrivant leurs modèles mathématiques. Par la suite, des outils numériques appropriés sont utilisés pour caractériser la dynamique de ce dernier. Les principaux résultats suivants ont été obtenus:

La thèse étend le système deterministe de pont-véhicule existant au cas de plusieurs véhicules en mouvement avec des vitesses stochastiques et analyse les vibrations des ponts poutres, des ponts dalles et des ponts à câbles. Nous démontrons que le caractère aléatoire des vitesses de véhicules a un effet spectaculaire sur la réponse dynamique du tablier, conduisant à un comportement non monotone de l'amplitude moyenne du tablier par rapport à l'intensité de la partie fluctuante de ladite vitesse et du poids du véhicule. Une étude portant sur le rôle des câbles dans un modèle de pont à câbles est faite. Il est montré que la présence de ces câbles dans ce type de système peut augmenter le degré de sécurité de ce dernier et paradoxalement peut aussi contribuer à sa déstabilisation. Dans la même perspective, une modélisation rigoureuse d'un système véhicules-plaque est présentée pour simuler l'interaction entre un tablier à plusieurs voies et les véhicules en mouvement. Les effets de certains paramètres du trafic sur la valeur moyenne et la variance de la déflection de la plate sont étudiés.

Une étude portant sur les effets des pistes de chemin de fer et les appuis (partie du pont comprise entre le tablier et les piliers) sur la dynamique des ponts ferroviaires et des ponts poutres respectivement est incluse dans cette thèse. On suppose que ces types de structures peuvent être constitués de matériaux viscoélastiques (tels que les élastomères) caractérisés par *l'effet de mémoire* et modélisé par le biais des dérivées fractionnaires. Nous démontrons que l'installation de ces types de dispositifs (pistes de chemin de fer et les appuis) peut contribuer à réduire les vibrations du tablier. Par ailleurs, un choix approprié du matériau utilisé pour la construction des pistes de chemin de fer peut contribuer à la suppression des comportements non désirés (tels que le chaos) dans la superstructure. Aussi surprenante que cela puisse être, le caractère turbulent du vent peut contribuer à réduire les chances pour le tablier d'atteindre plus rapidement la résonance des oscillations.

Mots-clés: Ponts, véhicules, vent, poutres, plaques, charges en mouvement, vitesses stochastiques, dérivation d'ordre fractionnaire, chaos aléatoire, amplitude des vibrations.

General Introduction

People have always been interested in transporting themselves and their goods from one place to another. So obstacles such as the rivers, mountains and valleys are considered as a fundamental difficulty that people have faced in their transportation and movement from one place to another. The solution is to pass the obstruction, for instance using a rope, or swimming. A more sophisticated solution is to use a bridge, presumably made of simple materials like rock, stone, timber and other materials. Thus, the history of development of bridge construction is closely linked with the history of human civilization. The first bridges were simple beam span of stone slabs or tree trunks, and for longer spans, single strands of bamboo or vine were stretched across the chasm or oops or baskets containing the traveller were pulled across the stretched rope.

In general, a bridge is a structure providing passage over an obstacle without closing the way beneath. The required passage may be for a road, a railway, a pedestrian passage, a canal or a pipeline. The obstacle to be crossed may be a river, a road, railway or a valley. This type of transportation infrastructure is an important factor for the development of a national economy. With the rapid advances in the field of high performance materials and construction techniques, the bridges are evolving towards long and flexible structures as those of the high-rise buildings. The inclusion of modern materials also results in a new generation of lightweight structures which are utterly susceptible to the action of wind. During the last two centuries, major structural failures due to the wind action has occurred and has provoked much interest in wind loadings by engineers. Long-span bridges have often produced the most dramatic failures, such as the Brighton Chain Pier Bridge in England in 1836, the Tay Bridge in Scotland in 1879, and the Tacoma Narrows Bridge in Washington State in 1940. In particular, the failure of the Tacoma Bridge has pushed engineers to conduct various scientific investigations on bridge aerodynamics [1,2]. The main categories of wind effects on bridges with boundary layer flow theory are flutter and buffeting. While flutter may result in dynamic instability and the collapse of the whole structures, large buffeting amplitude may cause serious fatigue damage to structural members or noticeable serviceability problems.

When excessive external loads occur, the bridges may suffer large deflections and even cause damages that will endanger human life and property. This situation is generally possible in highway and railway bridges. From the point of view of structural dynamics, a railway bridge is different from a highway bridge in that the sources of excitation caused by the moving vehicles are different. For example, the loading of highway bridges is characterized by the occurrence of millions of repetitive random load events per year. This type of load causes material fatigue and ultimately damage of the structure. A random sequence of moving forces would seem to be the most relevant model for the problem of reliability of highway bridges [3–7]. The vehicles constituting the highway traffic may vary in terms of the axle weight, axle interval, moving speed, and even the headway. However, a train moving over a railway bridge can generally be regarded as a sequence of identical vehicles in connection, plus one or two locomotives. Conventionally, a

train was simplified as a sequence of moving masses, or in the extreme case as a sequence of concentrated loads, at regular intervals [8]. The vibrations caused by the passage of vehicles have become an important consideration in the design of these bridges. In particular, the interaction problem between the moving vehicles and the bridge structure has attracted much attention during the last three decades. This is in part due to the rapid increase in the proportion of heavy vehicles and high-speed vehicles in the highway and railway traffic. From the civil engineer's point of view, the structural vibration caused by the passage of the vehicles or a train is one of the main concern of its structure design.

The combination scenarios of these two previous major service loads (moving vehicles and wind actions) may cause global failure of the bridge structure. To maintain resilient and sustainable bridges against these expected scenarios is also the key to any successful bridge design. Traditionally, bridges were analyzed under a single type of dynamic loads at a time without considering any other ones, such as buffeting analysis under turbulent wind loads, time-history seismic analysis, or bridge dynamic analysis with moving vehicle. Recent bridge, vehicle, or wind interaction studies have highlighted the importance of predicting the bridge dynamic behaviour by considering the bridge, the actual traffic load, and wind as a single system of interacting parts [9–13].

In order to prevent the damage of bridges, the bearings (part of bridge ranging between the bridge deck and the piers) are often used as base isolators for severe earthquakes load and/or for load transference to the foundation in bridge engineering. Conventionally, the bearings are built or installed at the supports of simply supported bridge and, when they are constituted by elastic material, provide some insulation for the earthquake forces transmitted from the ground to the superstructure. However, such devices may adversely result in amplification of the response of the bridge during the passage of a train [82]. This is certainly one disadvantage of the use of elastic bearings; hence our interest. The bearings can also be constituted by viscoelastic materials (such as elastomer). Therefore, the *long memory effects* of these viscoelastic materials can be modelled by means of fractional derivatives. We demonstrate that this viscoelastic physical property of the bearings can be beneficial for the bridge safety.

Predicting the dynamic performance of bridges under moving loads is a well-known challenging subject in structural dynamics and it is considered in this thesis. ***Notably, the dynamic of various types of bridges including girder bridges, railway bridges, slab bridges and cable-stayed bridges under the action of moving vehicles and wind actions is analyzed by using two dynamics approaches: vibratory and chaotic approaches***. More precisely, the aim of the research presented in this thesis is to:

- Give an analytical approach to characterize the probabilistic features of the nonlinear beam response, namely the mean square amplitude and the probability density function due to loads moving with stochastic velocities.

- Explore the effects of stochastic fluctuations of the load velocity and the number of cables on the possible appearance of horseshoes chaos in the cable-stayed bridge system.

- Propose a probabilistic evaluation approach to obtain the expected value and the standard deviation of a two lane slab-type-bridge deflection response due to two opposite series of stochastic moving loads.

- Explore the effects of loads number and their spacing, the load velocity, the order of the fractional viscoelastic shear layer material of the Pasternak foundation (as a track structure) and its strength on the amplitude of vibration of the beam, and especially the order of the fractional viscoelastic property of the shear layer on the appearance or disappearance of horseshoes chaos.

- Analyse the effect of the number of bearings and their fractional-order viscoelastic physical properties on the resonance vibrations of the beam, and to give some estimate of the additive and parametric wind turbulence effects on the stationary probability density function of the oscillations amplitude of the beam.

Following this introduction, the dissertation is organized as follows:

- **Chapter one** offers an overview of some key factors involved in the dynamic interaction between the bridge and service loads including roads traffic, train traffic and wind actions. We also briefly presents a state-of-art review of research based on this topic and the problems that we will have to solve in the thesis

- **Chapter two** is entirely devoted to our methodology of investigation, including the presentation of a general background on an approximate response methods for the reduced linear or nonlinear mathematical models of interest for this thesis.

- **Chapter three** presents and discusses our main results. We begin by first modelling the different types of bridges studied in this thesis. Secondly, we approach the resulting models by using the vibratory and chaotic dynamic procedures. Thereafter, the main results are presented and discussed.

- **General Conclusion**: This part provides the overall conclusions of the main results of the thesis and suggestions for future work.

Chapter I

Literature review on some key factors involved in the dynamic interaction between the bridge and service loads

I-1- Introduction

There are a large amount of vehicles passing through in-service bridges every day while considerable wind blows on the bridge decks at the same time. Vibration caused by these service loads is of great theoretical and practical significance in civil engineering. Excessive dynamic responses of the bridge under service loads may not only cause global failure of the bridge structure, but also traffic safety concern on moving vehicles. In this chapter, the key factors involved in the dynamic interaction between the bridge and service loads will be discussed.

The chapter is organized as follows: Section I-2- presents some models of two major service loads, namely wind and traffic actions. Section I-3- is devoted to the presentation of some bridge models. In Section I-4-, we briefly describe the different types of bridge supports models. Section I-5- deals with a state-of-art review of research based on the vibration of various types of bridges. Section I-6- will give more details on the problems solved in this thesis after the presentation of some dynamical features of bridges under the action of wind, roads or train traffic. Finally a brief conclusion (Section I-7-) will give at the end of the chapter.

I-2- Service loads models

Bridges support busy traffic and experience considerable wind loads on the bridge decks nearly every day. In addition to these two major service loads, some extreme loads such as hurricane, earthquake, blast, fire, and vehicle-ship collision may also occur on the bridges simultaneously [13]. Some models of these service dynamic loads for the bridge are introduced in the following.

I-2-1- Roads traffic actions

Road traffic flow modelling is an important initial step in the development of the analytical framework of the bridge-vehicles interaction system. Generally, the roads traffic are considered as a sequence of vehicles having random weights, travelling at the deterministic or random speed and arriving at the span at random times [14].

However the modelling of this kind of loading is very complex. Therefore, in the vibration's analysis some simplifications in the load model are necessary. For example, investigating the vibrations of bridge caused by a single vehicle is quite simple and it is possible to take into account the coupling between the vibrations of the structure and the vehicle [15]. In that case, vehicle modelling include the following three essential computational models: a moving force model, a moving mass model and a sprung mass model with two degree of freedom as illustrated in Fig. 1. The moving force model

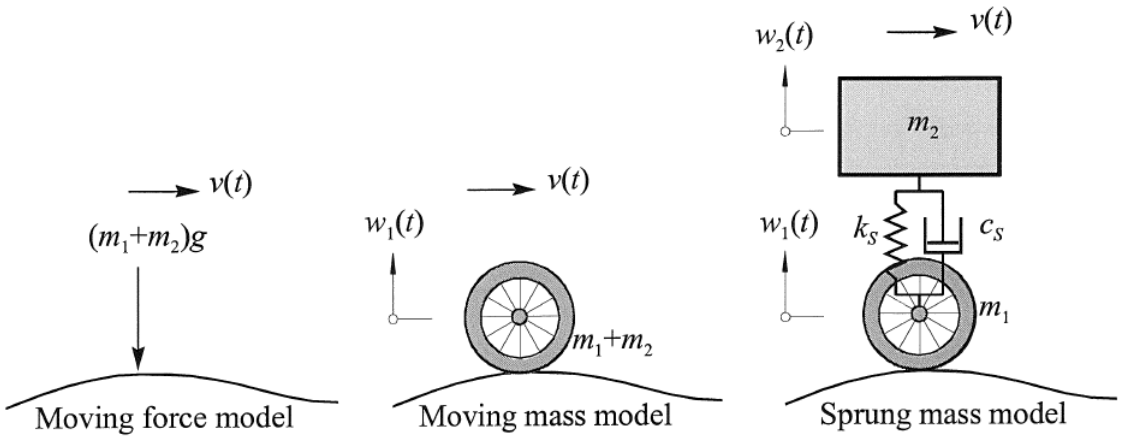

Figure 1: *Three essential vehicle models* [16].

(constant force magnitude) is the simplest model whereby researchers can capture the essential dynamic characteristics of a bridge under the action of a moving vehicle, although the interaction between the vehicle and bridge is ignored. It is sufficient if the inertia forces of the vehicle are much smaller than the dead weight of the vehicle. For a vehicle moving along a straight path at a constant speed, these inertia effects are mainly caused by bridge deformations (bridge-vehicle interaction) and bridge surface irregularities. Hence the factors that are believed to contribute in creating vehicle inertia effects include: high vehicle speed, flexible bridge structure, large vehicle mass, small bridge mass, stiff vehicle suspension system and large surface irregularities [16]. The sprung mass model is a one-axle vehicle model of a real multi-axle vehicle. This model is acceptable when the bridge span is considerably larger than the vehicle axle base [17].

Very detailed vehicle models are unnecessary and will not bring any great advantage, when the main purpose of this thesis is to study the dynamic response of bridges. ***In this thesis, the roads traffic model used assume that the sequence of vehicles moving with random or deterministic weights and stochastic velocities.***

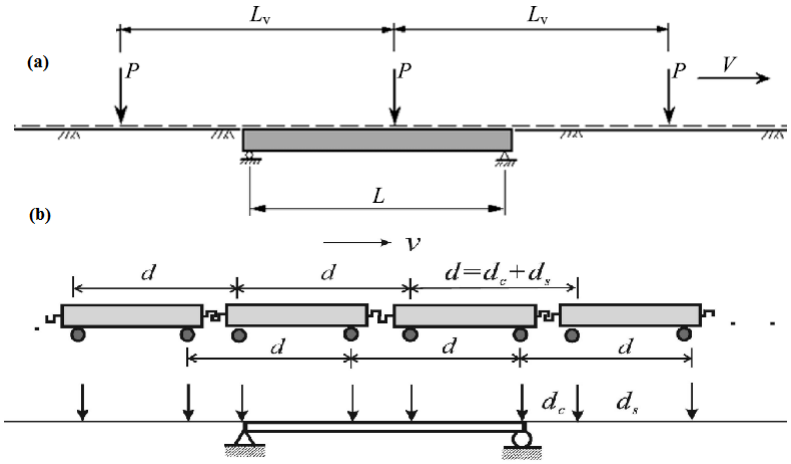

Figure 2: *Simplification of train loads on a single-span bridge: (a) composition of a train; (b) simplified regular uniform moving equidistant loads* [18].

I-2-2- Train or rail traffic actions

A train moving over a railway bridge can generally be regarded as a sequence of identical vehicles in connection, plus one or two locomotives. Conventionally, a train has been simplified as a sequence of moving masses, or in the extreme case as a sequence of concentrated loads, of regular uniform intervals (see Fig. 2) or of regular non-uniform intervals (see Fig. 3) to simulate the effect of a connected line of train loads [8].

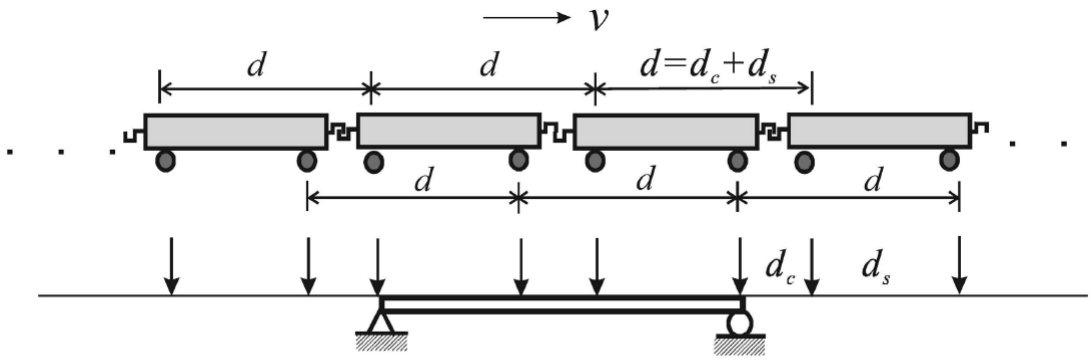

Figure 3: *Regular non-uniform train loads model* [8].

I-2-3- Wind actions

Wind is about air movement relative to the earth, driven by different forces caused by pressure differences of the atmosphere, by different solar heating on the earth's surface, and by the rotation of the earth. Wind loading offers a complicated set of loading conditions which must be idealized in order to provide a workable design. In general, the wind force shall be considered as a moving load acting in any horizontal direction. The interaction between the bridge vibration and this wind results in two kinds of forces: motion dependent and motion-independent. The former vanishes if the structures are rigidly fixed. The latter, being purely dependent on the wind characteristics and section geometry, exists whether or not the bridge is moving. In addition, bridge may responds dynamically to the effects of the wind flow over the deck section. This wind-induced dynamic response is generally classified into three major categories, depending on the mechanisms involved:

- Random response due to buffeting induced by wind turbulence
- Vortex-induced response
- Aerodynamic instability

In this thesis, the response of the bridge due to buffeting induced by turbulent wind and to aerodynamic instability will be analysed in details. Indeed,

Buffeting is the random response of the bridge due to wind forces associated with the pressure fluctuations on the bridge deck caused by gustiness of the wind flow over the section. It normally increases monotonically with the mean velocity and is thus more important at maximum wind. It is also a function of the turbulence intensity of the oncoming flow and of the structural damping of the bridge. Generally, aerodynamic instability occurs in the structure when the attack angle (that give the orientation of the force exerted by the wind flow on the structure) changes or varies. Therefore, the bridge oscillates due to the lift force (mean force in the direction normal to wind velocity), drag force (mean force in the direction of the wind velocity) and pitch moment.

I-3- Bridge models

Bridge design is a combination of art and science. Conceptual design is usually the first step. The conceptual design process includes selection of bridge systems, materials, proportions, dimensions, foundations, aesthetics, and consideration of the surrounding landscape and the environment. There are two kinds of models of bridges in the moving force identification systems: the Beam-Element Model and the Continuous Beam Model.

I-3-1- Beam-Element Model

In that case, a bridge can be modelled as an assembly of lumped masses interconnected by massless elastic beam elements [19]. The total modal responses, $[R]_{total}$, on the bridge equal to the equivalent static responses, $[R]_{static}$, caused by the external loads less the responses caused by the inertia forces, $[R]_{inertia}$, and the damping forces, $[R]_{damping}$, or equivalently as: $[R]_{total} = [R]_{static}$ - $[R]_{inertia}$ - $[R]_{damping}$. This model is usually used by the structural engineers.

I-3-2- Continuous Beam Model

This model assuming an Euler-Bernoulli or Timoshenko beam [20] of constant cross-section with constant mass per unit length, having linear, viscous proportional damping and with small deflections. From there follow four special cases:

- If the effect of rotatory inertia is neglected and only the effect of shear on the dynamic deflection of the beam is considered, it is called a shear beam.
- If the effect of shear is neglected and only the effect of rotatory inertia is considered, the so-called Rayleigh beam model results.
- If both the effect of shear and the effect of rotatory inertia are neglected, the classical Euler-Bernoulli beam model is obtained.

- Finally, if both the effect of shear and the effect of rotary inertia are considered, the so-called Timoshenko beam results.

In most problems encountered in practice the effects of rotatory inertia and shear can safely be neglected with little error (Euler-Bernoulli beam); however, for short, deep beams with height-span ratios larger than about 1/10 or beams made of materials sensitive to shear stresses, it is desirable to give consideration to the effect of shear and rotatory inertia. ***In this thesis the Rayleigh beam model will be used to refine the theory of Euler-Bernoulli beam which has some serious shortcomings for high frequency motion and for the analytical conveniences.***

I-4- Bridge supports models

Many structures, such as bridges, runways, rails, roadways, pipelines, etc., can be modelled as a beam structure on a elastic foundation. The modelling of this elastic foundation is based on an assumption for the behaviour of the subgrade reaction under loading. This elastic subgrade reaction is represented principally by [21]:

- One-parameter model
- Two-parameter models

I-4-1- One-parameter model

The one-parameter model developed by Winkler in [22] assumes that the vertical displacement of a point of the elastic foundation is proportional to the pressure at that point and does not depend on the pressure at the adjacent points. The Winkler model can be interpreted as a system of mutually independent vertical springs with stiffness k. The strain energy of the elastic foundation is

$$U_f = \frac{1}{2} kb \int_0^L w^2 \mathrm{d}x \tag{1}$$

where b and L are the width and the length of the deformed zone and w is the vertical displacement of the beam. The Winkler soil model assumes that the displacement appears only in the loaded zone. Outside this zone the deflections are zero. This assumption leads to a discontinuous displacement field and this is the main disadvantage of the Winkler model.

I-4-2- Two-parameter models

Two-parameter soil models restore the continuity of the elastic foundation by introducing a second parameter. The two-parameter models of Filonenko-Borodich [23], Hetenyi [24] and Pasternak [25] provide the continuity of the soil medium by adding a second spring which interacts with the first one. In [26] Kerr generalizes the Pasternak model by including a third spring in vertical direction. The models of Reissner [27] and Vlasov-Leontiev [28] make simplifying assumptions by introducing functions for distribution of the displacements or the stresses in the soil medium. The general expression for the strain energy in two parameter models is

$$U_f = \frac{1}{2}kb\int_0^L w^2 \mathrm{d}x + \frac{1}{2}Gb\int_0^L \left(\frac{\mathrm{d}w}{\mathrm{d}x}\right)^2 \mathrm{d}x \tag{2}$$

The second integral in Eq. (2) includes the second parameter G which represents the stiffness of a generalized rotation spring. Different interpretations exist of the physical meaning of G and the relation with the first parameter k:

- Filonenko-Borodich model: the G parameter is presented as an internal tension force in a virtual elastic string placed on the transversal springs which constrains the vertical displacements of the springs;
- Hetenyi model constrains the vertical displacements by adding an imaginary beam in bending. The second parameter represents the beam's stiffness;
- Pasternak model: the G parameter represents a shear modulus of a virtual layer that integrates the vertical spring elements;
- Vlasov-Leontiev model: the k and G parameters are obtained on the basis of the elastic continuum approach by making assumptions for the displacement field.

In this thesis the modified models of Pasternak and Winkler foundation will be investigated. These models include the damping effect, and the fractional order derivative rheological models are used to model this damping.

I-5- Brief review of the studies related to moving loads induced vibration of bridges

The first recorded research into bridge vibration appears to be a report published in 1849 by Willis [29], which discussed the reasons for the collapse of the Chester Railway Bridge. The research work on this subject has a long history of more than 150 years.

An overview of research related in this field in Europe, the United States, and Asia is given by Frýba [17]. Early research has led to closed-form or analytical expressions for simplified cases, e.g., considering a simply supported Euler-Bernoulli beam model for the bridge and a moving load model for the vehicle [30, 31] or for the wind force [18].

I-5-1- Bridges and vehicles

In bridges dynamic problem, there are two categories of vehicle: highway vehicles and railway vehicles. Highway vehicles are idealized by trains of concentrated forces (vehicle weights) of random (or not) values travelling at the different stochastic speed. The inter-arrival times of the moving forces are regarded as random or deterministic variables. While, railway vehicles are regarded as a sequence of moving masses, or in the extreme case as a sequence of concentrated loads, of regular uniform intervals or of regular non-uniform intervals. The dynamic response of bridge structures subjected to vehicles is very complicated. This is because the dynamic effects induced by moving on the bridge are greatly influenced by the interaction between vehicles and the bridge structure. Generally, this problem depends on the following factors:

- the speed, weight, and type of the vehicle
- road surface roughness
- dynamic characteristics of the vehicle, such as the number of axles, axle spacing, axle load, natural frequencies, suspension stiffness and damping
- the number of vehicles and their travel paths
- characteristics of the bridge structure, such as the bridge geometry, support condition, bridge mass and stiffness, damping and natural frequencies
- braking and acceleration of the vehicle.

Among the aforementioned factors, the first four have the greater influence on the dynamic response of a bridge. A number of research studies were carried out on the vibration of various types of bridges such as girder bridges, slab bridges, cable-stayed bridges, suspension bridges due to vehicles.

■ **Vibration of girder bridges**

A girder bridge is the most common and most basic bridge. The vibration of girder bridges under moving vehicles has been widely studied by analytical and numerical methods during the last three decades. In many papers, the problem has been studied in the deterministic manner (by considering that the moving vehicle is a deterministic load) and summarized in review articles by Frýba [31]. However, due to

many reasons the moving forces acting on highway bridges (vehicle axle pressures) are of random magnitude. Moreover, they arrive at the span at random times. Consequently, the traffic load on a bridge is a random process. Only a few authors approached the moving load problem from this point of view. Frýba considered vibration of a beam due to the passage of a single, time-dependent concentrated force, the variation of which is given by a stochastic process [32]. Knowles [33] dealt with the problem of an infinitely long beam subjected to a moving concentrated force, whose position is described by strictly stationary first order, stationary Gaussian, or Wiener stochastic process. The vibration of a beam under random moving continuous load was studied by Robson [34] and Bolotin [35]. Besides, the stochastic vibrations of the beam excited by a random set of moving forces was presented among others by Iwankiewicz and Śniady [36], and Sieniawska and Śniady [6, 7]. These authors approached the most realistic highway vehicles problem by employing a simple beam model of a bridge.

In the same impetus, Śniady and Śniady et *al.* [15,37] investigated on the problem of a dynamic response of a beam-like modelled girder bridge to the passage of a train of random forces. In this study they assumed that the random train of forces idealizes the flow of vehicles having random weights and travelling at the stochastic velocity. They shows the effect of theses stochastic quantities on the mean deflection of the beam. Zibdeh [38] investigated the vibrations of a simply supported elastic beam under the action of a point load moving with random non constant velocity, while the beam is also subject to axial deterministic forces. Closed form solutions for the mean and variance of the response were also obtained. The above mentioned works deal with bridge beams vibrations caused by a random stream of moving forces, assuming that the bridge is idealized by a single Euler-Bernoulli beam model.

To take into account the rotary and high frequency motion of beam elements, Chang [39] proposed to treat the deterministic and random vibration analysis of a Rayleigh-Timoshenko beam like girder bridge model on an elastic foundation. He used a modal analysis to compute the dynamic responses of the structure (such as the displacement and bending moment) and some statistical responses (such as the mean square values of the dynamic displacement and the mean bending moment). With the same method, Argento et *al.* [40] studied the response of a rotating Rayleigh beam with different boundary conditions subject to an axially accelerating distributed surface line load. Zibdeh and Juma [41] used an analytical and numerical methods to investigate the stochastic dynamic response of a rotating simply supported beam subjected to a random force with constant mean value moving with a constant speed along the beam. The beam is modelled by Euler-Bernoulli, Rayleigh, and Timoshenko beam models. They showed the effect of load speed, beam rotating speed, and geometrical size of the beam on the random response of the beam.

As far as bridge response to highway vehicles is concerned, the contributions given by Tung [3–5] seem to be most relevant to the problem. Based on the assumption that vehicles travel at the same constant speed, are of equal weight, and that the bridge response is a filtered Poisson or filtered renewal process. Tung obtained, by means of a numerical procedure, the probability density function of the response process and its expected rate of threshold crossings. He also estimated the fatigue life of bridges.

■ **Vibration of cable-stayed bridges**

Cable-stayed bridges have become very popular over the last three decades because of their aesthetic appeal, structural efficiency, enhanced stiffness compared with suspension bridges, ease of construction and comparatively small size of structures. In another development, enhanced by the use of lightweight and high-strength materials, more slender cross sections were adopted for the various components of cable-stayed bridges. As a consequence, response prediction of this type of bridge subjected to randomly moving excitations is important for engineering practice [42,43]. The dynamic behaviour of cable-stayed bridges is a source of interesting research. This includes free vibration and forced vibration due to wind and earthquake, see for example [44–46]. However, literature dealing with the dynamics of these bridges due to highway vehicles are relatively few.

Meisenholder and Weidlinger [47] simulated the cable-stayed bridge as a beam resting on an elastic foundation and proposed an approach for modeling the dynamic effects of cable-stayed guideways subjected to track-levitated vehicles moving at high speeds. By using an approximate bridge model, taking into account the nonlinear effect of cables, the dynamic response of cable-stayed bridges under moving loads was analyzed by Yang and Fonder [48]. Au et *al.* [49] investigated the impact effects of cable-stayed bridges under railway traffic using various vehicle models, and concluded that the moving force and moving mass models can significantly underestimate the impact effects. Based on a nonlinear dynamic finite-element analysis for the Vehicle-Bridge Interaction (VBI) system, Yau and Yang [50] pointed out that the larger of the number of stay cables of a cable-stayed bridge, the smaller of the impact response of the bridge; the same is also true for the riding comfort of the moving vehicles. Yau et et *al.* [51] studied the vibration reduction of cable-stayed bridges subjected to the passage of high-speed trains. The train is modeled as a series of sprung masses, the bridge deck and towers by nonlinear beam-column elements, and the stay cables by truss elements with Ernst's equivalent modulus. To suppress the multiple resonant peaks of train-induced vibrations on cable-stayed bridges, a hybrid Tuned Mass Damper (TMD) system that consists of several TMD subsystems, each of which is tuned for one dominant frequency of the main system, is proposed. The numerical results indicate that the proposed hybrid TMD system

can effectively suppress the main resonant peaks of the cable-stayed bridge subjected to the moving train loads at high speeds.

Yet, Zaman et *al.* [52] analysed the dynamic response of cable-stayed bridges subjected to moving loads by using the structural impedance method. In their study, the bridge deck was modelled as an elastic plate, the cables were idealised as springs for simplicity, and the vehicles were modelled as a series of masses with suspension systems moving at different speeds and accelerations. By using the same method, Rasoul [53] studied the dynamic response of bridges due to general traffic conditions. The bridge flexibility functions were evaluated by using a static analysis of the bridge subjected to unit loads. A simply supported beam, a continuous beam and very simple cable-stayed bridges were studied. For the cable-stayed bridges, two different analysis methods were used, namely an approximate method using the concept of continuous beam with intermediate elastic supports, fixed pylon heads and with the cables approximated by springs. The traffic load was modelled as a series of vehicles traversing along the bridge. Each vehicle was modelled with a sprung mass and an unsprung mass giving a vehicle model with two Degrees Of Freedom (2 DOF). Different traffic conditions were studied, and the effect of vehicle speed and bridge damping on the Dynamic Amplification Factor (DAF) was presented.

■ **Vibration of suspension bridges**

Compared with other types of bridges, publications on the vibration of suspension bridges caused by moving vehicles are relatively few. Hirai and Ito [54] studied theoretically and experimentally the dynamic response of two hinged suspension bridges due to a railway vehicle modelled either as a single constant force with a constant velocity, a pulsating force with a constant velocity, or a distributed load with a uniform intensity and a constant velocity. The modal superposition method was employed for the analysis and only the few lower natural modes were taken into consideration. Karoumi [16] derived approaches for solving the moving load problem of cable-stayed and suspension bridges. An efficient finite element program was developed to carry out dynamic analysis of bridges. The implemented program is verified by comparing the analysis results with literature and a commercial finite element code. Parametric studies were performed, investigating the effect of damping, bridge-vehicle interaction, cables vibration, road surface roughness, vehicle speed and tuned mass dampers. It concluded that road surface roughness has great influence on the dynamic response and should always be considered if possible.

Subsequently, Yasoshima et *al.* [55] carried out a comprehensive study using the modal superposition method on the running stability of railway vehicles on suspension bridges. The vertical response of the bridge was obtained by modelling the moving railway vehicle as either a moving constant force or a moving constant load with a uniform intensity. The lateral vibration of the bridge induced by

the side thrusts of the wheels of the running railway vehicles was also obtained. Chatterjee et *al.* [56] presented a continuum analysis for determining the coupled vertical-torsional vibration of multi-span suspension bridges under vehicular movement. They employed the modal superposition method and obtained the dynamic response in time domain using an iterative scheme. Three different types of vehicle models, namely one-, two- and three-dimensional mass-spring-damper systems were used in the analysis.

The above-mentioned research work was carried out taking the problem as a deterministic one. Some researchers investigated the random vibration of suspension bridges due to highway traffic. By treating the moving vehicle loads as random concentrated weights and their arrivals as a Poisson process. Bryja and Śniady [14] performed the random non-linear dynamic analysis of a single-span suspension bridge under the passage of moving vehicles. Subsequently, they extended their studies to a general case of spatially coupled flexural-torsional vibration of a single-span suspension bridge under the passage of trains of concentrated forces with random magnitudes [57]. In this study, the bridge is modelled by a single-span prismatic thin-walled stiffening girder underslung to two whipped cables. They used both iterative and linearization methods to determine the solution for the expected value and variance of the bridge deflections.

■ **Vibration of slab bridges**

The beam model was often adopted to study the vibration of girder bridges under moving vehicles and trains. However, it is inadequate to model the response of wide bridge decks such as slab bridges, particularly under moving vehicles whose paths are not along the centre-line of the bridge. The vibration of slab bridges modelled as isotropic or orthotropic plates under the action of vehicles was investigated by many authors but in most of their works the moving vehicle was regarded as deterministic. A concise review of several related research studies is carried out in the following paragraph.

Nikkhoo and Rofooei [58] scrutinized the inertial effects and the trajectory of the moving load on the dynamic response of a simply-supported edge thin rectangular plate. Wu [59] examined an inclined flat plate vibration due to traveling loads. Vaseghi Amiri et *al.* [60] provided a semi-analytical simulation of a shear deformable plate vibration due to traveling inertial loads considering a general load distribution pattern and plate boundary condition. Zhu and Law [61] analysed the dynamic behavior of an orthotropic plate simply supported on a pair of parallel edges and under a system of moving loads based on Lagrange equation and modal superposition. Preliminary results of the paper indicate that the multi-lane loading case is less critical than a single-lane loading case. Nikkhoo et *al.* [62] considered two series of moving inertial loads traversing the plate surface along parallel rectilinear trajectories with opposite directions and studied the resonance caused by this loads.

This investigation done by Nikkhoo et *al.* is of significance in engineering mechanics dealing with the vibration of two-lane slab-type bridges under the moving vehicles. They showed that, the plate displays resonance behavior for specific values of spacing of the loads. In addition, they also demonstrated that for a specific velocity, the loads inertia can alter the aforementioned distance.

In real situation the load process has stochastic nature. So, the problem of vibrations of a plate-like modelled slab bridges subjected to this kind of load was considered in some papers in stochastic approaches. Rystwej and Śniady [63] investigated the problem of a dynamic response of an infinite beam and a plate resting on a two-parametric foundation (Pasternak foundation) to the passage of a sequence of random forces. This sequence of forces idealizes the flow of vehicles having random weights and travelling at the same speed. They assumed that this occurrence process of moving loads is either a Poisson process or a renewal (Erlang) process. An analytical technique was developed to determine the two first probabilistic characteristics of the beam and plate responses. Li et *al.* [64] investigated the dynamic response of a rectangular plate on a viscoelastic foundation under moving loads with varying velocity. The deflection distribution of the plate and the effects of the type of motion, initial speed of the load and foundation damping on the plate response are illustrated and analysed.

By using the method of modal analysis, Wang and Lin [65] analysed the vibration of multi-span Mindlin plates under a moving load. The effects of span number, rotary inertia and transverse shear deformation on the critical velocity, the maximum displacement and the maximum moment of plates were discussed. They further studied the random vibration of multi-span Mindlin plates due to random moving loads [66]. Here, the moving load is considered to be a stationary process with a constant mean value and a variance. Four types of variances were considered in this study: white noise, exponential, exponential cosine, and cosine. The effect of both velocity and statistical characteristics of the load and the effect of the span number of the multi-span plate on the mean value, variance of deflection and moment of the structure were investigated.

Nurkan yagiz and sakman [67] analyzed the vibrations of a bridge modeled as an isotropic plate with all sides simply supported under the effect of a moving load due to a full vehicle having seven DOF. A mathematical model of the bridge is obtained by applying Lagrange's formulation to orthogonal mode shapes and the non-conservative moving forces. The time responses at the mid-span and quarter-span of the bridge were obtained. The transverse vibration of the bridge and the body bounce, pitch, and roll of the vehicle were presented for different vehicle speeds. They also presented the bending moment at the mid-span for different vehicle speeds to aid in the structural design of the bridge. In the same way, Paul and Talukdar [68] analyzed an orthotropic bridge deck to find out non-stationary response statistics

when subject to moving vehicle at variable velocity. In that work statistics of the responses were presented and DAF for constant velocity and variable velocity was discussed.

■ **Vibration of railway bridges**

The dynamic response of railway bridges under moving train loads is one of the fundamental problems to be solved in bridge design. On the one hand, the train running with high speed induces dynamic impact on the bridge structure, influencing their working state and service life. On the other hand, the vibration of the bridge in turn affects the running stability and safety of the train vehicles, and thus becomes an important factor for evaluating the dynamic parameters of the bridge in design. Therefore, great efforts were constantly attached to the subject.

The book of Frýba [17] and the one of Garg and Dukkipati [69] described well the dynamics of railway bridge and railway vehicle modelling. Frýba [17] gave a comprehensive treatise on this field of research. Yang et *al.* [8] presented a literature review of research work on the dynamic interaction between moving vehicles and bridges, with particular emphasis on the analysis of high-speed railway bridges. Indeed, based on an analytical approach, Yang et *al.* [70] obtained the closed form solution for the response of simple beams subjected to the passage of a high-speed train modeled as a sequence of moving loads with regular non-uniform intervals, in which the conditions for the phenomena of resonance and cancellation to occur were identified. Based on these conditions, optimal design criteria that are effective for suppressing the resonant response of the VBI systems was proposed. In the study done by Wu et *al.* [71], a bridge containing two railway tracks was considered, with which two trains are allowed to move over the bridge in opposite directions. Such a vehicle-rails-bridge interaction model was adopted by Wu [72] and Yang and Wu [73] in evaluating the risk of derailment for trains traveling over a bridge and simultaneously subjected to an earthquake excitation.

Out of Frýba an Yang, the dynamic response of railway bridges subjected to vehicles has received much attention from those researchers. For example, Museros et *al.* [74] investigated the influence of sleepers and ballast layers, as well as train-bridge interactions, on the response of short high-speed railway bridges. They concluded that inclusion of these factors can result in smaller maximum displacements and accelerations on the bridge, compared with those obtained using barely the moving loads model. Bolotin [75] studied a beam subjected to an infinite sequence of equal loads with uniform interval and constant speed. In his study, the period of the moving loads was identified as a key parameter.

The dynamic response of track structures resting on bridges under the action of moving trains is also of great theoretical and practical significance in railway engineering. It was often studied by modelling the railway track system as either

a beam on Winkler elastic foundation or a beam supported on a series of discrete spring-damper units. Steele [76] obtained an analytical solution for a finite simply supported Euler-Bernoulli beam, with and without an elastic foundation, subjected to a moving force. He further solved the problem of a semi-infinite Timoshenko beam on elastic foundation with a step load moving from the supported end at a constant velocity [77]. Subsequently, Suzuki [78] obtained the dynamic response of a finite beam on elastic foundation subjected to travelling loads with acceleration. Kargarnovin and Younesian [79, 80] used the first order perturbation method to analyse the response of an infinite Timoshenko beam on the viscoelastic foundation under a moving load. To simulate the behaviour of the foundation, Pasternak viscoelastic model was used. This model includes a Kelvin foundation in conjunction with a shear viscous layer [79] or with a shear elastic layer [80]. These studies clearly show that the shear layer material of the foundation can have viscoelastic physical properties.

I-5-2- Wind-vehicles-bridge system, bearings devices

■ Wind-vehicles-bridge interaction

Slender long-span bridges exhibit unique features which are not present in short and medium-span bridges such as higher traffic volume, simultaneous presence of multiple vehicles, and sensitivity to wind load. In recent years, some efforts were put forth on studying more realistic load combination scenarios including wind and vehicles, for long-span bridges. A few number of researches showed the significance of coupling effects existing among vehicles, wind, and long-span bridges. For instance, Xu et *al.* [9] investigated the dynamic response of suspension bridges to high wind and a moving train, while no wind loading was considered on the train moving inside the suspension bridge deck. In this analysis it was found that the suspension bridge response was dominated by wind force in high wind speed. The coupled dynamic analysis of vehicle and cable-stayed bridge system under turbulent wind was also recently conducted by Xu and Guo [10] under low wind speed and neglecting the vehicle number and speed. Chen and Wu [11] proposed a simulation approach for the bridge performance under the combined effect of wind and stochastic traffic flow that provides a realistic estimate of the bridge response. In the same view, Zhou and Chen [13] established a general simulation platform to investigate the dynamic performance of the bridge-traffic system under multiple service and extreme loads. The approach allows to explore the vertical and lateral responses for the bridge and a representative vehicle in different loading scenarios. Zhang et *al.* [12] investigated a comprehensive framework for fatigue reliability analysis of long-span bridges under the combined dynamic loads of vehicles and wind. Li et *al.* [81] presented an analytical model to simulate dynamic interactions among wind, rail

vehicle and bridge. The analysis on an engineering example indicates the important role of wind excitation in vibration of the coupled wind-vehicles-bridge system, which prominently enlarges the dynamic responses of both bridge and vehicles.

■ **Bearings devices**

To prevent the damage of bridges, the bearings (part of bridge ranging between the bridge deck and the piers) were often used as base isolators for severe earthquakes load and/or for load transference to the foundation in bridge engineering. The problem of elastically supported beams subjected to moving loads received little attention in the literature. Yang *et al.* [83] explained by using an analytical approach the mechanism involved in the phenomena of resonance and cancellation in the train induced vibrations of railway bridges with elastic bearings. They concluded that there is doubt that the installation of elastic bearings can prevent the transmission or dissipation of vehicle-induced forces from the superstructure to the ground. Thus, the huge amount of vibration energy brought by a train may be accumulated and amplified on the bridge during its passage. A method based on modal superposition and regularisation technique is used by Zhu and Law [84] to identify the moving loads on the elastically supported bridge deck. Their main conclusion was that the stiffness of the bearings should be large relative to the stiffness of the bridge deck. Naguleswaran [85] analysed the transverse vibration of a uniform Euler-Bernoulli beam on five resilient supports (including ends).

I-6- Problem statement of the present study

This thesis covers the dynamic analysis of girder bridges, railway bridges, slab bridges as well as cable-stayed bridges under the action of moving vehicles and wind actions. In order to distinguish the present work from the above pertinent literature, we extend the work done by others researchers by identifying and proposing the solutions to some of the limits encountered in this field of research. The following improvements have been achieved in the study.

- **Effects of load random velocities on the probabilistic features of the non-linear Rayleigh beam subjected to a train of forces moving with stochastic velocity**

  In previous studies on the vibration analysis of girder bridges under moving vehicles, most of them deal with bridge beams vibrations caused by a random stream of moving forces, assuming that the loads move with an exactly determined velocity [3–5, 38, 41]. A step further is to consider the velocities as stochastic variables [15, 37, 87]. If the beam is loaded by stochastically moving loads, the problem is more complicated and, generally, only numerical methods allow to retrieve the resulting vibrations [88]. ***In this thesis, we give an analytical approach to***

characterize the mean-square amplitude of the beam response and the probability density function due to loads moving with stochastic velocities. The effects of the mean and disturbances velocity on the dynamics of the beam are also analysed.

- **Cable-stayed bridge loaded by a sequence of moving forces with stochastic velocity: A chaotic dynamics approach**
  In all of the above mentioned research concerning the dynamic of the cable-stayed bridge under the action of moving vehicles, only the effect of vehicle parameters on the DAF of the system response was presented. Also, due to the complexity of the cable-stayed bridge structure, only the finite-element analysis for the VBI system was generally pointed out to find for example the effect of the number of stay cables on the system response. ***To the best of our knowledge, the effects of stochastic fluctuations of the load velocity and the number of stay cables on the possible appearance of some nonlinear phenomenon such as horseshoes chaos in the cable-stayed bridge system remain unaddressed. In this thesis, based on one of a chaotic dynamics approach: Melnikov technique which is widely used by most researchers [89, 91–94], all theses effects are investigated.***

- **Dynamic response of a two lane slab-type-bridge due to traffic flow: Probabilistic or statistic approach**
  From the above pertinent literature concerning the dynamic of slab bridges loaded by vehicles, the contributions given by Nikkhoo et *al.* [62] seem to be most relevant to the problem. They considered two series of moving inertial loads traversing the plate surface along parallel rectilinear trajectories with opposite directions and studied the resonance caused by this loads. This investigation done by Nikkhoo et *al.* is of significance in engineering mechanics dealing with the vibration of two lane slab-type bridges under the moving vehicles.

  Nevertheless, the assumed model of the loads is a serious shortcoming of their work if they are supposed to idealize the loads due to moving vehicles. In this model all the forces (vehicles) arriving at the plate at different, deterministic time instants and with constant velocity. An adequate modelling of highway traffic loads was proposed by Tung [3–5]. We propose here to extend the work done by Nikkhoo et *al.* [62] by taking into account this more realistic model of moving loads (when it idealizes the vehicles in highway traffic). In this model all the forces (vehicles) arrive at the plate at the random time instant, with stochastic velocities. ***To summarize, in this thesis, an analytical approach for obtaining the probabilistic characteristics of a two lane slab-type-bridge response due to two opposite series of stochastic moving loads is investigated.***

- **Rayleigh beams on viscoelastic Pasternak foundation supporting a sequence of equidistant moving loads: Vibratory and chaotic dynamics approaches**

  Amongst those previous investigations concerning the vibration analysis in railway bridges, the ones of Kargarnovin and Younesian [79, 80] were attracted our attention. The authors used the first order perturbation method to analyse the response of an infinite Timoshenko beam on the viscoelastic foundation under a moving load. To simulate the behaviour of the foundation, Pasternak viscoelastic model was used. This model includes a Kelvin foundation in conjunction with a shear viscous layer [79] or with a shear elastic layer [79]. These studies clearly show that the shear layer material of the foundation can have viscoelastic physical properties.

  It is well known that, the shear layer of material that constitutes the railway track can be constituted by some viscoelastic materials such as elastomer. Therefore, the long memory effects of this viscoelastic materials may be considered through a fractional-order derivative concept. ***So, we focus in our work on the analytical and numerical analysis of Rayleigh beams subject to uniform moving loads resting on Pasternak foundations considering their shear layer as fractional-order viscoelastic material.***

- **Vibration analysis of Rayleigh beams laying on fractional order viscoelastic bearings subject to moving loads and stochastic wind**

  Elastic bearings often exist at the supports of bridge girders for load transference to the foundation or for earthquakes load isolator. However, such devices may result in amplification of the response of the bridge during the passage of a train [82]. This is certainly one disadvantage with the use of elastic bearings. Hence our interest. It is well known that, the bearings can also be constituted by some viscoelastic materials (such as elastomer) [86]. Therefore, the long memory effects of these viscoelastic materials may be modelled by means of fractional derivatives. Or, in the above mentioned studies of bridge/vehicle/wind interaction analysis [9,11–13,81], the effects of bearings having fractional-order viscoelastic material on the vibration performance of bridge deck have not yet been explored. Also, most of these studies focus on the dynamic displacements and accelerations using a simple finite element model of the bridge. ***In this thesis, we firstly, analyse the effect of the number of bearings and their fractional-order viscoelastic physical properties on the resonance vibrations of the bridge deck. Secondly, we give some estimate of the additive and parametric wind turbulence effects on the stationary probability density function of the oscillations amplitude of the bridge deck.***

I-7- Conclusion

In this chapter, we have provided the reader with some key factors involved in the dynamic interaction between the bridge and service loads including roads traffic, train traffic and wind actions. A briefly state-of-art review of research based on this topic has been presented. The main challenge of the thesis concerning notably, the problem of transverse vibrations of bridges subject to the passage of randomly moving loads has been presented and will be solved in chapter III of the dissertation by using some approximate response methods. Therefore, in the following chapter a general background of these methods will be presented.

Chapter II

Research methodology: approximate response methods for the reduced linear or nonlinear mathematical bridge models

II-1- Introduction

Generally, the whole excited bridge system is modelled with a Partial Differential Equation (PDE) that is reduced to a linear or nonlinear one-dimensional system by applying the Galerkin's method. This chapter presents a general background on approximate response methods for these reduced mathematical models. These approximate response methods are subdivided in two major categories: analytical and numerical techniques. Therefore, five analytical techniques including the classical stochastic averaging technique to approach the nonlinear Stochastic Differential Equations (SDEs), Melnikov's method to predict Smale horseshoe type chaos, Fourier transform and theory of residues to characterize the probabilistic features of the nonlinear Ordinary Differential Equations (ODEs), Routh-Hurwitz criterion to give the decision on the stability of the non-trivial steady-states solutions of the nonlinear ODEs, and the Itô differential rule associated with the averaging method to approximate solutions for statistical moments of the reduced mathematical models are presented in Section II-2-. In Section II-3-, four numerical methods are presented: the Stochastic Fourth-order Runge-Kutta (SRK4) algorithm to integrate the nonlinear SDEs, the deterministic one (RK4) for the nonlinear ODEs, the Newton-Leipnik and the Adams-Bashforth-Moulton (A-B-M) predictor-corrector schemes to integrate the nonlinear Fractional Differential Equations (FDEs), the dichotomy method to solve complex or non-trivial polynomial equations. The conclusion of the chapter appears in Section II-5-.

II-2- Approximate response methods for the reduced mathematical bridge models - Analytical techniques

To predict the response and to give the decision on its stability, various analytical techniques [96–103] are used to approach the reduced mathematical bridge models (nonlinear ODEs, SDEs and FDEs or linear equations) and will present in the following subsection.

II-2-1- Stochastic averaging method for the nonlinear stochastic differential equations

In the quest for approximate solution for random vibration problems, the method of stochastic averaging has proved to be a powerful analytic tool. This method was originally introduced by Stratonovich [96] in 1963, based on a combination of physical and mathematical arguments, in connection with non-linear self-excited oscillations in electrical systems, due to the presence of noise. It may be viewed as an extension of the

deterministic averaging procedure of Bogoliubov and Mitropolsky [104]. The success of the stochastic averaging method is mainly due to its two advantages: the equations of motion of a system are much simplified and the dimensions of the equation is often reduced while the essential behaviour of the system is retained; the averaged response is a diffusive Markov process and the method of Fokker-Planck-Kolmogorov (F-P-K) equation can be applied.

The solvability of a nonlinear stochastic system is enhanced if the dimensionality of the system can be reduced. This is accomplished with two averaging techniques, applicable under certain conditions. The first, known as stochastic averaging, is applied to systems with linear or weakly nonlinear stiffness. The second averaging technique, known as quasi conservative averaging, is applicable even when the stiffness term in the governing physical equation is strongly nonlinear. In this thesis, we have used the first one which is now illustrated with the following single-degree-of-freedom-system of linear stiffness:

$$\ddot{Y} + \omega_0^2 Y = \varepsilon f\left(Y, \dot{Y}\right) + \varepsilon h\left(Y, \dot{Y}\right) D^{\alpha}\left[Y\left(t\right)\right] + \varepsilon^{1/2} \sum_k g_k\left(Y, \dot{Y}\right) \xi_k\left(t\right) \tag{3}$$

where ε is a small parameter, indicating that the damping term is of order ε, and the random excitations $\xi_k\left(t\right)$ are of order $\varepsilon^{1/2}$. $f\left(Y, \dot{Y}\right)$, $h\left(Y, \dot{Y}\right)$ and $g_k\left(Y, \dot{Y}\right)$ are linear or nonlinear functions with respect to Y and $\dot{Y}$. We assume that $\xi_k\left(t\right)$ are weakly stationary process, namely:

$$E\left[\xi_r\left(t\right)\xi_s\left(t+\tau\right)\right] = R_{rs}\left(\tau\right) \tag{4}$$

$D^{\alpha}\left[Y\left(t\right)\right]$ is Caputo-type fractional derivative and defined by

$$D^{\alpha}\left[Y\left(t\right)\right] = \frac{1}{\Gamma\left(n-\alpha\right)} \int_0^t \frac{Y^{(n)}\left(t-\tau\right)}{\tau^{\alpha}} \mathrm{d}\tau \tag{5}$$

where $n-1 < \alpha \leq n$ and $\Gamma\left(z\right)$ is Gamma function that satisfies $\Gamma\left(z+1\right) = z\Gamma\left(z\right)$. At first, the original system (3) is transformed into a diffusion differential equation by using the following generalized Van der Pol transformation:

$$Y = A\left(t\right)\cos\theta, \quad \dot{Y} = -A\left(t\right)\omega_0 \sin\theta, \quad \theta = \omega_0 t + \phi\left(t\right) \tag{6}$$

Therefore, the joint response process $\left(Y, \dot{Y}\right)$ is needed to be transformed to a pair of slowly varying processes (A, ϕ). After some elementary calculations, Eq. (3) may be replaced by the following two first-order equations:

$$\begin{aligned} \dot{A} = -\tfrac{\sin\theta}{\omega_0} \Big[& \varepsilon f\left(A\cos\theta, -A\omega_0\sin\theta\right) + \varepsilon h\left(A\cos\theta, -A\omega_0\sin\theta\right) D^{\alpha}\left[A\cos\theta\right] \\ & + \varepsilon^{1/2} \sum_k g_k\left(A\cos\theta, -A\omega_0\sin\theta\right)\xi_k\left(t\right) \Big] \end{aligned} \tag{7}$$

$$\dot{\phi} = -\frac{\cos\theta}{A\omega_0}\left[\varepsilon f\left(A\cos\theta, -A\omega_0\sin\theta\right) + \varepsilon h\left(A\cos\theta, -A\omega_0\sin\theta\right) D^{\alpha}\left[A\cos\theta\right] + \varepsilon^{1/2}\sum_k g_k\left(A\cos\theta, -A\omega_0\sin\theta\right)\xi_k\left(t\right)\right] \tag{8}$$

The right hand side of Eqs. (7) and (8) are associated only with ε and $\varepsilon^{1/2}$ terms. Physically, $A\left(t\right)$ represents the random amplitude, and $\phi\left(t\right)$ represents the random phase, and their values are nearly unchanged within a time-span $1/\varepsilon$.

Define a correlation time between random excitations $\xi_r\left(t\right)$ and $\xi_s\left(t\right)$:

$$\tau_{rs} = \frac{1}{\left[R_{rr}\left(0\right)R_{ss}\left(0\right)\right]^{1/2}}\int_{-\infty}^{0}\left|R_{rs}\left(\tau\right)\right|\mathrm{d}\tau \tag{9}$$

which is a measure of memory of the present $\xi_r\left(t\right)$ with respect to the past $\xi_s\left(t\right)$. If the system variables $\{A,\,\phi\}$ are observed at time instants at Δt apart, and if $\Delta t \gg \tau_{rs}$ for all r and s, then the observed variation of the system variables is Markov-like. However, Δt should be much smaller than ε^{-1} in order that sufficient details of the system behaviour can be observed. In other words, the observed $\{A,\,\phi\}$ is approximately a Markov vector if $\varepsilon^{-1} \gg \tau_{rs}$ for all r and s. If this condition is satisfied, then the amplitude process may be approximated as a one-dimensional Markov process, governed by an Itô equation:

$$\mathrm{d}A = m\left(A\right)\mathrm{d}t + \sigma\left(A\right)\mathrm{d}B\left(t\right) \tag{10}$$

where the drift and diffusion coefficients $m\left(A\right)$ and $\sigma\left(A\right)$ can be obtained as follows:

$$m\left(A\right) = \varepsilon\left\langle -\frac{1}{\omega_0}\sin\theta_t f\left(A\cos\theta_t, -A\omega_0\sin\theta_t\right) + h\left(A\cos\theta, -A\omega_0\sin\theta\right)D^{\alpha}\left[A\cos\theta\right] + \frac{1}{\omega_0^2}\int_{-\infty}^{0}\sum_k\sum_j\left\{\frac{\partial}{\partial A}\left[\sin\theta_t g_k\left(A\cos\theta_t, -A\omega_0\sin\theta_t\right)\right]\sin\theta_{t+\tau} + \frac{1}{A}\frac{\partial}{\partial\theta_t}\left[\sin\theta_t g_k\left(A\cos\theta_t, -A\omega_0\sin\theta_t\right)\right]\cos\theta_{t+\tau}\right\} g_j\left(A\cos\theta_{t+\tau}, -A\omega_0\sin\theta_{t+\tau}\right)R_{kj}\left(\tau\right)\mathrm{d}\tau\right\rangle_t \tag{11}$$

$$\sigma^2\left(A\right) = \varepsilon\left\langle\frac{1}{\omega_0^2}\sum_k\sum_j\int_{-\infty}^{+\infty}\left\{\sin\theta_t\sin\theta_{t+\tau}g_k\left(A\cos\theta_t, -A\omega_0\sin\theta_t\right) g_j\left(A\cos\theta_{t+\tau}, -A\omega_0\sin\theta_{t+\tau}\right)R_{kj}\left(\tau\right)\right\}\mathrm{d}\tau\right\rangle_t \tag{12}$$

in which θ_t and $\theta_{t+\tau}$ are abbreviations for $\omega_0 t + \phi\left(t\right)$ and $\omega_0\left(t+\tau\right) + \phi\left(t\right)$, respectively, and $\left\langle . \right\rangle_t$ denotes a deterministic time-averaging operation of the enclosing quantity. That is,

$$\left\langle\left[.\right]\right\rangle_t = \lim_{T\to\infty}\frac{1}{T}\int_{t_0}^{t_0+T}\left[.\right]\mathrm{d}t \tag{13}$$

If the quantities in Eqs. (11) and (12) are periodic, with period T_0 for example, then Eq. (13) becomes

$$\langle [.] \rangle_t = \frac{1}{T_0} \int_{t_0}^{t_0+T_0} [.] \, \mathrm{d}t \tag{14}$$

It is seen that the fractional derivative with Caputo definition is essentially a generalized integral with derivative of time-delay in it, usually, it is very difficult to deal with a higher fractional order in mathematics. Herein only the case $0 < \alpha \leq 1$ in this thesis is considered, other values for α will be discussed further in our future work. So, according to formula (5) and Eq. (6), the Caputo-type fractional derivative can be rewritten as

$$\frac{1}{\Gamma(1-\alpha)} \int_0^t \frac{\dot{Y}(t-\tau)}{\tau^\alpha} \mathrm{d}\tau = \frac{A\omega_0}{\Gamma(1-\alpha)} \left[\cos\theta \int_0^t \frac{\sin\omega_0\tau}{\tau^\alpha} \mathrm{d}\tau - \sin\theta \int_0^t \frac{\cos\omega_0\tau}{\tau^\alpha} \mathrm{d}\tau \right] \tag{15}$$

It turns out that how to calculate or approximate the integrals appeared in (15) is an important task to replace the complicated Caputo-type fractional derivative in terms of envelope and frequency. Fortunately, the following two generalized integrals can play a role to solve this problem, they are respectively

$$\int_0^t \frac{\sin\omega_0\tau}{\tau^\alpha} \mathrm{d}\tau = \omega_0^{\alpha-1} \left[\Gamma(1-\alpha) \cos\frac{\pi\alpha}{2} - \frac{\cos\omega_0 t}{(\omega_0 t)^\alpha} + o(\omega_0 t)^{-\alpha} \right], \tag{16a}$$

$$\int_0^t \frac{\cos\omega_0\tau}{\tau^\alpha} \mathrm{d}\tau = \omega_0^{\alpha-1} \left[\Gamma(1-\alpha) \sin\frac{\pi\alpha}{2} + \frac{\sin\omega_0 t}{(\omega_0 t)^\alpha} + o(\omega_0 t)^{-\alpha} \right]. \tag{16b}$$

After that, the drift function and diffusion function in differential equation (10) can be computed out completely by means of stochastic averaging method mentioned ahead.

With the knowledge of the Itô Eq. (10), or equivalently, the corresponding F-P-K equation, one obtains the Probability Density Function (PDF) of the averaged amplitude as follows:

$$P(a) = \frac{C}{\sigma^2(a)} \exp\left(\int \frac{2m(a)}{\sigma^2(a)} \mathrm{d}a \right) \tag{17}$$

where a is the state variable for A, and C is a normalization constant.

In the case of combined harmonic and random excitations, the stochastic averaging method was usually used for obtaining the analytic solution of a nonlinear stochastic systems. This case is also investigated in this thesis and the procedure to obtain the exact PDF of the averaged amplitude and phase is more complex. The principle is as follows: first, the amplitude and phase process are approximated as a two-dimensional Markov process, governed by the averaged Itô equations. Then the equivalent stochastic systems of the averaged equations are obtained by using differential forms and exterior differentiation [105, 106]. After that, the exact stationary solutions to the equivalent

systems are obtained. Pertinent and more informations about this procedure can be get in the article of Huang and Zhu [107].

II-2-2- Melnikov's method to predict Smale horseshoe chaos

Melnikov's method [108] is one of relatively few analytical methods used to predict the onset of chaotic motion in dynamical systems with deterministic or random perturbation. It gives a bound on the parameters of a system such that chaos is predicted not to occur. It is applicable to conservative one DOF systems which include a separatrix loop, and which are perturbed by small forcing and damping.

The idea is to show by perturbation expansions that there exists an intersection of the stable and unstable manifolds of an equilibrium point in a two-dimensional Poincare map M. This implies that there is a horseshoe in the map M, which in turn implies that there exist periodic motions of all periods, as well as motions which are not periodic. The horseshoe map also exhibits sensitive dependence on initial conditions. The method was first applied by Holmes [109] to study a periodically forced Duffing oscillator with negative linear stiffness.

To perform the general Melnikov technique for horseshoe chaos analysis, let's Consider a single-degree-of-freedom Hamiltonian system subject to light damping and external or parametric excitation. This system has the following form:

$$\begin{cases} \dot{x} = \frac{\partial H}{\partial y} \\ \\ \dot{y} = -\frac{\partial H}{\partial x} - \varepsilon\lambda\left(x,y\right)\frac{\partial H}{\partial y} + \varepsilon f\left(x,y\right)\eta\left(t\right) \end{cases} \tag{18}$$

where x and y are generalized displacement and velocity respectively; $H = H\left(x,y\right)$ is Hamiltonian with continuous first-order derivatives; ε is a small positive parameter; $\eta\left(t\right)$ is the external perturbation which can be purely periodic excitation or random noise excitation. $\lambda\left(x,y\right)$ represents the coefficient of damping; $f\left(x,y\right)$ represents the amplitude of excitation.

We assume that $\left(x_0\left(t\right), y_0\left(t\right)\right)$ is a solution on the separatrix loop in the $\varepsilon = 0$ system. The separatrix loop in the $\varepsilon = 0$ system will generally be "broken" when the perturbation is applied. The question of whether or not chaos can occur in a particular system depends upon what happens to the broken pieces of the separatrix loop (the stable and unstable manifolds of the saddle), that is, whether they intersect or not. In the case of Eq. (18) and based on a formula given by Wiggins [91], Melnikov's method involves the following integral:

$$M\left(t_0\right) = \int_{-\infty}^{+\infty} \frac{\partial H}{\partial y}\left[-\lambda\left(x,y\right)\frac{\partial H}{\partial y} + f\left(x,y\right)\eta\left(t+t_0\right)\right]\mathrm{d}t \tag{19}$$

where before integrate the previous Eq. (19), the couple (x, y) is substituted by the orbit $(x_0(t), y_0(t))$.

II-2-2-1- Melnikov method for chaos analysis: Deterministic state of the system

When a system (18) is under purely periodic excitation ***(case where $\eta(t)$ is periodic function of time)***, the system is said to respond in a deterministic state. In this case, the deterministic Melnikov method need to be adopt in other to define the condition for the appearance of the so-called transverse intersection points between the perturbed and the unperturbed separatrix, thus identifying possible chaotic response by the Smale-Birkhoff theorem, in a two dimensional vector field [91, 110]. This transverse intersection manifests itself by the fractality on the basin of attraction of the system.

According to the assumption made in this section, $M(t_0)$ in Eq. (19) is a deterministic function which characterizes the size of the gap between the stable and unstable manifolds of the saddle. If $M(t_0)$ vanishes for some t_0 , then the stable and unstable manifolds intersect and system (18) is predicted to contain a horseshoe. If $M(t_0)$ does not vanish for any t_0, then Melnikov's method predicts that there is no intersection of the stable and unstable manifolds, and hence no associated horseshoe or chaos in system (13). All these results assume that ε is a small quantity.

II-2-2-2- Melnikov method for chaos analysis: Stochastic state of the system

When a system (18) is under random noise excitation ***(case where $\eta(t)$ is a random function of time)***, the system is said to respond in a stochastic state. Due to the presence of random noise, the deterministic boundary of the safe region indicated by the invariant manifolds no longer applies. Stochastic analyses of the system response and interpretation from a probabilistic aspect are needed. A generalized stochastic Melnikov method or random Melnikov process can be developed to provide a criterion for the existence of "noisy" chaotic system response. Since $\eta(t)$ is assumed to be random in this case (generally, considered as bounded noise with zero mean), the function $M(t_0)$ in Eq. (18) is now a random process rather than a deterministic function and it can be treated only in some statistical sense. This function measures the random distance between the stable and the unstable manifolds.

First, consider the mean of random Melnikov process (19)

$$\mathrm{E}[M(t_0)] = -\int_{-\infty}^{+\infty} \lambda(x, y) \left(\frac{\partial H}{\partial y}\right)^2 \mathrm{d}t \tag{20}$$

where $\mathrm{E}[.]$ is an expectation operator. Eq. (20) gives a negative constant for positive damping. It implies that in mean sense chaos never occurs in system (18). Next, consider if random Melnikov process (19) has simple zeros in mean-square sense. Let

$$\sigma_d^2 = \mathrm{E}\left[\left\{\int_{-\infty}^{+\infty} \lambda(x,y)\left(\frac{\partial H}{\partial y}\right)^2 \mathrm{d}t\right\}^2\right], \tag{21a}$$

$$\sigma_Z^2 = \mathrm{E}\left[\left\{\int_{-\infty}^{+\infty} f(x,y)\left(\frac{\partial H}{\partial y}\right)\eta(t+t_0)\,\mathrm{d}t\right\}^2\right]. \tag{21b}$$

The integral in Eq. (21a) yields a positive constant since $x = x_0(t)$, $y = y_0(t)$. The integral in Eq. (21b) is a convolution one and it can be rewritten as

$$Z(t_0) = \int_{-\infty}^{+\infty} f(x,y)\left(\frac{\partial H}{\partial y}\right)\eta(t+t_0)\,\mathrm{d}t \quad = \quad h(t) * \eta(t) \tag{22}$$

where $h(t) = f(x,y)\left(\frac{\partial H}{\partial y}\right)\Big|_{x=x_0(t),\ y=y_0(t)}$ can be regarded as the impulse response function of a time-invariant linear system, while $\eta(t)$ is an input of the system. Thus, as the output of the system can be obtained in frequency domain as follows:

$$\sigma_Z^2 = \int_{-\infty}^{+\infty} |\mathrm{H}(\omega)|^2 S_\eta(\omega)\,\mathrm{d}\omega \tag{23}$$

where $\mathrm{H}(\omega)$ is the frequency response function of the system, i.e., the Fourier transformation of $h(t)$, and $S_\eta(\omega)$ is the spectral density of $\eta(t)$. The threshold value for the rising of the chaotic response will depend on the property of the random excitation process, and may deviate from the mean value. Then, the random Melnikov process has simple zeros in a mean-square sense if

$$\sigma_Z^2 = \sigma_d^2 \tag{24}$$

Eq. (24) is the criterion of judging the threshold condition for onset of horseshoes chaos of nonlinear random system.

It is important to remember that the existence of a horseshoe does not imply the existence of a chaotic attractor. Although the horseshoe itself is chaotic, its presence may show up as transient chaos if it coexists with a periodic attractor.

II-2-3- Approximate Solutions for Statistical Moments

To obtain various statistical moments of the response, it is more convenient to work with the Itô-type stochastic differential equations of the form:

$$\mathrm{d}X_i\left(t\right) = m_i\left(\mathrm{X}\right) + \sum_j \sigma_{ij}\left(\mathrm{X}\right)\mathrm{d}B_j\left(\mathrm{X}\right) \tag{25}$$

where $B_j\left(\mathrm{X}\right)$ are known as the Wiener (or Brownian motion) processes, and m_i and σ_{ij} are known as drift and diffusion coefficients, respectively, which can be determined in the same manner as the first and second derivate moments. A vector $X_i(t)$ is supposed to be a diffusional Markov process. The greatest advantage in using stochastic differential Eq. (25) of the Itô-type is the ease with which another Itô equation for an arbitrary scalar function $F(\mathrm{X},\mathrm{t})$ can be obtained:

$$\mathrm{d}F\left(\mathrm{X},t\right) = \left(\frac{\partial F}{\partial t} + \sum_j m_j\frac{\partial F}{\partial X_j} + \frac{1}{2}\sum_j\sum_k\sum_l \sigma_{kl}\sigma_{kl}\frac{\partial^2 F}{\partial X_j \partial X_k}\right)\mathrm{d}t + \sum_j\sum_k \sigma_{jk}\frac{\partial F}{\partial X_j}\mathrm{d}B_k\left(t\right) \tag{26}$$

Eq. (26) is known as the Itô differential rule. The applicability of this rule requires that F is differentiable with respect to t, and twice differentiable with respect to the components of X. For the purpose of obtaining statistical moments, we let $F\left(\mathrm{X},t\right) = X_r^{n_r}X_s^{n_s}...$, where $n_r, n_s...$, are nonnegative integers, and then take ensemble average of the resulting Itô equations.

As an example, consider a two-dimensional Markov vector $\mathrm{X} = \{X_1, X_2\}$. Let $F\left(\mathrm{X},t\right) = X_1^{n_1}X_2^{n_2}$. Application of Itô differential rule yields:

$$\begin{aligned}
&\mathrm{d}\left(X_1^{n_1}X_2^{n_2}\right)\\
&= \left\{n_1 m_1 X_1^{n_1-1}X_2^{n_2} + n_2 m_2 X_1^{n_1}X_2^{n_2-1} + \tfrac{1}{2}\left[n_1\left(n_1-1\right)\sum_l \sigma_{1l}\sigma_{1l}X_1^{n_1-2}X_2^{n_2}\right]\right.\\
&\left.+\tfrac{1}{2}\left[n_2\left(n_2-1\right)\sum_l \sigma_{2l}\sigma_{2l}X_1^{n_1}X_2^{n_2-2} + 2n_1n_2\sum_l\sum_l \sigma_{1l}\sigma_{2l}X_1^{n_1-1}X_2^{n_2-1}\right]\right\}\mathrm{d}t\\
&+\sum_k\left(n_1X_1^{n_1-1}X_2^{n_2}\sigma_{1k} + n_2X_1^{n_1}X_2^{n_2-1}\sigma_{2k}\right)\mathrm{d}B_k\left(t\right)
\end{aligned} \tag{27}$$

Taking ensemble average of Eq. (27), and recognizing that the ensemble average of the last term is zero, we obtain:

$$\begin{aligned}
&\tfrac{\mathrm{d}}{\mathrm{d}t}\mathrm{E}\left[X_1^{n_1}X_2^{n_2}\right]\\
&= n_1\mathrm{E}\left[m_1X_1^{n_1-1}X_2^{n_2}\right] + n_2\mathrm{E}\left[m_2X_1^{n_1}X_2^{n_2-1}\right] + \tfrac{1}{2}n_1\left(n_1-1\right)\mathrm{E}\left[\sum_l \sigma_{1l}\sigma_{1l}X_1^{n_1-2}X_2^{n_2}\right]\\
&+\tfrac{1}{2}n_2\left(n_2-1\right)\mathrm{E}\left[\sum_l \sigma_{2l}\sigma_{2l}X_1^{n_1}X_2^{n_2-2}\right] + n_1n_2\mathrm{E}\left[\sum_l\sum_l \sigma_{1l}\sigma_{2l}X_1^{n_1-1}X_2^{n_2-1}\right]
\end{aligned} \tag{28}$$

A sequence of equations for the statistical moments can be obtained by substituting nonnegative integers for n_1 and n_2. Of course, any X_j with a negative power on the right hand side of Eq. (28) should be replaced by zero. It is clear that this sequence of equations for the statistical moments constitute an infinite hierarchy; therefore, they cannot be solved exactly. Several schemes have been proposed for obtaining approximate solutions, one of which is known as Gaussian closure. In this scheme, higher statistical moments are expressed in terms of the first- and second-order moments, using the same relationships as if they were moments of Gaussian random variables, or equivalently, neglecting those cumulants of X_1 and X_2 of an order higher than the second.

II-2-4- Practical use of the Fourier transform technique associated with residue theory

The Fourier transform is beneficial in differential equations because it can transform them into equations which are easier to solve. The derivative property of Fourier transforms is especially appealing, since it turns a differential operator into a multiplication operator. In many cases this allows us to eliminate the derivatives of one of the independent variables. The resulting problem is usually simpler to solve. Of course, to recover the solution in the original variables, an inverse transform is needed. This is typically the most labor intensive step. Generally, the original solution contains a complex Fourier integral which can compute by using residue theorem and proposition. In complex analysis, the residue theorem sometimes called Cauchy's residue theorem is a powerful tool to evaluate line integrals of *analytic functions* over closed curves; it can often be used to compute real integrals as well. This theorem is expressed as follows:

Theorem [111]
Let C be a simple closed positively oriented path. Suppose that f is analytic inside and on C, except at finitely many isolated singularities $z_1, z_2, ..., z_n$ inside C. Then

$$\int_C f(z)\,\mathrm{d}z = 2\pi i \sum_{j=1}^{n} \mathrm{Res}\,(f, z_j) \tag{29}$$

After this transformation, a search of the poles of f is needed. Hence the following Proposition

Proposition [111]
(i) Suppose that z_0 is an isolated singularity of f. Then f has a simple pole at z_0 if and only if

$$\mathrm{Res}\,(f, z_0) = \lim_{z \to z_0} \{(z - z_0) f(z)\} \neq 0 \tag{30}$$

(ii) If $f(z) = \frac{p(z)}{q(z)}$, where p and q are analytic at z_0, $p(z_0) \neq 0$, and $q(z)$ has a simple zero at z_0, then

$$\mathrm{Res}\left(\frac{p(z)}{q(z)}, z_0\right) = \frac{p(z_0)}{q'(z_0)} \tag{31}$$

Let us look at an example to see how this method is used for differential equations involving a function of only one variable. The well known ODE that governing the harmonic oscillator with single degree of freedom and pulsation ω_0 excited by the Dirac impulse function $\delta(t)$ is considered as example.

$$\ddot{q}(t) + \omega_0^2 q(t) = \delta(t) \tag{32}$$

Many Fourier transformations can be made simply by applying predefined formulas to the Eq. (32). The most used for the ODEs are:

$$\begin{aligned}
&\mathrm{TF}(f(t)) = \int_{-\infty}^{+\infty} f(t)\, e^{-i\omega t} \mathrm{d}t = F(\omega) \\
&\mathrm{TF}^{-1}(F(\omega)) = \tfrac{1}{2\pi} \int_{-\infty}^{+\infty} F(\omega)\, e^{i\omega t} \mathrm{d}\omega = f(t) \\
&\mathrm{TF}\left(f^{(n)}(t)\right) = \int_{-\infty}^{+\infty} f^{(n)}(t)\, e^{-i\omega t} \mathrm{d}t = (i\omega)^n F(\omega), \quad i^2 = -1 \\
&\mathrm{TF}(\delta(t)) = 1
\end{aligned} \tag{33}$$

where TF(.) is the Fourier transform operator. Therefore, the transform of both sides of Eq. (32) can be accomplished using Eq. (33), giving

$$\left(-\omega^2 + \omega_0^2\right) Q(\omega) = 1 \tag{34}$$

This is just an algebraic equation whose solution is

$$Q(\omega) = -\frac{1}{\omega^2 - \omega_0^2} = -\frac{1}{(\omega - \omega_0)(\omega + \omega_0)} \tag{35}$$

We can then recover the original solution $q(t)$ by an inverse transform

$$q(t) = -\frac{1}{2\pi} \int_{-\infty}^{+\infty} \frac{e^{i\omega t}}{(\omega - \omega_0)(\omega + \omega_0)} \mathrm{d}\omega \tag{36}$$

Since that the integrand has two poles located respectively at $\omega = +\omega_0$ and $\omega = -\omega_0$, the residue theorem can be applied and the solution is given as

$$q(t) = -\frac{1}{2\pi} \times 2\pi i \times [\mathrm{Res}(+\omega_0) + \mathrm{Res}(-\omega_0)] = -i \times \left[\frac{e^{i\omega_0 t}}{2\omega_0} + \frac{e^{-i\omega_0 t}}{-2\omega_0}\right] \tag{37}$$

Finally,

$$q(t) = \frac{\sin \omega_0 t}{\omega_0} \tag{38}$$

II-2-5- Stability of the non-trivial steady states solutions of the nonlinear system response

It is well known that the steady states solutions of any nonlinear system only exist if they are stable. Hence the interest to perform a stability analysis of these solutions. To do so, we shall define first what we mean by a steady state solution and how can appreciate their stability. So, formally, we can say that

Definition [112]
The constant vector $Y_0 \in C^n$ is a steady state solution of the system of differential equations

$$\frac{\mathrm{d}Y(t)}{\mathrm{d}t} = F(Y(t)) \tag{39}$$

if it satisfies the equation $F(Y(t)) = \mathbf{0}$, where $\mathbf{0}$ is the null vector and $F(Y(t))$ is a differentiable vector function. When $Y_0 \neq 0$, the steady state solution is non-trivial.

As we have seen, if such a system is required to satisfy the initial condition given by $Y(0) = Y_0$, then its solution will be $Y(t) = Y_0$ for all times t. (So, Y_0 will be a constant solution of the system). What about the stability of this solution? We can get some information about the stability of the solution of the nonlinear systems models by using Taylor's Theorem to "relate" it to a linear system. In fact, the version of Taylor's Theorem which we shall use is the following

Theorem [Taylor's Theorem] [112]
If $F : C^n \to C^n$ is a continuously differentiable function and Y_0 is some constant vector in C^n, then for a vector $\delta Y(t) \in C^n$,

$$F(Y_0 + \delta Y(t)) = F(Y_0) + DF(Y_0) + R(\delta Y(t)) \tag{40}$$

Note that if the function $F(Y) = (f_1(Y), f_2(Y), ..., f_n(Y))$, then DF is the Jacobian

$$DF = \begin{pmatrix} \frac{\partial f_1}{\partial Y_1} & \cdots & \frac{\partial f_1}{\partial Y_n} \\ \vdots & \ddots & \vdots \\ \frac{\partial f_n}{\partial Y_1} & \cdots & \frac{\partial f_n}{\partial Y_n} \end{pmatrix} \tag{41}$$

and the matrix $DF(Y_0)$ is the Jacobian evaluated at Y_0. Further, $R(\delta Y)$ has the property that: $\frac{R(\delta Y)}{\|\delta Y\|} \to 0, \quad as \quad \delta Y \to 0$

Loosely speaking, this means that if each entry of δY is small, then

$$F(Y_0 + h) \simeq F(Y_0) + DF(Y_0) \tag{42}$$

where $\simeq$ can be interpreted as "is approximately".

Now, suppose that Y_0 is a steady state solution of the previous system (39), i.e. $F(Y_0) = 0$, and take $Y(t)$ to be a solution of the system such that $Y(0) - Y_0$ is small. If we now take $Y(t) = Y_0 + \delta Y(t)$, system (39) becomes

$$\frac{\mathrm{d}}{\mathrm{d}t}\left\{Y_0 + \delta Y(t)\right\} = F(Y_0 + \delta Y) \tag{43}$$

Consequently, using Taylor's theorem, we have

$$\frac{\mathrm{d}\delta Y(t)}{\mathrm{d}t} = \frac{\mathrm{d}}{\mathrm{d}t}\left\{Y_0 + \delta Y(t)\right\} = DF(Y_0)\,\delta Y(t) + R(\delta Y(t)), \tag{44}$$

and if $\delta Y(t)$ is small, we can ignore the term $R(\delta Y(t))$. This means that if the quantity $\delta Y(0) = Y(0) - Y_0$ is small, then the behaviour of the vector $\delta Y(t) = Y(t) - Y_0$ is *qualitatively* the same as the solution to the linear system

$$\frac{\mathrm{d}\delta Y(t)}{\mathrm{d}t} = DF(Y_0)\,\delta Y(t) \tag{45}$$

This analysis results in the following theorem:

Theorem [112]
Let the constant vector Y_0 be a steady state solution of the system (39) and let the matrix $DF(Y_0)$ denote the Jacobian evaluated at Y_0.

- If the n eigenvalues of the Jacobian matrix $DF(Y_0)$ have real parts less than zero, then the steady state solution Y_0 is stable.

- If at least one of the n eigenvalues of the Jacobian matrix $DF(Y_0)$ has real part greater than zero, then the steady state solution Y_0 is unstable.

Generally, the determination of the sign of the real parts of the eigenvalues is carried out by using the *Routh-Hurwitz* criterion [103].

This mathematical formalism will be used in the following chapter to analyze the stability of the steady state solutions of the beam responses.

II-3- Approximate response methods for the reduced mathematical bridge models - Numerical techniques

When analytic solutions are not apparent, numerical integration is the only way to obtain information about the trajectory. Many different methods were proposed and used in an attempt to solve accurately various types of the ODEs, SDEs and FDEs. Unfortunately it is seldom that these equations have solutions that can be expressed in closed form, so it

is common to seek approximate solutions by means of numerical methods; nowadays this can usually be achieved very inexpensively to high accuracy and with a reliable bound on the error between the analytical solution and its numerical approximation. In this thesis, four numerical methods including a SRK4 method to integrate the SDEs, a classical RK4 to integrate the ODEs, Newton-Leipnik and A-B-M predictor-corrector schemes to integrate the FDEs and the bisection method to solve a complex or non-trivial polynomial equations are presented.

II-3-1- Stochastic Fourth-order Runge-Kutta method for the stochastic differential equations

SDEs are the differential equations which contain a stochastic process. These type of equations play an important role in physics but existing numerical methods for solving it are of low accuracy and poor stability. The efficient SRK4 scheme [118] developed by Jeremy N. Kasdin is used in this thesis to numerically treat the random process of the systems models.

Consider for simulation the following Itô stochastic differential equation:

$$\begin{cases} \frac{\mathrm{d}X(t)}{\mathrm{d}t} = F\left(t, X\left(t\right)\right) + G\left(t, X\left(t\right)\right)\xi\left(t\right) \\ X\left(t_0\right) = X_0 \end{cases} \tag{46}$$

where $X(t) = (x_1(t), x_2(t), ..., x_n(t))$ is a vectorial variable with $n-$dimensional, $F = (f_1, f_2, ..., f_n)$ and $G = (g_1, g_2, ..., g_n)$ the vectorial flows. $\xi\left(t\right)$ is a random (stochastic) processes. This excitation is parametric (multiplicative) if its accompanying coefficient $G\left(t, X\left(t\right)\right)$ is a function of X. Otherwise, it is external (additive). $\xi\left(t\right)$ can be:
- a white noise defines as [119]:

$$\prec \xi\left(t\right) \succ = 0, \quad \text{and} \quad \prec \xi\left(t\right)\xi\left(t'\right) \succ = 2\delta\left(t - t'\right); \tag{47}$$

- a colored (Ornstein-Uhlenbeck) noise defines as [119]:

$$\prec \xi\left(t\right) \succ = 0, \quad \text{and} \quad \prec \xi\left(t\right)\xi\left(t'\right) \succ = \frac{1}{2\,\tau}\, e^{-\frac{|t - t'|}{\tau}}; \tag{48}$$

- a bounded noise which is a harmonic function with constant amplitude and random phase defines as [119]:

$$\begin{gathered} \prec \xi\left(t\right) \succ = 0, \quad \prec \xi\left(t\right)\xi\left(t'\right) \succ = \frac{\sigma^2}{2}\, \exp\left(-\frac{\gamma^2|t - t'|}{2}\right)\, \cos\Omega\left(t - t'\right), \\ \xi\left(t\right) = \sigma\cos\left(\Omega t + \gamma B\left(t\right) + \Gamma\right) \end{gathered} \tag{49}$$

where σ and γ are positive constants, $B(t)$ is a standard Wiener process, Γ is a random variable uniformly distribution in $[0, 2\pi]$. The brackets $\prec ... \succ$ denote the time average.

Let us consider the SDE gives by Eq. (46) and assuming that $\xi(t)$ is a bounded noise (since that it is the type of noise used in our work) defined as shown in (49). Introducing a new variable $Z(t)$, the system (46) can be rewritten as

$$\begin{cases} \frac{\mathrm{d}X(t)}{\mathrm{d}t} = F\left(t, X\left(t\right)\right) + \sigma G\left(t, X\left(t\right)\right)\cos\left(Z\left(t\right)\right) \\ \frac{\mathrm{d}Z(t)}{\mathrm{d}t} = \Omega + \gamma\zeta\left(t\right) \\ X\left(t_0\right) = X_0 \\ Z\left(t_0\right) = Z_0 \end{cases} \tag{50}$$

The SRK solution for k , X_k and Z_k is given by the following set of equations:

$$\begin{aligned} &x_{0,j} = X_0 \\ &z_{0,j} = Z_0 \\ &x_{k+1,j} = x_{k,j} + \alpha_1 K_{1,j} + \alpha_2 K_{2,j} + \alpha_3 K_{3,j} + \alpha_4 K_{4,j} \\ &z_{k+1,j} = z_{k,j} + \alpha_1 M_{1,j} + \alpha_2 M_{2,j} + \alpha_3 M_{3,j} + \alpha_4 M_{4,j} \\ &\\ &K_{1,j} = \left[f_j\left(t_k, x_{k,j}\right) + \sigma\cos\left(z_{k,j}\right) g_j\left(t_k, x_{k,j}\right)\right]\Delta t \\ &M_{1,j} = \Omega\Delta t + \zeta_1 \\ &\\ &K_{i,j} = \left[f_j\left(t_k + c_i\Delta t, x_{k,j} + A_{i,j}\right) + \sigma\cos\left(z_{k,j} + B_{i,j}\right) g_j\left(t_k + c_i\Delta t, x_{k,j} + A_{i,j}\right)\right]\Delta t \\ &M_{i,j} = \Omega\,\Delta t + \zeta_i \end{aligned} \tag{51}$$

where

$$\begin{aligned} &A_{i,j} = \sum_{n=1}^{i-1} a_{in} K_{n,j},\ B_{i,j} = \sum_{n=1}^{i-1} a_{in} M_{n,j},\ \zeta_1 = r_1\sqrt{2q_1\gamma\Delta t},\ \zeta_i = r_i\sqrt{2q_i\gamma\Delta t}, \\ &c_2 = a_{21},\ \ c_3 = a_{31} + a_{32},\ \ c_4 = a_{41} + a_{42} + a_{43};\ \ i = 2,\, 3,\, 4 \end{aligned} \tag{52}$$

Here, r_m (m = *1,...,4*) are the Gaussian white noise from random numbers y_p (p = *1,...,8*) generated by using the Box-Mueller algorithm as [120].

$$r_m = \sqrt{-2\log\left(y_p\right)}\cos\left(2\pi y_p\right) \tag{53}$$

The coefficients (see Table I) α_i, q_i and a_{in} are chosen in the deterministic case to ensure that $x_{k,j}$ and $z_{k,j}$ simulate the solution $X(t)$ and $Z(t)$ with error of order Δt^5. That is,

$$x_j(t_k) = x_{k,j} + O\left(\Delta t^5\right),\ \ z_j(t_k) = z_{k,j} + O\left(\Delta t^5\right) \tag{54}$$

These coefficients are given in Table I.

This method will be used in the next chapter to approach numerically the reduced nonlinear SDEs of our mathematical models in order to check the validity of the results obtained by the mathematical formalism.

Table I: *Coefficients of the SRK4 method* [118]

Coefficient	Value	Coefficient	Value
α_1	0.25001352164789	a_{41}	-2.32428921184321
α_2	0.67428574806272	a_{42}	2.69723745129487
α_3	-0.00831795169360	a_{43}	0.29093673271592
α_4	0.08401868181222	q_1	3.99956364361748
a_{21}	0.66667754298442	q_2	1.64524970733585
a_{31}	0.63493935027993	q_3	1.59330355118722
a_{32}	0.00342761715422	q_4	0.26330006501868

II-3-2- Fourth-order Runge-Kutta method for ordinary differential equations

Runge-Kutta methods are among the most popular ODEs solver. It was first studied by Carle Runge and Martin W. Kutta around 1900. Their modern developments are mostly due to John Butcher in the 1960s. Generally, we distinguish 04 important families of Runge-Kutta methods: Second-order, Fourth-order, Five-order and Six-order Runge-Kutta Methods. But the most used method is the Fourth-order one since that it is easy to use and no equations need to be solved at each stage, highly accurate for moderate values of the normalization integration time step and easy to code.

Let us consider the same problem given in Eq. (46) but by taking $\xi(t) = 0$

$$\begin{cases} \frac{\mathrm{d}X(t)}{\mathrm{d}t} = F(t, X(t)) \\ X(t_0) = X_0 \end{cases} \tag{55}$$

Define h to be the time step size and $t_i = t_0 + ih$. Then the classical RK4 flow for this problem is given by [113]:

$$\begin{aligned} &x_{0,j} = X_0 \\ &L_{1,J} = hf_j(t_i, x_{i,j}) \\ &L_{2,J} = hf_j\left(t_i + \tfrac{h}{2}, x_{i,j} + \tfrac{L_{1,j}}{2}\right) \\ &L_{3,J} = hf_j\left(t_i + \tfrac{h}{2}, x_{i,j} + \tfrac{L_{2,j}}{2}\right) \\ &L_{4,J} = hf_j(t_i + h, x_{i,j} + L_{3,j}) \\ &x_{i+1,j} = x_{i,j} + \tfrac{1}{6}(L_{1,j} + 2L_{2,j} + 2L_{3,j} + L_{4,j}) \end{aligned} \tag{56}$$

where i runs for time incrementation and j labels the variables related to x_j. $L_{1,j}$, $L_{2,j}$, $L_{3,j}$, $L_{4,j}$ are intermediate coefficients.

This method will be used in the following chapter in order to solve a first moment and second moment equations that will permit to get the probabilistic features such as the expected and variance values of one of our system model response.

II-3-3- Numerical methods for fractional differential equations

To solve a fractional differential equation, one has to approximate the corresponding derivative operator, which means including information about previous states of the system (the so-called *memory effect*). For numerical solutions of the FDEs, the Newton-Leipnik and A-B-M predictor-corrector schemes [114–117] are the most used. Accordingly, particular attention will be put on these two numerical methods in this section.

Firstly, a method on the basis of the A-B-M type predictor-corrector scheme is suitable for Caputo's fractional order derivative because it just requires the initial conditions and for unknown function it has clear physical meaning. The method is based on the fact that fractional differential equation

$$\begin{cases} D_t^q Y(t) = \frac{\mathrm{d}^q Y(t)}{\mathrm{d}t^q} = F(t, Y(t)) \\ Y^{(k)}(0) = Y_0^{(k)}, \ k = 0, 1, ..., m-1 \end{cases} \tag{57}$$

is equivalent to the Volterra integral equation

$$Y(t) = \sum_{k=0}^{[q]-1} Y_0^{(k)} \frac{t^k}{k!} + \frac{1}{\Gamma(q)} \int_0^t (t-\tau)^{q-1} F(\tau, Y(\tau)) \, \mathrm{d}\tau \tag{58}$$

Discretizing the Volterra equation Eq. (58) for uniform grid $t_n = nh \quad (n = 0, 1, ..., N)$, $h = Tsim/N$ and using the short memory principle (fixed or logarithmic) [114, 121], we obtain a close numerical approximation of the true solution $Y(t_n)$ of fractional differential equation while preserving the order of accuracy. Assume that we have calculated approximations $Y_h(t_j), j = 1, 2, ..., n$ and we want to obtain $Y_h(t_{n+1})$ by means of the equation

$$\begin{aligned} Y_h(t_{n+1}) = \sum_{k=0}^{m-1} Y_0^{(k)} \frac{t_{n+1}^k}{k!} + \frac{h^q}{\Gamma(q+2)} F[t_{n+1}, Y_h^p(t_{n+1})] + \\ \frac{h^q}{\Gamma(q+2)} \sum_{j=0}^{n} a_{j,n+1} F[t_j, Y_n(t_j)] \end{aligned} \tag{59}$$

where

$$a_{j,n+1} = \begin{cases} n^{q+1} - (n-q)(n+1)^q, & \text{if } j = 0, \\ (n-j+2)^{q+1} + (n-j)^{q+1} + 2(n-j+1)^{q+1}, & \text{if } 1 \le j \le n, \\ 1, & \text{if } j = n+1. \end{cases} \tag{60}$$

The preliminary approximation $Y_h^p(t_{n+1})$ is called predictor and it is given by

$$Y_h^p(t_{n+1}) = \sum_{k=0}^{m-1} Y_0^{(k)} \frac{t_{n+1}^k}{k!} + \frac{1}{\Gamma(q)} \sum_{j=0}^{n} b_{j,n+1} F[t_j, Y_n(t_j)] \tag{61}$$

where

$$b_{j,n+1} = \frac{h^p}{q} \left[(n+1-j)^q - (n-j)^q \right] \tag{62}$$

Secondly, a method on the basis of the Newton-Leipnik algorithm is suitable for Grünwald-Letnikov fractional order derivative. This approach is based on the fact that for a wide class of functions, three definitions - Grünwald-Letnikov, Riemman-Liouville and Caputo's are equivalent. In this case, the relation to the explicit numerical approximation of qth derivative at the points $kh, (k = 1, 2, ...)$ has the following form [121]:

$$_{k-L_m/h}D^q_{t_k} f(t) \approx h^{-q} \sum_{j=0}^{k} (-1)^j \begin{pmatrix} q \\ j \end{pmatrix} f(t_{k-j}) \tag{63}$$

where L_m is the "memory length", $t_k = kh$, h is the time step of calculation and $(-1)^j \begin{pmatrix} q \\ j \end{pmatrix}$ are binomial coefficients $c_j^{(q)}$ $(j = 0, 1, ...)$. For their calculation we can use the following expression

$$c_0^{(q)} = 1, \qquad c_j^{(q)} = \left(1 - \frac{1+q}{j}\right) c_{j-1}^{(q)} \tag{64}$$

According to the short memory principle [114, 121], the length of system memory can be substantially reduced in the numerical algorithm to get reliable results. Therefore, general numerical solution of the following fractional differential equation

$$_aD^q_t Y(t) = F(t, X(t)), \tag{65}$$

can be expressed as

$$Y(t_k) = F(t_k, Y(t_k)) h^q - \sum_{j=1}^{k} c_j^{(q)} Y(t_{k-j}) \tag{66}$$

In Eq. (66), the memory term is expressed by the sum. As shown in paper [122], both mentioned time-domain numerical methods (Newton-Lepnik and A-B-M) have approximately the same order of accuracy and good match of numerical solutions. Since that the last one method is easy to code, we will used it in the following chapter to approximate the numerical solutions of the FDEs decribing our reduced systems models.

II-3-4- Bisection method for a complex polynomial equations

Bisection method is the simplest among all the numerical schemes to solve the complex polynomial equations. The method is also called the interval halving method, the binary search method, or the dichotomy method. The bisection method is based on the following result from calculus:

The Intermediate Value Theorem:

Assume $f : R \to R$ is a continuous function and there are two real numbers a and b such that $f(a)f(b) < 0$. Then $f(x)$ has at least one zero between a and b.

In other words, if a continuous function has different signs at two points, it has to go through zero somewhere in between!

The bisection method consists of finding two such numbers a and b, then halving the interval $[a, b]$ and keeping the half on which $f(x)$ changes sign and repeating the procedure until this interval shrinks to give the required accuracy for the root. An algorithm of this method could be defined as follows. Suppose we need a root for $f(x) = 0$ and we have an error tolerance of ϵ (the absolute error in calculating the root must be less that ϵ).

Bisection Algorithm:

Step 1: Find two numbers a and b at which f has different signs.

Step 2: Define $c = \frac{a+b}{2}$.

Step 3: If $b - c \leq \epsilon$ then accept c as the root and stop.

Step 4: If $f(a)f(c) \leq 0$ then set c as the new b. Otherwise, set c as the new a. Return to **Step 1**

Let α be the value of the root, $a \leq \alpha \leq b$. Let a_n, b_n and c_n be the values of a, b and c on the nth iteration of the algorithm. Then the error bound for c_n is given by

$$|\alpha - c_n| \leq \frac{1}{2^n}(b - a) \tag{67}$$

This inequality can give us the number of iterations needed for a required accuracy ϵ

$$n \geq \frac{\log\left(\frac{b-a}{\epsilon}\right)}{\log(2)} \tag{68}$$

Advantages and disadvantages of the bisection method

- The method is guaranteed to converge
- The error bound decreases by half with each iteration
- The bisection method converges very slowly
- The bisection method cannot detect multiple roots

This method will be used in the next chapter in order to get the non-trivial steady states solutions of some nonlinear Amplitude-Frequency equations governing one of our systems models response.

II-4- Hardware and software

During the course of this work, we used a Laptop computer having the following performances (Operating system: Windows 8.1 single language 64-bit(6.3, Build 9600), Processor: Intel(R)Core(TM)i3-3110M CPU @2.40GHz(4CPUs), ˜2.4GHz, Memory: 4096MB RAM) and four major software's: Fortran for differential equations, Matlab for data analysis, Maple and Mathematica for integral calculus.

II-5- Conclusion

In this chapter, we have presented some analytical and numerical methods used to solve the differential equations describing the reduced mathematical models of our excited bridge systems as well as the hardware and software used. These methods will be used in the next chapter to: obtain the analytical solutions of the ODEs, SDEs and FDEs describing the mathematical models of our systems; analyse the stability of these solutions; find the behavior of small amplitudes vibrations; obtain time histories, phase diagram, amplitudes diagrams, Probability distribution diagram and basin of attraction diagram.

Chapter III

Dynamical behaviors of various models of bridge subjected to loads dynamics: main results and their discussion

III-1- Introduction

Vibration of the bridges subjected to loads dynamics is of great theoretical and practical significance in structural engineering. Vibrations connected with this issue occur for example in the roadways or railways loaded by traffic. Frýba [31] and Ouyang [123] are addressed a variety of engineering problems concerning this subject.

Our aim in this chapter is to extend the work done by others researchers by proposing the solutions to some of the limits encountered in this field of research which are identified and listed in chapter I (for example, when the beam is loaded by stochastically moving loads, the problem is more complicated and, generally, only numerical methods allow to retrieve the resulting vibrations [88]. In almost all the research concerning the dynamic of the cable-stayed bridge under the action of moving vehicles, only the effect of vehicle parameters on the DAF of the system response was presented. Also, due to the complexity of the cable-stayed bridge structure, only the finite-element analysis for the VBI system was generally pointed out to find the effect of the number of stay cables on the system response. The bearings often exist at the supports of bridge girders for load transference to the foundation or for earthquakes load isolator and always use as elastic structure may result in amplification of the response of the bridge during the passage of a train [82].). We address these issues with a joint analytical and numerical analysis that permit to give an estimate of the system behavior. The chapter is organized as follows. In Section III-2-, we present and discuss our main results concerning the dynamic response analysis of various models of bridge as structure subjected to vehicles modelled as random moving loads [125–127]. In Section III-3-, we first present a fractional order derivative rheological models of the damping of the track structure and of the bearings devices; thereafter we present and discuss our main results concerning the dynamic analysis of railway track and bridge-bearings systems supporting a sequence of equidistant moving loads and stochastic wind load [128, 129]. The last section III-4- summarizes our results and concludes the chapter.

III-2- Mathematical modeling and dynamic analysis of various models of bridge subjected to randomly moving loads

This Section is devoted to the presentation and discussion of the main results come from the study of three type of bridges submitted to vehicles. Here a bridge deck is modelled by using the Rayleigh beam theory [124] or the thin rectangular plate theory [145] and the vehicles by the series of random forces moving over the bridge deck with stochastic velocities. The first model (subsection III-2-1-) presented in this section describes well the

dynamic of the girder bridges under moving vehicles; the second model (subsectionIII-2-2-), the dynamic of a model of cable-stayed bridge under the action of moving vehicles and the last one, the analysis of the two lane slab-type bridges under the moving vehicles (subsectionIII-2-3-).

III-2-1- Amplitude stochastic response of Rayleigh beams to randomly moving loads

III-2-1-1- Description of the physical system and mathematical formalism

Let us consider a beam of finite length L, that is a nonlinear elastic structure. In particular, our attention is paid to the geometric nonlinearities described due to the Euler-Bernoulli law, that states that the bending moment of the beam is proportional to the change in the curvature produced by the load [130–132]. To take into account the high frequency motion of the beam, a Rayleigh beam correction (up to the second order of the bending angle) [124] is used to refine the theory of Euler-Bernoulli beam for high frequency motion. When the governing equation for the vertical displacement of the beam incorporates the Rayleigh term into the analysis, the correction affects the summing moments produced in the simple Euler-Bernoulli theory.

Vibrations of the beam are caused by a set of point forces of constant amplitudes P, the inter-arrival times are different, deterministic variables t_i and the forces are moving along the beam with stochastic velocities v_i (see Fig. 4).

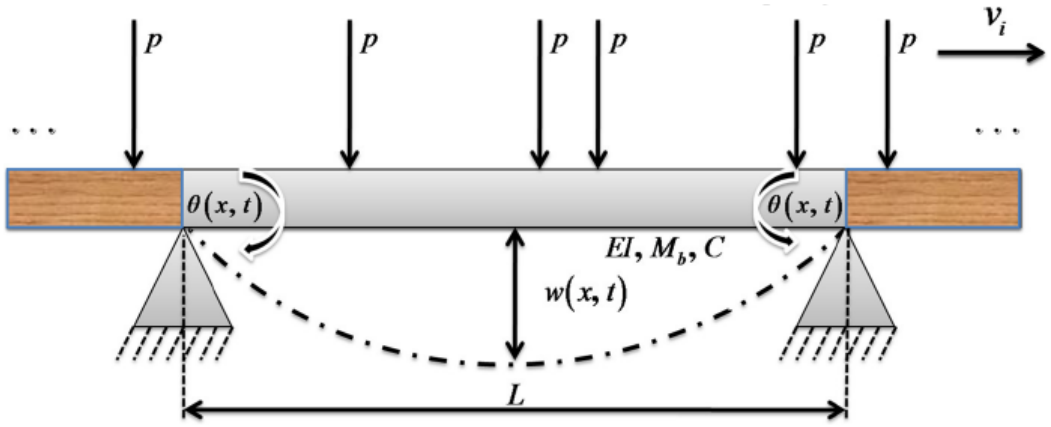

Figure 4: *Sketch of a beam under stochastic moving loads. The gravitational forces are represented by arrows P, whose separations are not uniform, for the speeds v_i are not identical.*

Considering the classical viscous damping for the viscosity materials and Newton second law of motion, for an infinitesimal element of the beam, the equation of motion for the small deformations: $\theta(x,t) \approx \partial w(x,t)/\partial x$ (here $w(x,t)$ is the transverse defection of the beam at point x and time t) is obtained as [124, 132] (from the derivation of this equation (see AppendixIII-4-))

$$M_b \frac{\partial^2 w(x,t)}{\partial t^2} - R_a \frac{\partial^4 w(x,t)}{\partial t^2 \partial x^2} + C \frac{\partial w(x,t)}{\partial t} + EI \frac{\partial^2}{\partial x^2} \left[\frac{\partial^2 w(x,t)}{\partial x^2} \left(1 - \frac{3}{2} \left(\frac{\partial w(x,t)}{\partial x} \right)^2 \right) \right] = P \sum_{i=1}^{N_v} \varepsilon_i \delta \left[x - x_i(t - t_i) \right] \tag{69}$$

with the boundary and initial conditions

$$\begin{aligned} & w\left(x,t\right)\big|_{x=0,L} = 0, \quad \frac{\partial^2 w(x,t)}{\partial x^2}\Big|_{x=0,L} = 0. \\ & w\left(x,t\right)\big|_{t=0} = 0 \ , \ \frac{\partial w(x,t)}{\partial t}\Big|_{t=0} = 0. \end{aligned} \tag{70}$$

Here EI denotes the flexural rigidity of the beam, M_b the beam mass per unit length, C the damping coefficient, R_a the transverse Rayleigh beam coefficient and $\delta[...]$ the Dirac delta function. The position of the i^{th} force at the time t reads $x_i\left(t - t_i\right)$, where $t_i = (i-1)d/v_0$ is the deterministic arriving time of the i^{th} load at the beam. The average spacing loads is d, v_0 the average speed of the moving loads, and N_v the number of the applied loads. In Eq. (69), $M_b \frac{\partial^2 w(x,t)}{\partial t^2}$ represents the inertia force of the beam per unit length, $R_a \frac{\partial^4 w(x,t)}{\partial x^2 \partial t^2}$ is the rotary inertia force of the beam element (per unit length), $C \frac{\partial w(x,t)}{\partial t}$ is the damping force of the beam per unit length, $EI \frac{\partial^2}{\partial x^2} \left[\frac{\partial^2 w(x,t)}{\partial x^2} \left(1 - \frac{3}{2} \left(\frac{\partial w(x,t)}{\partial x} \right)^2 \right) \right]$ is the nonlinear rigidity of beam essentially due to the Euler law [130–132]. This nonlinear term is obtained by using the Taylor expansion of the exact formulation of the curvature up to the second order. To facilitate a compact representation of the equations, a window function ε_i is employed [62]: $\varepsilon_i = 0$ when the load has left the beam and $\varepsilon_i = 1$ while the load is crossing the beam.

A more realistic and useful model of highway traffic loads takes into account random arrival times, in the form, for examples, of Poisson process [3, 4] or renewal counting process [5], to represent the vehicular traffic fluctuations. Load fluctuations are thus assumed to be a set of point forces of constant amplitudes whose inter-arrival times are different, for the forces are moving with stochastic velocities. Thus, let us consider that the velocities $v_i(t - t_i)$ are Gaussian distributed around the average speed v_0 [15]. These velocities are a function of the difference between the time t and the instant at which the vehicles enter the bridge, t_i

$$\begin{aligned} & \frac{dx_i(t-t_i)}{dt} = v_i(t - t_i) = v_0 + \sigma_v \xi_i(t - t_i), \\ & 0 \leq x_i(t - t_i) \leq L. \end{aligned} \tag{71}$$

Here $v_i(t - t_i)$ is the stochastic velocity of the i^{th} force, σ_v its standard deviation and $\xi_i(t - t_i)$ the velocity disturbances which it is assumed to be independent and stationary

white noise random processes; i.e.

$$\langle v_i(t-t_i)\rangle = v_0\,, \quad \langle \xi_i(t-t_i)\rangle = 0,$$

$$\langle \xi_i(t-t_i)\xi_j(t-t_i)\rangle = 0 \quad \text{for} \quad i \neq j, \tag{72}$$

$$\langle \xi_i(t-t_i)\xi_i(t-t_i+\zeta)\rangle = \ \gamma_v^2\delta(\zeta).$$

The brackets $\langle ... \rangle$ denote the time average and $\gamma_v = v_0\sigma_v$.

In the presence of the stochastic term there is a finite probability that the fluctuations produce a negative velocity, that become sizeable when fluctuations σ_v are comparable with the average speed v_0. We do not exclude such negative velocities, that we interpret as a vehicle moving in the opposite direction, thus assuming that the beam represents in fact a two-way bridge.

If one takes into account the boundary conditions given by Eq. (70) , the transversal deflection $w(x,t)$ for the simply supported beam can be represented in a series form as

$$w\,(x,t) = \sum_{n=1}^{\infty} q_n\,(t) \sin\left(\frac{n\pi x}{L}\right) \tag{73}$$

Here, $q_n\,(t)$ is the amplitude of the nth mode, and $\sin\,(n\pi x/L)$ is the solution of the eigen value problem, that depends on the boundary conditions of the free oscillations of the beam. It is convenient to adopt the following dimensionless variables:

$$\chi_n = \frac{q_n}{r} \ , \ \tau = \frac{\tilde{v}t}{L} \ , \ v = \frac{v_0}{\tilde{v}} \tag{74}$$

The equivalent stochastic dimensionless modal equation is obtained substituting Eq. (71) and Eq. (73) into Eq. (69), taking into account the dimensionless variables given in Eq. (74) and considering the first mode only. We have limited the analysis to the first mode, inasmuch the first mode of vibrations is expected to carry most of the energy, and therefore one hopes that it could suffice to obtain a first estimate of the system behavior. If we indicate with $W_i(\tau-\tau_i)$ a unit Wiener stochastic process:

$$\ddot{\chi}(\tau) + \lambda\dot{\chi}(\tau) + \chi(\tau) + \beta\chi^3(\tau) = \mathit{\Gamma}\sum_{i=1}^{N_v} \varepsilon_i \sin\left[\Omega\tau + \gamma W_i\,(\tau-\tau_i)\right] \tag{75}$$

with

$$\begin{array}{l} \Omega = \frac{\pi v_0}{\tilde{v}}\,, \ \ \mathit{\Gamma} = \frac{2PL^3}{rEI\pi^4} \ \ , \ \ \beta = -\frac{3}{8}\left(\frac{\pi r}{L}\right)^2\,, \ \ \lambda = \frac{CL^3}{\pi^2\sqrt{EI(L^2M_b+R_a\pi^2)}} \\ R_a = M_b r^2\ , \ \ \tilde{v} = \pi^2\sqrt{\frac{EI}{L^2M_b+R_a\pi^2}}\ , \ \ r = \sqrt{\frac{I}{S}}\ , \quad \gamma = \pi\sigma_v\ , \quad \tau_i = \frac{\tilde{v}t_i}{L}. \end{array} \tag{76}$$

The ansatz (73) of the modal analysis is but the simplest method to deal with this intrinsically nonlinear problem, for the nonlinear terms of Eq. (69) only results in the

cubic nonlinearity of Eq. (75). However, the method is capable both to retain (to a limited and approximated extent) the essential nonlinearity of the full partial differential equation, and at the same time allow for an analytical treatment, as we shall see in the following. Also, the roughness of the method calls for detailed numerical simulations to validate the analysis. As we shall see in the following, numerical simulations support the usefulness of the method.

Eq. (75) amounts to a stochastic Duffing oscillator which describes the unbounded or catastrophic motion of the beam. The catastrophic behavior of the beam is related to the configuration of the potential of the system, as described in details in Ref. [133]

III-2-1-2- Analytical investigation of the system response

It has been shown by Iwankiewicz and Śniady [36] that the influence of the free vibration ($\varepsilon_i = 0$) on the probabilistic characteristics of the structure response is negligibly small when the speed of the moving forces is below 130.0 km/h (about 36.0 m/s). Therefore, for simplicity, it is assumed in the first case ($\varepsilon_i = 0$) that the dynamic response function is equal to zero ($\chi(\tau) = 0$) and for the second case ($\varepsilon_i = 1$) the response function is calculated from the equation (considering the case of a single moving load):

$$\ddot{\chi}(\tau) + \lambda\dot{\chi}(\tau) + \chi(\tau) + \beta\chi^3(\tau) = \Gamma \sin\left[\Omega\tau + \gamma W(\tau)\right] \tag{77}$$

It is observed that the right hand side of Eq.(77) is a harmonic function with constant amplitude and random phases (mathematically equivalent to frequency fluctuations of a nonmonochromatic drive [134]), and therefore it amounts to a bounded or sine-Wiener noise $\eta(\tau)$ [135] , whose covariance is given by

$$C_\eta(\tau, \tau') = \langle \eta(\tau)\eta(\tau') \rangle = \frac{\Gamma^2}{2} \exp\left(-\frac{\gamma^2|\tau - \tau'|}{2}\right) \cos\Omega(\tau - \tau'). \tag{78}$$

The response of the stochastic Eq. (77) is obtained using the Fourier transform associated with the residues theorem (where the background has been given in detail in chapter II) [136], as will be shown in the following.

(a) - Root mean square displacement of the beam

The equivalent linearization of Eq.(77) is

$$\ddot{\chi}(\tau) + \lambda\dot{\chi}(\tau) + \omega^2\chi(\tau) = \eta(\tau) \tag{79}$$

where

$$\omega^2 = 1 + \frac{3}{4}\beta A^2, \tag{80a}$$

$$\eta(\tau) = \Gamma \sin\left[\Omega\tau + \gamma W(\tau)\right] \tag{80b}$$

and A is the root mean square displacement. The solution of Eq. (79) in Fourier space reads

$$\chi(\omega') = \frac{\eta(\omega')}{\omega^2 - \omega'^2 + i\lambda\omega'} \tag{81}$$

From Eq. (78), one have

$$\langle \eta(\omega')\, \eta(\omega'') \rangle = \delta\left(\omega' + \omega''\right) S_\eta(\omega') \tag{82}$$

where $S_\eta(\omega')$ is the spectral density of the noise $\eta(\tau)$ defined by

$$S_\eta(\omega') = \frac{(\Gamma\gamma)^2}{2\pi}\left[\frac{1}{4(\omega' - \Omega)^2 + \gamma^4} + \frac{1}{4(\omega' + \Omega)^2 + \gamma^4}\right] \tag{83}$$

Hence,

$$\begin{aligned} \langle \chi(\omega')\chi(\omega'') \rangle &= \frac{\langle \eta(\omega')\eta(\omega'') \rangle}{\left(\omega^2 - \omega'^2 + i\lambda\omega'\right)\left(\omega^2 - \omega''^2 + i\lambda\omega''\right)} \\ &= \frac{\delta\left(\omega' + \omega''\right)\ S_\eta(\omega')}{\left(\omega^2 - \omega'^2 + i\lambda\omega'\right)\left(\omega^2 - \omega''^2 + i\lambda\omega''\right)} \end{aligned} \tag{84}$$

The mean square amplitude can be calculated as

$$A^2 = \langle \chi^2(\tau) \rangle \tag{85}$$

It follows from the above definitions that:

$$\begin{aligned} A^2 &= \int \tfrac{\mathrm{d}\omega_1}{2\pi}\tfrac{\mathrm{d}\omega_2}{2\pi} \prec \chi(\omega_1)\chi(\omega_2) \succ e^{i(\omega_1+\omega_2)\tau} \\ &= \int \tfrac{\mathrm{d}\omega_1}{2\pi}\tfrac{\mathrm{d}\omega_2}{2\pi} \frac{\delta(\omega_1+\omega_2) S_\eta(\omega_1) e^{i(\omega_1+\omega_2)\tau}}{\left(\omega^2 - \omega_1^2 + i\lambda\omega_1\right)\left(\omega^2 - \omega_2^2 + i\lambda\omega_2\right)} \\ &= \frac{(\Gamma\gamma)^2}{2\pi} \int \tfrac{\mathrm{d}\omega_1}{2\pi} \frac{2\gamma^4 + 8\left(\omega_1^2 + \Omega^2\right)}{\left[4(\omega_1 - \Omega)^2 + \gamma^4\right]\left[4(\omega_1 + \Omega)^2 + \gamma^4\right]\left[\left(\omega^2 - \omega_1^2\right)^2 + \lambda^2\omega_1^2\right]} \\ &= \frac{(\Gamma\gamma)^2}{4\pi\lambda} \cdot \frac{\left[\gamma^4 + 4\left(\omega^2 + (\lambda - \Omega)^2\right)\right]}{\omega^2\left[\gamma^8 + 16(\omega^2 + (\lambda-\Omega)\Omega)^2 + 4\gamma^4(\lambda^2 + 2(\omega^2 + \Omega^2 - \lambda\Omega))\right]} \end{aligned} \tag{86}$$

This is the main result of this part: the dependence of the oscillations amplitude upon the beam parameters (damping λ, natural frequency $\omega_0 = 1$ and nonlinear component β) and of the loads traffic (loads weights intensity Γ, average velocity Ω, and velocity fluctuation intensity γ). In fact substituting Eq. (80a) into Eq. (86), the amplitude can be found from the roots of

$$\Theta_4 A^8 + \Theta_3 A^6 + \Theta_2 A^4 + \Theta_1 A^2 = \Theta_0 \tag{87}$$

with

$$\Theta_0 = \Gamma^2 \left[\gamma^6 + 4\gamma^2 \left(1 + (\lambda - \Omega)^2\right)\right] \tag{88a}$$

$$\Theta_1 = 4\pi\lambda \left[\gamma^8 + 4\left(\lambda^2 + 2\left(1 + \Omega^2 - \lambda\Omega\right)\right)\gamma^4 - \frac{3\beta\Gamma^2}{4\pi\lambda}\gamma^2\right] + 64\pi\lambda\Omega\left[2\lambda + \Omega\left(\Omega^2 + \lambda^2 - 2 - 2\lambda\Omega\right)\right] \tag{88b}$$

$$\Theta_2 = 3\lambda\pi\beta\left[\gamma^8 + 4\left(4 + \lambda^2 + 2\Omega\left(\Omega - \lambda\right)\right)\gamma^4\right] + 48\lambda\pi\beta\left[3 + \Omega^4 + \Omega\left(\Omega\lambda^2 - 2\lambda\Omega^2 + 4\left(\lambda - \Omega\right)\right)\right] \tag{88c}$$

$$\Theta_3 = 18\lambda\pi\beta^2\left[\gamma^4 + 6 + 4\Omega\left(\lambda - \Omega\right)\right] \tag{88d}$$

$$\Theta_4 = 27\lambda\pi\beta^3 \tag{88e}$$

III-2-1-3- Numerical investigation of the system response

To check the validity of the analytical estimates, we have compared some analytical results with numerical simulations. But before that, the random process of the nonlinear Eq. (77) is numerically treated according to the SRK4 algorithm developed by Kasdin [118] and well described in the previous chapter.

The physical parameters of the beam and moving loads used for this first model are given in Table II

Table II: *Properties of the Beam and Moving loads* [16]

Item	Notation	Value
Beam		
Length	L	34.0 m
Young's modulus (steel)	E	3.0×10^{10} N/m^2
Cross-sectional area	S	0.02 m^2
Mass per unit length	M_b	11400.0 kg/m
Moment of inertia	I	3.07 m^4
Beam viscosity	C	350.5 N.S/m
Moving loads		
Load	P	350.0 kN
Mean velocity	v_0	30.0 m/s

The mean response of the amplitude of the oscillators, as estimated with the modal equations method, Eq. (87), compared with numerical simulations of Eq. (75) obtained through the stochastic RK algorithm is displayed in Fig. 5(a). The Figure demonstrates that there is a resonant velocity $v \simeq 0.32$ where the amplitude of the oscillations increases, in both the theoretical prediction and the numerical simulations.

The analysis of a single load cannot be extended to the multiple vehicles case described by Eq.(75), inasmuch the superposition principle of a linear system is not established for

the nonlinear dynamics system (75). As the present analysis cannot be rigorously extended to multiple load cases, the limits of validity of the extension can only be numerically verified, as shown in Fig. 5(b). In the Figure it is observed that the resonance is made more pronounced by the increase of the number of loads N_v. Another interesting feature of Fig. 5(b) is the reentrant behavior. For some values below the resonant velocity $v = 0.32$ there are as many as three different amplitudes that correspond to the same speed. It is interesting to notice that the peculiar behavior is observed in both the analytical treatment for the noise value $\gamma = 0.1$, see Fig. 5(a). At this level fluctuations are comparable with the resonant speed $v_0 = 0.32$ in Fig. 5(a). Physically, it corresponds to rare but sizeable negative velocities. Instead, in Fig. 5(b) fluctuations are so small that it practically represents the case of a one way bridge. We conclude that the analytical treatment captures the main effect, as the agreement is fairly good and the resonance is correctly captured by the analysis in a wide range of parameters.

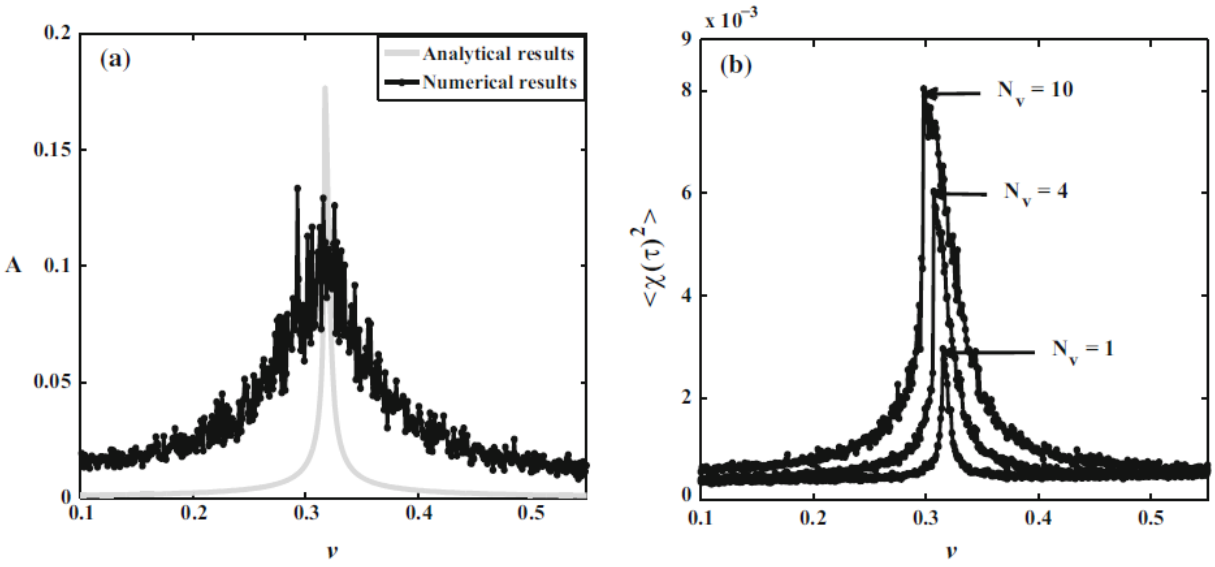

Figure 5: *(a) Comparative analysis of mean-square response through the stochastic average analysis (Eq. (87), light gray line) and numerical simulations of the full model Eq. (75) (black line with circle) for a single load ($N_v = 1$) and for noise intensity $\gamma = 0.1$. (b) Numerical simulations of the mean square response of a different number of loads N_v for $\gamma = 0.001$. The other dimensionless parameters read: $\beta = -0.52$, $\lambda = 0.00078$, $\Gamma = 0.0022$.*

The reentrant behavior is further analyzed in Fig. 6, where the mean-square amplitude as a function of the noise intensity for different values of the loads speed v is displayed. In Fig. 6 the peak of the oscillations, marked by an oval, occurs at relatively high noise values ($\gamma \simeq 1.4$) for low speed ($v = 0.1$) speeds, decreases at lower noise levels ($\gamma \simeq 0.4$) for higher speed ($v = 0.35$), and moves again to higher fluctuations ($\gamma \simeq 0.6$) with a further increase of the speed ($v = 0.4$). Thus, not only the amplitude has a maximum response for a finite value of the noise intensity, but also the peak position exhibits a nontrivial behavior. In general these features can be ascribed to the peculiar character

of bounded noise in model Eq. (75) [137]. We note that the amplitude decrease occurs for fluctuation levels that are comparable or higher than the average speed, and therefore they basically describe a two way bridge.

It is always found from Fig. 6 that, velocity noise first causes an increase of the mean-square amplitude of the beam oscillations, and after a maximum a further increase of the noise causes a *decrease* of the mean-square displacement, a behavior that closely follows stochastic resonance phenomena [139, 140]. In fact, high levels of noise appear to be paradoxically beneficial for the beam safety, inasmuch the amplitude only increases up to a special noise value where it exhibits a maximum damage to the beam wearing. Such counterintuitive effect of the random disturbance has been extensively debated in signal detection [141] and biological systems [142], and are generally connected with suboptimal detection observable as the observed amplitude of the oscillations [143]. There are the

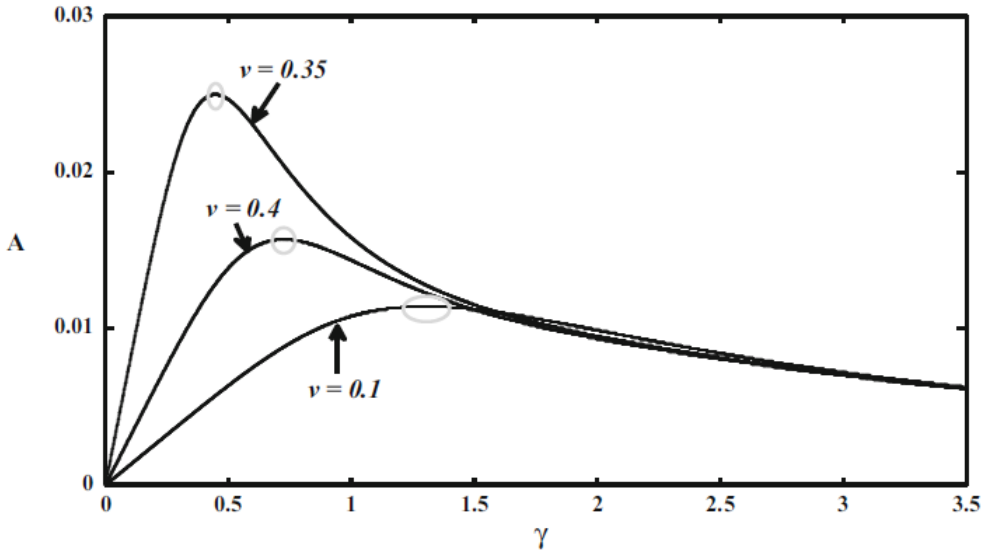

Figure 6: *Influence of the intensity of the stochastic velocity on the mean amplitude of vibration for different values of the mean velocity v in the simplified system Eq.(77). The other parameters are the same as in Fig.5.*

values of γ for which the amplitude is almost constant at the maximum; a further increase of the noise amplitude γ leads to a decrease of the amplitude (see Fig. 6).

Beside the reentrant effect, it is noticed that the noise intensity tends to broad the resonance, and the number of loads increases both the mean square amplitude and the width of the peak. These features are naturally expected on physical grounds; more surprising is the effect of the single load weight on the mean square amplitude, as shown in Fig. 7. Increasing the load of each moving weight, one observes that the mean amplitude also shows a reentrant behavior with multiple solutions below the resonance speed (Fig. 7). It is significant to note that when the speed is below the resonance, one observes critical values of the weight load where we have a bifurcation of the system. On a general ground this could be again attributed to the presence of bounded noise, that can produce bimodal

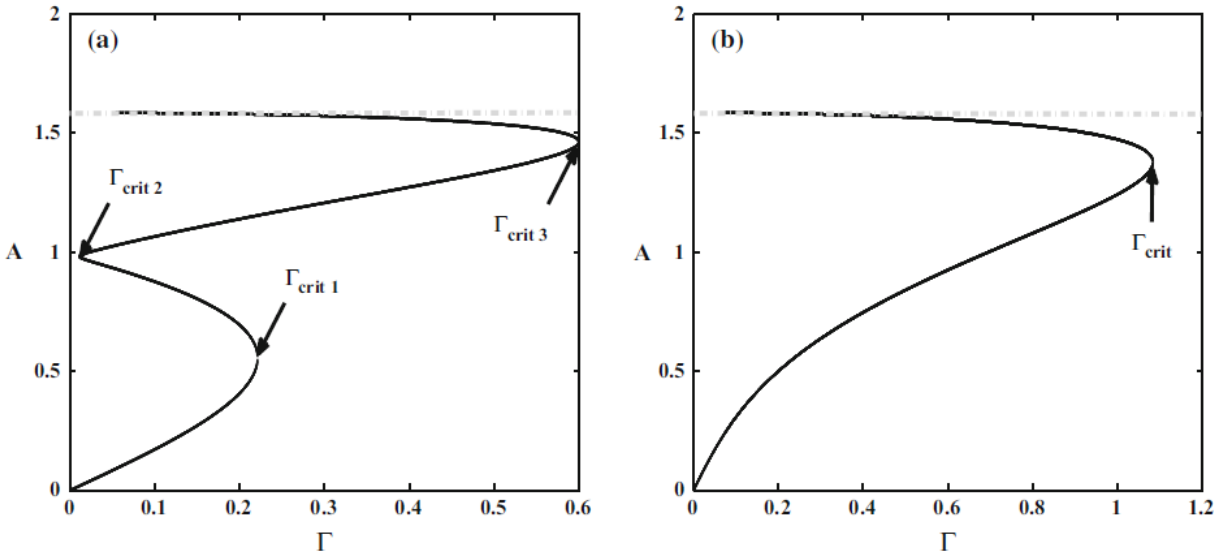

Figure 7: *The mean square amplitude versus the weight load for (a)* $v = 0.25$ *and (b)* $v = 0.35$. *It is assumed here that,* $\gamma = 0.1$. *The other parameters are the same as in Fig.5.*

distributions [135]. More specifically, the effect can be related to the special features of the bounded noise spectral density (83), combined with the nonlinear amplitude-frequency relation of Eq.(87). These features give rise to the intricate effects above described, inasmuch the spectral content determined by Eq. (83) is, at variance with the uniform case of white noise, peaked around some frequencies. Thus, the frequency of the peaks depends upon the noise intensity: increasing the noise intensity the harmonic content is altered. This is the physical origin of the reentrant behavior observed in Fig. 6: when the noise intensity is increased it first moves the harmonic content towards the resonance of the beam, increasing the amplitude of the oscillations. The effect, however, saturates and eventually the term at the denominator γ dominates.

In Figs. 5,6,7, the mean amplitude of the oscillations of the beam has been displayed. A more complete description in terms of the full distribution is presented in the following subsection, where the probability distribution of the representative coordinate χ is analysed.

III-2-1-4- Stationary probability distribution of a catastrophic monostable system

In this subsection, a Duffing oscillator with bounded Gaussian noise described by Eq. (77) is considered. In particular, the stationary probability distribution analytically with the method of stochastic averaging method [96, 98, 99, 138] is sought as describe in the previous chapter. To do so, it is assumed that the noise intensity is small and the

following change in variables is introduced,

$$\chi(\tau) = a(\tau)\cos\theta, \qquad \dot{\chi}(\tau) = -\Omega a(\tau)\sin\theta, \qquad \theta = \Omega\tau + \varphi(\tau). \tag{89}$$

Substituting Eqs. (89) into Eq. (77), we obtain

$$\begin{cases} \dot{a} = -\lambda a \sin^2\theta + \\ \quad \frac{1}{\Omega}\left\{a\left(1-\Omega^2\right)\cos\theta + \beta a^3\cos^3\theta - \Gamma\sin\left[\Omega\tau + \gamma W(\tau)\right]\right\}\sin\theta \\ \\ a\dot{\varphi} = -\lambda a\sin\theta\cos\theta + \\ \quad \frac{1}{\Omega}\left\{a\left(1-\Omega^2\right)\cos\theta + \beta a^3\cos^3\theta - \Gamma\sin\left[\Omega\tau + \gamma W(\tau)\right]\right\}\cos\theta. \end{cases} \tag{90}$$

The steady state response for the case of perfect periodicity is considered first, $\gamma = 0$, and Eqs. (90) become

$$\begin{cases} \dot{a} = -\lambda a \sin^2\theta + \\ \quad \frac{1}{\Omega}\left\{a\left(1-\Omega^2\right)\cos\theta + \beta a^3\cos^3\theta - \Gamma\sin\left[\theta - \varphi\right]\right\}\sin\theta \\ \\ a\dot{\varphi} = -\lambda a\sin\theta\cos\theta + \\ \quad \frac{1}{\Omega}\left\{a\left(1-\Omega^2\right)\cos\theta + \beta a^3\cos^3\theta - \Gamma\sin\left(\theta - \varphi\right)\right]\right\}\cos\theta. \end{cases} \tag{91}$$

By applying the standard averaging method [102, 104], Eqs. (91) reduce to

$$\begin{cases} \dot{a} = -\frac{\lambda a}{2} - \frac{\Gamma}{2\Omega}\cos\varphi \\ \\ a\dot{\varphi} = \frac{1}{\Omega}\left[\frac{a\left(1-\Omega^2\right)}{2} + \frac{3}{8}\beta a^3\right] + \frac{\Gamma}{2\Omega}\sin\varphi. \end{cases} \tag{92}$$

The steady states solutions of Eqs. (92) can be found by putting $a = a_0, \varphi = \varphi_0$ and $\dot{a} = 0$, $\dot{\varphi} = 0$, this leads to the following result:

$$\frac{9}{16}\beta^2 a_0^6 + \frac{3}{2}\beta\left(1-\Omega^2\right)a_0^4 + \left[\lambda^2\Omega^2 + \left(1-\Omega^2\right)^2\right]a_0^2 = \Gamma^2. \tag{93}$$

This equation has more than one steady-state solution for some parameters. The variation of steady-state response a_0 as a function of the speed v is compared with the numerical simulation of Eq. (77) and shown in Fig. 8. It can be seen from this figure that the deterministic response predicted by the standard averaging method is in good agreement with that obtained by the numerical simulations. In particular the resonance is correctly captured by the analysis. The time response of the system (75) and phase plot are shown in Fig. 8 for the noiseless case $\gamma = 0$, and for $v = 0.32$, $N_v = 1$, $\lambda = 0.0078$. Clearly, the response is periodic and the phase trajectory is a limit cycle. Next, the stationary response of system (75) in the noisy case is determined, $\gamma \neq 0$. To do so, Eqs. (90) are

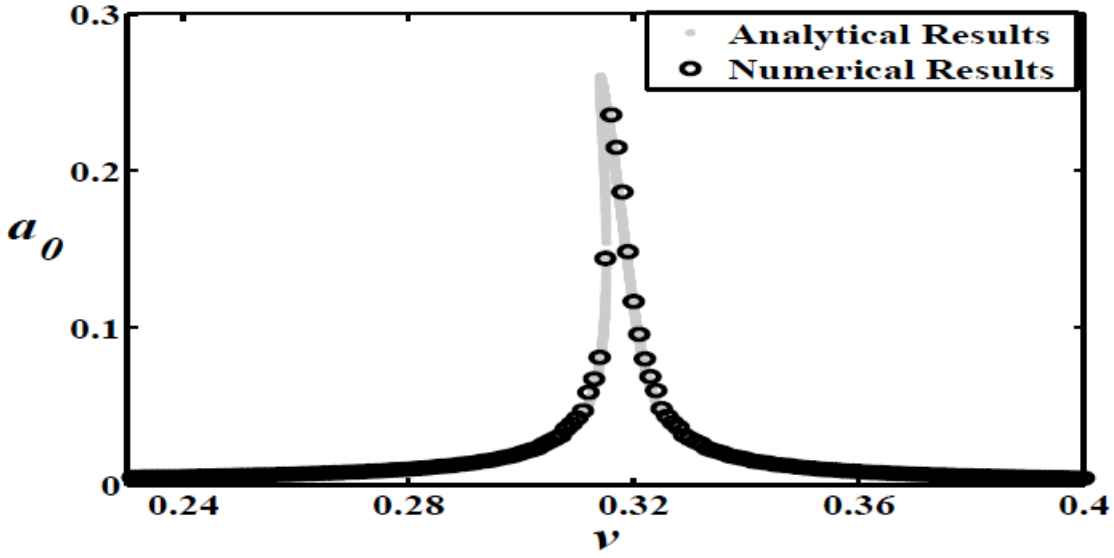

Figure 8: *Variations of the steady-state response of deterministic system Eq. (75) with* $\gamma = 0$ *(the other parameters read:* $\Gamma = 0.002, N_v = 1, \lambda = 0.0078$*): the light gray dots represent the theoretical prediction and the black circles the numerical solution.*

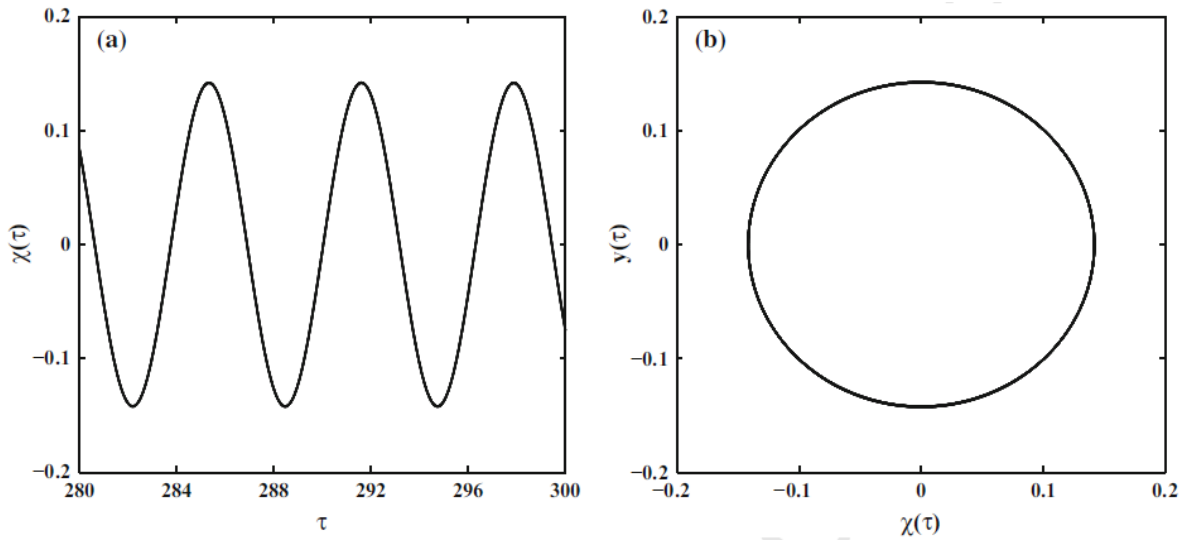

Figure 9: *Time evolution and phase portrait of the deterministic system, Eq. (75) with* $\gamma = 0$ *(the other parameters read:* $v = 0.32, \Gamma = 0.002, N_v = 1, \lambda = 0.0078$*): (a) time history of* $\chi(\tau)$ *and (b) phase plot.*

rewritten as:

$$\begin{cases} \dot{a} = -\lambda a \sin^2\theta + \frac{1}{\Omega}\left[a\left(1-\Omega^2\right)\cos\theta + \beta a^3 \cos^3\theta - \eta(\tau)\right]\sin\theta, \\ \\ \dot{\varphi} = -\lambda \sin\theta\cos\theta + \frac{1}{a\Omega}\left[a\left(1-\Omega^2\right)\cos\theta + \beta a^3 \cos^3\theta - \eta(\tau)\right]\cos\theta. \end{cases} \tag{94}$$

To apply the method [96, 98, 138], one average at the frequency Ω and the following pair of stochastic equations for amplitude $a(\tau)$ and the phase $\varphi(\tau)$ is obtained:

$$\mathrm{d}a = \left[-\tfrac{1}{2}\lambda a + \frac{(\Gamma\gamma)^2}{8a\Omega^2}\frac{2\Omega^2+\frac{\gamma^4}{4}}{\left(\frac{\gamma^4}{4}\right)^2+\Omega^2\gamma^4}\right]\mathrm{d}\tau \; + \; \frac{\Gamma\gamma}{2\Omega}\sqrt{\frac{2\Omega^2+\frac{\gamma^4}{4}}{\left(\frac{\gamma^4}{4}\right)^2+\Omega^2\gamma^4}}\mathrm{d}W_1(\tau) \tag{95a}$$

$$\mathrm{d}\varphi = \frac{1}{\Omega}\left[\frac{\left(1-\Omega^2\right)}{2} + \frac{3}{8}\beta a^2\right]\mathrm{d}\tau + \frac{\Gamma\gamma}{2a\Omega}\sqrt{\frac{2\Omega^2+\frac{\gamma^4}{4}}{\left(\frac{\gamma^4}{4}\right)^2+\Omega^2\gamma^4}}\mathrm{d}W_2(\tau) \tag{95b}$$

Here $W_1(\tau)$ and $W_2(\tau)$ are independent normalized Weiner processes. Clearly, Eq. (95a) governing the amplitude $a(\tau)$ does not depend on $\varphi(\tau)$; thus, one can consider the probability density for $a(\tau)$, rather than a joint density for $a(\tau)$ and $\varphi(\tau)$. The probability density function $P(a(\tau),\tau|a(\tau_0),\tau_0)$ for the amplitude is governed by the Fokker-Planck-Kolmogorov equation:

$$\begin{aligned} \tfrac{\partial P(a,\tau)}{\partial\tau} = \tfrac{\partial}{\partial a}\left[\left(-\tfrac{1}{2}\lambda a + \tfrac{(\Gamma\gamma)^2}{8a\Omega^2}\tfrac{2\Omega^2+\frac{\gamma^4}{4}}{\left(\frac{\gamma^4}{4}\right)^2+\Omega^2\gamma^4}\right)P(a,\tau)\right] \\ +\tfrac{1}{2}\left(\tfrac{(\Gamma\gamma)^2}{4\Omega^2}\tfrac{2\Omega^2+\frac{\gamma^4}{4}}{\left(\frac{\gamma^4}{4}\right)^2+\Omega^2\gamma^4}\right)\tfrac{\partial^2 P(a,\tau)}{\partial a^2} \end{aligned} \tag{96}$$

In the stationary case, $P: \frac{\partial P(a,\tau)}{\partial\tau} = 0$, the solution of Eq. (96) is:

$$P(a) = \frac{Na}{\Lambda}\exp\left[2\int\frac{\Delta(a)}{\Lambda}\mathrm{d}a\right], \tag{97}$$

where

$$\Delta(a) = -\frac{1}{2}\lambda a + \frac{(\Gamma\gamma)^2}{8a\Omega^2}\frac{2\Omega^2+\frac{\gamma^4}{4}}{\left(\frac{\gamma^4}{4}\right)^2+\Omega^2\gamma^4}, \tag{98a}$$

$$\Lambda = \frac{(\Gamma\gamma)^2}{4\Omega^2}\frac{2\Omega^2+\frac{\gamma^4}{4}}{\left(\frac{\gamma^4}{4}\right)^2+\Omega^2\gamma^4}. \tag{98b}$$

Combining Eq. (97) and Eqs. (98), we get

$$P(a) = \frac{\lambda a}{\Lambda}\exp\left(-\frac{\lambda}{2\Lambda}a^2\right) \tag{99}$$

where N has been determined by the normalization condition:

$$\int_0^\infty P(a)\mathrm{d}a \equiv 1, \tag{100}$$

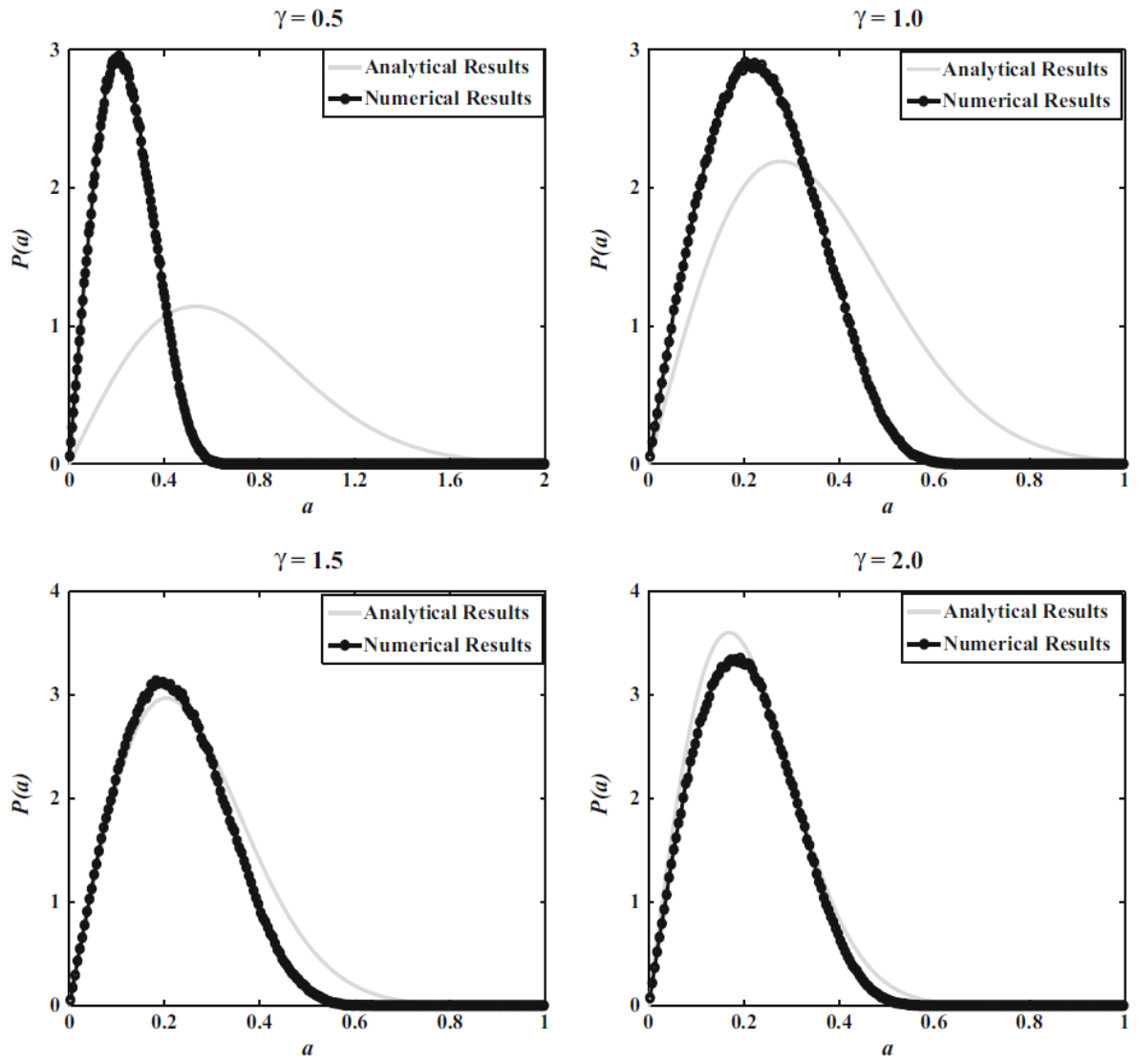

Figure 10: *Stationary probability distributions for different values of the standard deviation of stochastic velocity γ versus the amplitude a. The parameters used are: $v = 0.25$, $\Gamma = 0.2$, $\lambda = 0.28$, $N_v = 1$. The curves with solid light gray lines denote the algebraic calculations using Eq. (99) and the curves with solid black lines (with circles) represent the numerical solutions for the oscillator, Eq. (75).*

Moreover, one can find the peaks of the distribution Eq. (99) in the points where $\partial P\,(a)/\partial a = 0$:

$$a_m = \sqrt{\frac{\Lambda}{\lambda}} \tag{101}$$

As the amplitude of the oscillations in the ansatz Eq. (89) is defined positive, it is concluded that, the distribution should exhibit just a peak. In Fig. 10 the stationary probability density as a function of the amplitude a for different noisy velocity intensity γ is displayed, compared with numerical solutions of Eq. (75). The numerical results confirm that the distribution has only one maximum. It is also evident that the analytic solution predicts a peak of the probability distribution at higher values than the numerical solution. The discrepancy, however, decreases as noise increases, and the agreement is fairly good when fluctuations are very large (compared to the average speed $v = 0.25$). We therefore conclude that there is a better agreement for a two way bridge.

The results obtained in this subsection confirm that an increase of the noise intensity γ leads to a decrease of the amplitude of the oscillations, Eq.(101). This is in qualitative agreement with the findings of the Fourier analysis, as it confirms the counter-intuitive role of noise, that tends to decrease the amplitude of the oscillations. However, it is underlined that the stochastic averaging does not capture the amplitude of the oscillations at low noise values.

By way of short summary of this part, we have retrieved what is the effect of the load random velocities on the behavior of the mean amplitude versus the parameters. Some nonlinear dependences are new but not fully unexpected: the number of vehicles changes the resonant velocity (Figs. 5,8). More interesting is the unexpected influence of the load, that is not just nonlinear, but reentrant (Fig. 7). To single out what we regard as the most relevant finding, we focus on the non-monotonic effect of the noise intensity, Fig. 6, that discloses an unexpected beneficial role of noise intensity on the bridge stability.

III-2-2- Cable stayed-bridge subject to random moving loads: A chaotic dynamics approach

III-2-2-1- Description of a cable stayed-bridge model and mathematical formalism

The dynamic model of a cable-stayed bridge system investigated in this thesis and shown in Fig. 11(a) is the semi-harp type with two symmetrical spans. The cable-stayed bridge is modelled by using a Rayleigh beam theory [124] (in order to take into account the high frequency motion of the beam) of finite length L with geometric nonlinearities on elastic supports with linear stiffness K_k^c. This model is subjected to an axial compressive loads T_h^c due to the total contribution of the horizontal component of the tensile cables and a series of lumped loads P moving along the beam in the same direction with the same stochastic velocity v_i (See Fig. 11(b)). We assume that the mass of the cables is negligible and they are regularly spaced on the beam. Since all the stay cable anchorage sections are fixed to move both horizontally and vertically, the whole pylon is assumed to

be fixed. The deformed beam can be described by the transverse deflection $w(x,t)$ and

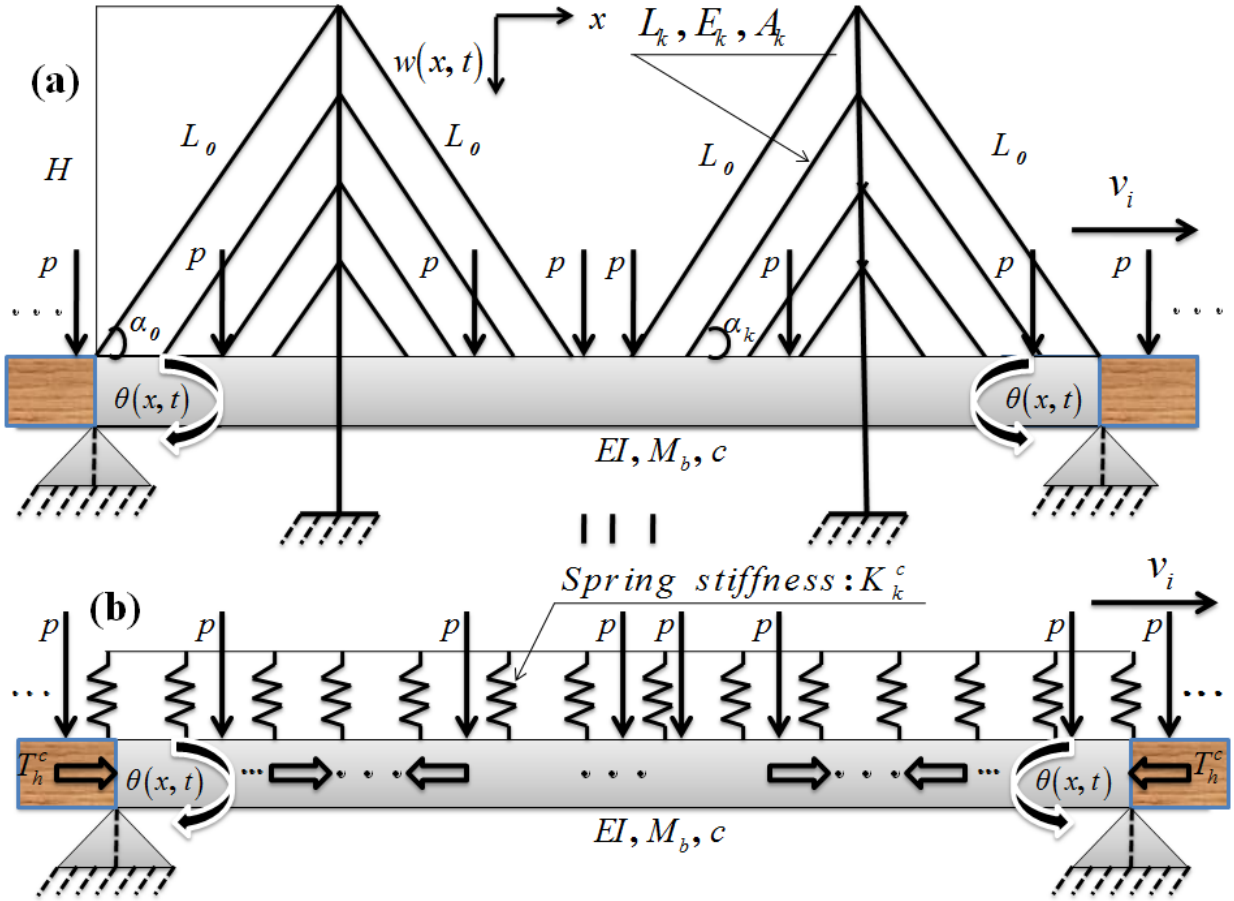

Figure 11: *Sketch of (a) the cable-stayed bridge system, (b) equivalent model under stochastic moving loads. The gravitational forces are represented by arrows P, whose separations are not uniform, for the speeds v_k are not identical.*

the rotation of the cross section of the beam $\theta(x,t)$. The equation of motion for the small deformations $\left(\theta(x,t) \backsimeq \frac{\partial w(x,t)}{\partial x}\right)$ for this system is then given by

$$\begin{aligned} M_b \frac{\partial^2 w(x,t)}{\partial t^2} - R_a \frac{\partial^4 w(x,t)}{\partial x^2 \partial t^2} + c \frac{\partial w(x,t)}{\partial t} + \sum_{k=0}^{N_c} K_k^c \delta\left[x - k\frac{L}{N_c}\right] w(x,t) + T_h^c \frac{\partial^2 w(x,t)}{\partial x^2} \\ + EI \frac{\partial^2}{\partial x^2}\left[\frac{\partial^2 w(x,t)}{\partial x^2}\left(1 - \frac{3}{2}\left(\frac{\partial w(x,t)}{\partial x}\right)^2\right)\right] = P \sum_{i=1}^{N_v} \varepsilon_i \delta\left[x - x_i(t - t_i)\right] \end{aligned} \tag{102}$$

In which M_b, EI, ρ, R_a, c, $w(x,t)$ are the beam mass per unit length, the flexural rigidity of the beam, beam material density, the transverse Rayleigh beam coefficient, the damping coefficient and the transverse defection of the beam at point x and time t respectively. T_h^c is the axial compressive loads due to the total contribution of the horizontal component of the tensile cables. In Eq. (102), $T_h^c \frac{\partial^2 w(x,t)}{\partial x^2}$ is the axial compressive load (per unit length) due to the horizontal component of the stay cables, $\sum_{k=0}^{N_c} K_k^c \delta\left[x - k\frac{L}{N_c}\right] w(x,t)$ is the tension of cables per unit length. The term on the right-hand side of Eq. (102) is used to describe the series of random moving loads over the beam. $x_i(t - t_i)$ is the distance

covered by the i^{th} force to the time t. $t_i = (i-1)d/v_0$ is a deterministic arriving time of the i^{th} load at the beam. d is the average spacing loads, $\delta[...]$ denotes the Dirac delta function, N_v is the total number of moving loads. ε_i is a window function defined as previously [58]. N_c is the number of cables acting on the bridge and $\delta[x - k\frac{L}{N_c}]$ give the position of each action. K_k^c is the linear stiffness of the cables. Their expression according to the particular characteristics of the stay cables is given by [16]

$$K_k^c = \frac{E_k A_k}{L_k} \sin^2(\alpha_k) \tag{103}$$

where α_k is the angle between the k^{th} cable and the bridge deck, E_k, A_k, L_k are the Youngs Modulus, the cross section and the length of the k^{th} cable respectively. The boundary and initial conditions of the beam are given in Eq. (70).

By taking into account Eq. (73) and considering the following adopted dimensionless variables:

$$\vartheta_n = \frac{q_n}{l_r} \ , \ \tau = \omega_0 t \tag{104}$$

The equivalent stochastic dimensionless modal equation is obtained, considering only the first mode of vibration as

$$\begin{aligned} \ddot{\vartheta}(\tau) + \lambda\dot{\vartheta}(\tau) + \left[1 - \tfrac{T_h^c}{T_{h_{cr}}^c} + \chi \sum_{k=0}^{N_c} \tfrac{E_k A_k}{L_k} \sin^2(\alpha_k) \sin^2\left(\tfrac{\pi k}{N_c}\right)\right] \vartheta(\tau) + \beta\vartheta^3(\tau) \\ = \Gamma \sum_{i=1}^{N_v} \varepsilon_i \sin\left[\Omega\tau + \gamma W_i(\tau - \tau_i)\right] \end{aligned} \tag{105}$$

with

$$\begin{gathered} \Omega = \tfrac{\pi v_0}{L\omega_0}\,, \quad \Gamma = \tfrac{2PL^3}{l_r EI\pi^4}\,, \quad \lambda = \tfrac{cL^3}{\pi^2\sqrt{EI[L^2 m_b + R_a\pi^2]}}\,, \quad \tau_i = \omega_0 t_i \\ \beta = -\tfrac{3}{8}\left(\tfrac{\pi l_r}{L}\right)^2, \ \gamma = \pi\sigma_v\,, \quad \chi = \tfrac{2L^3}{EI\pi^4}\,, \quad T_{h_{cr}}^c = \tfrac{EI\pi^2}{L^2}. \end{gathered} \tag{106}$$

and

$$\omega_0 = \frac{\pi^2}{L}\sqrt{\frac{EI}{L^2 M_b + R_a\pi^2}}\,, \quad R_a = M_b r^2\,, \quad r = \sqrt{\frac{I}{S}}\,, \quad l_r = \frac{L}{2}. \tag{107}$$

Here l_r is a reference length of the beam and $W_i(\tau - \tau_i)$ is a unit Wiener stochastic process. Eq. (105) amounts to a stochastic Duffing oscillator which describes the unbounded or catastrophic motion of the beam for:

$$T_h^c < \left(1 + \chi \sum_{k=0}^{N_c} \frac{E_k A_k}{L_k} \sin^2(\alpha_k) \sin^2\left(\frac{\pi k}{N_c}\right)\right) T_{h_{cr}}^c \tag{108}$$

The catastrophic behavior of the beam is related to the configuration of the potential of the system, as described in details in Ref. [133].

For the analytical purpose, let us consider the simplest case when the beam is subjected to the passage of a single moving load ($N_v = 1$). Also, we assume in the first case ($\varepsilon_i = 0$)

that the dynamic response function is equal to zero ($\vartheta(\tau) = 0$) and for the second case ($\varepsilon_i = 1$) the response function is calculated from the equation

$$\ddot{\vartheta}(\tau) + \lambda\,\dot{\vartheta}(\tau) + (1+\alpha)\;\vartheta(\tau) + \beta\,\vartheta^3(\tau) = \eta\,(\tau) \tag{109}$$

where:

$$\sigma = \chi \sum_{k=0}^{N_c} \frac{E_k A_k}{L_k} \sin^2(\alpha_k) \sin^2\left(\frac{\pi k}{N_c}\right),\ \alpha = \sigma - \frac{T_h^c}{T_{h_{cr}}^c},\ \eta\,(\tau) = \Gamma \sin\left[\Omega\,\tau + \gamma W\,(\tau)\right]$$

α is the total contribution of the stay cables structures on the dynamics of the cable-stayed bridges system. In the following, the prediction of chaotic behavior for Eq.(109) will be investigated.

III-2-2-2- Melnikov analysis and random chaos prediction

The aim of this subsection is to show the effect of stochastic velocity of the moving loads and the cables contribution on the basin boundaries. This is done by one of a few methods allowing analytical prediction of chaos occurrence: Melnikov method [89, 91–94].

This method was extended to study stochastic dynamical system by Frey and Simiu [90]. To apply this method, we introduce a small parameter μ in Eq. (109) and rewrite the governing system as the following set of first order differential equation :

$$\begin{cases} \dot{\vartheta}(\tau) = y(\tau) \\ \\ \dot{y}(\tau) = -\,(1+\alpha)\,\vartheta(\tau) - \beta\,\vartheta^3(\tau) + \mu\,\left[-\lambda\,y(\tau) + \eta(\tau)\right] \end{cases} \tag{110}$$

For $\mu = 0$, and after assuming that $\vartheta = \vartheta(\tau); y = y(\tau)$, the system of Eq. (110) is the Hamiltonian system with Hamiltonian function

$$H\,(\vartheta, y) = \frac{1}{2}\,y^2 + \frac{1}{2}\;(1+\alpha)\,\vartheta^2 + \frac{\beta}{4}\,\vartheta^4 \tag{111}$$

and the potential function

$$V\,(\vartheta) = \frac{1}{2}\,(1+\alpha)\,\vartheta^2 + \frac{\beta}{4}\vartheta^4 \tag{112}$$

Fig. 12(a) shows an increases of an energy barrier of our system when the contribution of cables α varies. As $\beta < 0$, the system has three equilibrium points: a center point $\vartheta_{e0} = (0,0)$ and two saddles $\vartheta_{e1} = \left(-\sqrt{-(1+\alpha)/\beta}\,, 0\right)$ and $\vartheta_{e2} = \left(\sqrt{-(1+\alpha)/\beta}\,, 0\right)$, as shown in Fig. 12(b). The saddle points are connected by heteroclinic orbits that satisfy

the following equation:

$$\begin{aligned} \vartheta_{het}(\tau) &= \pm\sqrt{-\tfrac{1+\alpha}{\beta}}\tanh\left[\sqrt{\tfrac{1+\alpha}{2}}.\tau\right] \\ y_{het}(\tau) &= \pm(1+\alpha).\sqrt{-\tfrac{1}{2\beta}}\sec h^2\left[\sqrt{\tfrac{1+\alpha}{2}}.\tau\right] \end{aligned} \tag{113}$$

Melnikov theory defines the condition for the appearance of the so-called transverse inter-

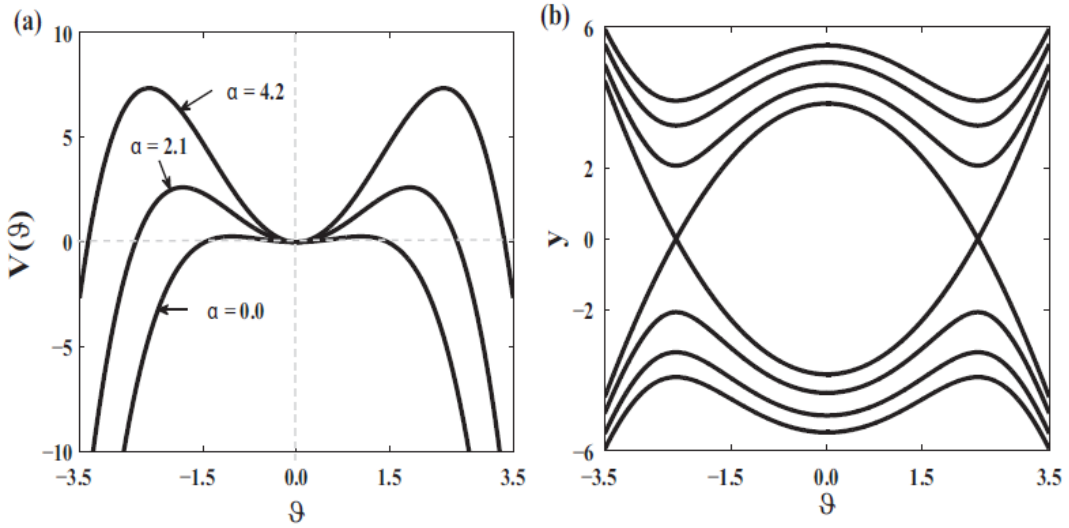

Figure 12: *Potential for different value of α (a), Separatrix (closed curve) and phase space portrait (open lines) of the Catastrophic system Eq. (109) for $\alpha = 4.2$ (b).*

section points between the perturbed and the unperturbed separatrix or the appearance of the fractality or erosion on the basin of attraction. This theory can be applied to Eq. (109) by using formula given by Wiggins in [91] as follows:

$$\begin{aligned} M_R(\tau_0) &= -\lambda\int_{-\infty}^{+\infty} y_{het}^2(\tau)\,\mathrm{d}\tau + \int_{-\infty}^{+\infty} y_{het}(\tau)\,\eta(\tau+\tau_0)\mathrm{d}\tau \\ &= I \pm Z(\tau_0) \end{aligned} \tag{114}$$

Where:

$$I = \frac{\lambda\sqrt{8(1+\alpha)^3}}{3\beta}, \quad Z(\tau_0) = (1+\alpha).\sqrt{-\frac{1}{2\beta}}\int_{-\infty}^{+\infty}\sec h^2\left[\sqrt{\frac{1+\alpha}{2}}.\tau\right]\eta(\tau+\tau_0)\mathrm{d}\tau$$

In the following, we consider the simple zeros of the mean-square of the output analyzed through the random Melnikov function. The impulse response function of the system (109) is [95]

$$h(\tau) = \vartheta_{het}(\tau).y_{het}(\tau) = \sqrt{\frac{(1+\alpha)^3}{2\beta^2}}\tanh\left[\sqrt{\frac{1+\alpha}{2}}.\tau\right]\sec h^2\left[\sqrt{\frac{1+\alpha}{2}}.\tau\right] \tag{115}$$

The associated frequency response can be expressed as follows

$$\mathrm{H}(\omega)=\int_{-\infty}^{+\infty}h(\tau)e^{-j\omega\tau}\mathrm{d}\tau=-\frac{j\pi\omega^{2}\csc h\left[\frac{\pi\omega}{2\sqrt{1+\alpha}}\right]}{2\sqrt{2\beta^{2}}} \tag{116}$$

Consequently, the variance of $Z(\tau_0)$, considered as the output of the system, is

$$\begin{aligned}\sigma_{z}^{2}&=\int_{-\infty}^{+\infty}|\mathrm{H}(\omega)|^{2}S_{\eta}\left(\omega\right)\mathrm{d}\omega\\&=\frac{\pi}{2}\left(\frac{\Gamma\gamma}{4\beta}\right)^{2}\int_{-\infty}^{+\infty}\omega^{4}\csc h^{2}\left[\frac{\pi\omega}{2\sqrt{1+\alpha}}\right]\left\{\frac{\Omega^{2}+\omega^{2}+\frac{\gamma^{4}}{4}}{\left(\omega^{2}-\Omega^{2}+\frac{\gamma^{4}}{4}\right)^{2}+\Omega^{2}\gamma^{4}}\right\}\mathrm{d}\omega\end{aligned} \tag{117}$$

Here $S_\eta(\omega)$ is the spectral density of the noise $\eta(\tau)$ defined in Eq. (83). Therefore, smale chaos appears (in mean-square response) when condition $I^2 \leq \sigma_z^2$ is satisfied, i.e.

$$\begin{aligned}\left(\frac{\lambda\sqrt{8(1+\alpha)^{3}}}{3\beta}\right)^{2}\leq\frac{\pi}{2}\left(\frac{\Gamma\gamma}{4\beta}\right)^{2}\times\\\int_{-\infty}^{+\infty}\omega^{4}\csc h^{2}\left[\frac{\pi\omega}{2\sqrt{1+\alpha}}\right]\left\{\frac{\Omega^{2}+\omega^{2}+\frac{\gamma^{4}}{4}}{\left(\omega^{2}-\Omega^{2}+\frac{\gamma^{4}}{4}\right)^{2}+\Omega^{2}\gamma^{4}}\right\}\mathrm{d}\omega\end{aligned} \tag{118}$$

Or simply,

$$\frac{\lambda}{\Gamma}\leq\frac{3\gamma}{16}\sqrt{\frac{\pi\int_{-\infty}^{+\infty}\omega^{4}\csc h^{2}\left[\frac{\pi\omega}{2\sqrt{1+\alpha}}\right]\left\{\frac{\Omega^{2}+\omega^{2}+\frac{\gamma^{4}}{4}}{\left(\omega^{2}-\Omega^{2}+\frac{\gamma^{4}}{4}\right)^{2}+\Omega^{2}\gamma^{4}}\right\}\mathrm{d}\omega}{\left(1+\alpha\right)^{3}}}=\left(\frac{\lambda}{\Gamma}\right)_{cr} \tag{119}$$

where $(\lambda/\Gamma)_{cr}$ is the critical parameter for the chaotic motion of the nonlinear system. The integral in Eq. (119) can be computed numerically.

In calculation, the structural and material properties of a cable-stayed bridge model are given in Table III as (See Refs. [51, 144])

The other lengths of the cables are calculated by using the *theorem of Thalès*, by assuming of course that the cables on both sides of the towers which support them are parallel between them. Moreover, the various angles ranging between the cables and the bridge deck are evaluated by using the relation: $\alpha_k=\cos^{-1}\left(\frac{l_c}{2L_k}\right)$ where l_c is the distance separating the two impacts points on the bridge deck of the two symmetrical cables.

One can thus get the threshold of bounded excitation amplitude versus the standard deviation of the stochastic velocity for different values of the mean driving frequency Ω, for $\alpha = 0.0$ (no cables) (as shown in Fig. 13(a)) and for $\alpha = 4.2$ (with 18 cables) (as shown in Fig. 13(b)). From Fig. 13, we can see that the threshold curve is a continuous line in the space $(\gamma, \lambda/\Gamma) \in R^2$. We observe that the area above the curves indicate the domain where the system goes from periodic to random as γ increases progressively, while

Table III: *Values of the physical parameters of a cable-stayed bridge model* [51, 144]

Physical parameters	Symbols	values
Length of the bridge (m)	L	628.1
Young modulus of the bridge deck (kg/m)	E	200.0
Cross-sectional area of the bridge deck (m^2)	S	4.8
Moment of inertia of the bridge deck (m^4)	I	12.0
Mass per unit length of the bridge deck (kg/m)	M_b	37680.0
Damping coefficient of the bridge deck (N.s/m)	c	68.0
High length of the stay cables (m)	L_0	158.13
Young modulus of the cables (MPa)	E_k	131.0
Cross-sectional area of the cables (m^2)	A_k	5.48×10^{-4}
Horizontal tension of the cables (N/m)	T_h^c	5.3×10^6
Length of the pylon (m)	H	45.7

below them the motion of system goes from chaos to random chaos as γ increases from zero and becomes more and more random and less chaotic as γ further increases. This domain is especially sensitive to initial conditions and fractal basin boundaries. Likewise, for certain values of the intensity of stochastic velocity ($\gamma \in [0, \gamma_{limit}]$), the increasing of mean driving frequency Ω still increases the chaotic field of the system. This effect doesn't appear any more for $\gamma > \gamma_{limit}$ (see Fig. 13(a)), the case is opposite. Fig. 13(b) illustrates the same effect while showing the contribution of the stay cables on the results obtained previously.

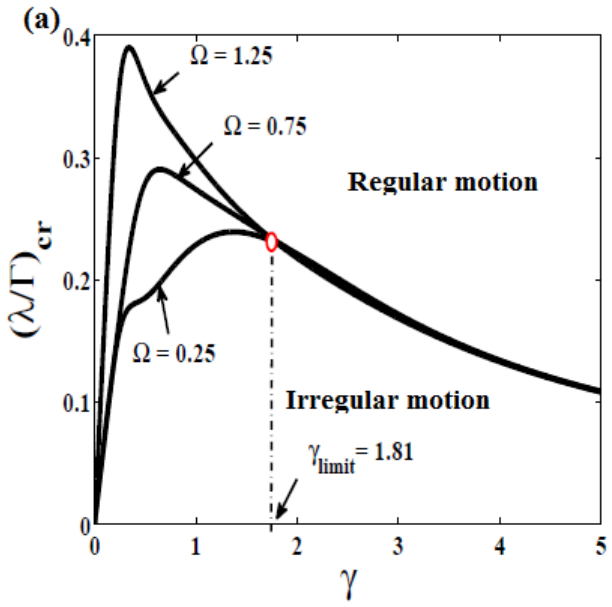

Figure 13: *Effects of the mean driving frequency Ω on the threshold curve of horseshoes chaos. (a): for $\alpha = 0.0$ (no cables) (b): for $\alpha = 4.2$ (with 18 cables).*

On the other hand, the effect of cable connections on the threshold amplitude of sine-Wiener noise excitation for the onset of chaos in the model is investigated as shown in Fig. 14. It is clear that the increase of number of stay cables first increases the threshold,

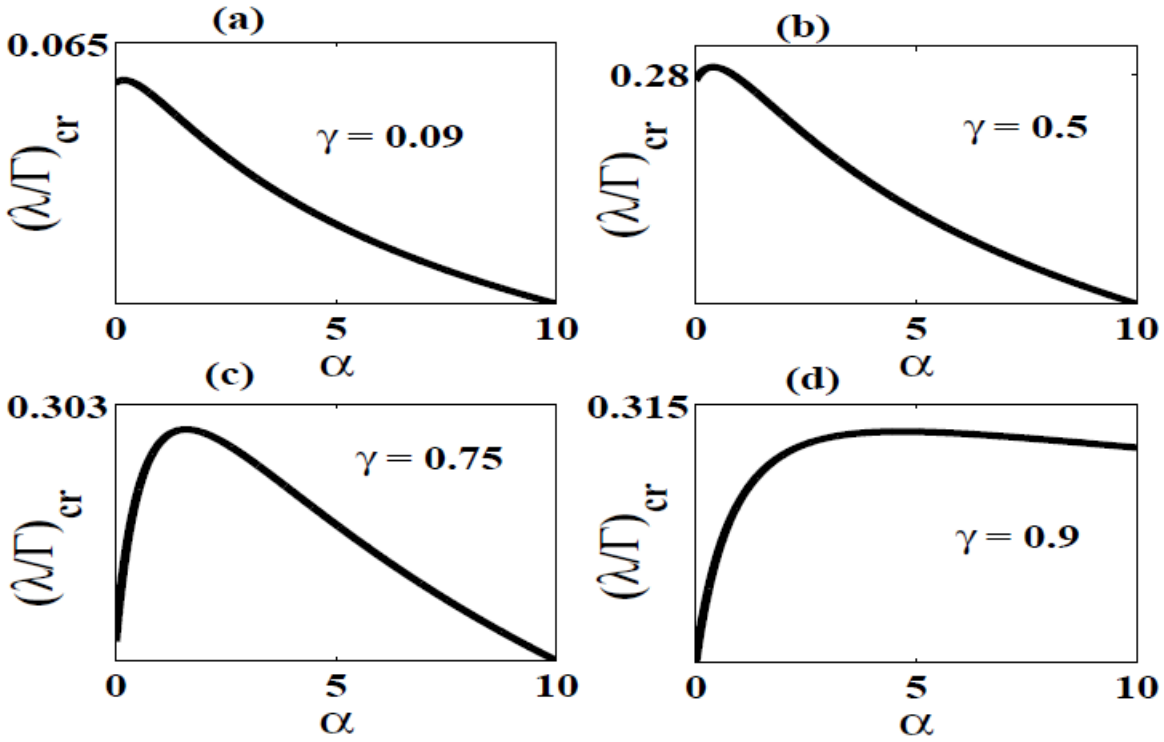

Figure 14: *Effects of stay cables contributions α on the threshold amplitude of sine-Wiener noise excitation. for $\Omega = 0.75$.*

and then decreases it. It is also shown from this figure that the lowest number of cables is dangerous for the stability of the structure, while the highest number contributed to increase the degree of safety of the bridge. The intensity of the random component of the loads velocity γ influences considerably this previous results as shown in Fig. 14.

Fig. 15 shows the correspondence between the parameter σ and the number of connections N_c. This result is obtained after a rigorous dimensioning of the model (Noticed that the dimensioning of the model only takes into account the case of eighteen cables). We observe that by increasing the number of cables, their contribution on the dynamic of the bridge also increase and then starting from the 16^{th} cable, saturates.

To validate the accuracy of the proposed analytical predictions, we solve numerically Eq. (109) using the SRK4 method [118] to display the shape of the basin of attraction.

Fig. 16 shows the sequence of the safe basin of system (109) plotted in order to verify the results provided by the Melnikov analysis. We first observe that for $\Omega = 0.75$ and $(\lambda/\Gamma) = 0.9$, the shape of the basins boundaries is regular. This reliability can be periodic for lower values of noise (Fig. 16(a), $\gamma = 0.003$) or random for higher values of noise (Fig. 16(b), $\gamma = 1.0$). These observations had already been predicted by the analytical developments. Second, we take $\Omega = 0.75$ and $(\lambda/\Gamma) = 0.15$, the fractal boundaries of the safe basins have turned up, especially when the intensity of stochastic velocity is low (Fig. 16(c), $\gamma = 0.003$). By considering the highest values of this intensity, another rich motion occurred in our system: "Random chaos motion" (see Fig. 16(d), $\gamma = 1.0$),

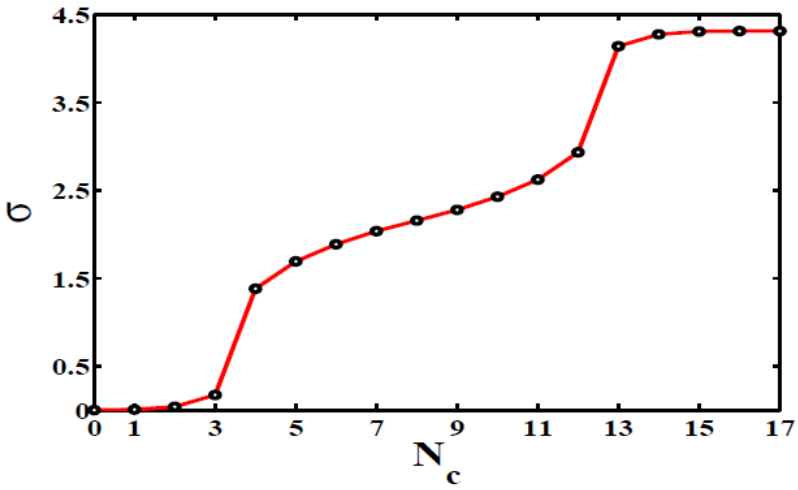

Figure 15: *Transversal contribution of cable connections* σ *as function of their number* N_c.

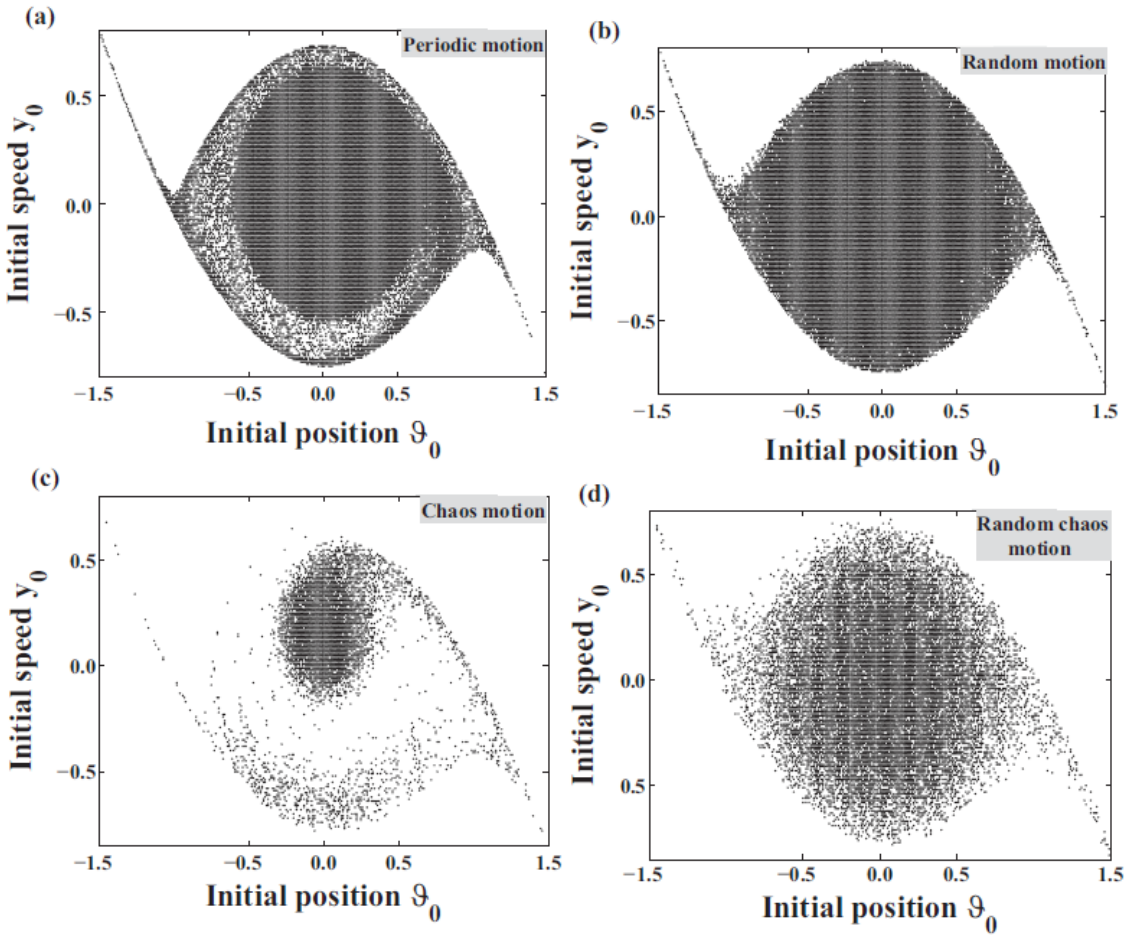

Figure 16: *Basins of attraction showing the confirmation of the analytical prediction for* $\alpha = 0.0$, $\Omega = 0.75$*:* $(\lambda/\Gamma) = 0.9$*; (a)* $\gamma = 0.003$*, (b)* $\gamma = 1.0$ *and* $(\lambda/\Gamma) = 0.15$*; (c)* $\gamma = 0.003$*, (d)* $\gamma = 1.0$.

as predicted by the frontier of Fig. 13(a). Fig. 17 reveals the interesting role of cables stayed on the bridge safety. In fact, by increasing the number of cables (increasing of α) on the bridge, that enlarges the basin of attraction area and the fractality disappears progressively (for the chosen parameters here, the system goes from random chaos motion to random motion as α increases), increasing consequently the degree of predictibility of the system. This leads us to the conclusion that, the numerical range is closed to the analytical one.

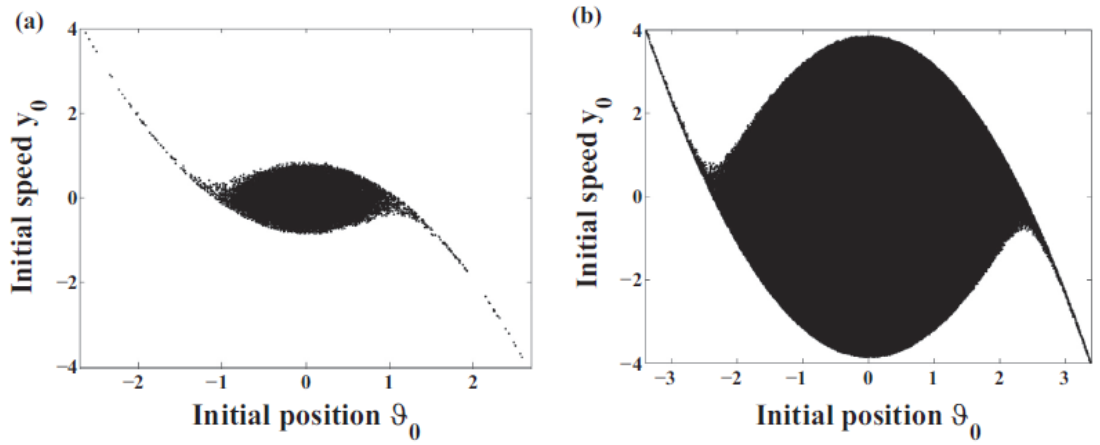

Figure 17: *Effects of cable contribution α on the basins of attraction: (a) $\alpha = 0.1$ (b) $\alpha = 4.2$. For $(\lambda/\Gamma) = 0.15$, $\Omega = 0.75$ and $\gamma = 1.0$*

As short conclusion of this part, notice that the identification of some rich dynamical behaviors such as periodic, random, chaos and random chaos in a cable-stayed bridge model has been investigated analytically and validated numerically. We have found that, the intensity of the random component of the loads velocity and stay cables contribution influence strongly the structure failure, the struture unpredictibility and the possible appearance of horseshoes chaos in system.

III-2-3- Probability or statistics response of a two lane slab-type-bridge due to traffic flow

III-2-3-1- The Bridge model and the mathematical formulation

The beam model was often adopted to study the vibration of girder bridges under moving vehicles and trains. However, it is inadequate to model the response of wide bridge decks such as slab bridges, particularly under moving vehicles whose paths are not along the centre-line of the bridge. For this reason and in order to come more close to the reality, the vibration of slab bridge modelled as thin rectangular plate under the action of vehicles is investigated in this subsection.

Let us consider a two lane slab-type-bridge modelled by a Simply Supported (SS) thin rectangular plate (of length a, width b and thickness h) with two separate rectilinear

paths and subjected to two opposite series of moving forces with random values A_{ij} (vehicle weights) appearing at random times t_{ij}, as shown in Fig. 18.

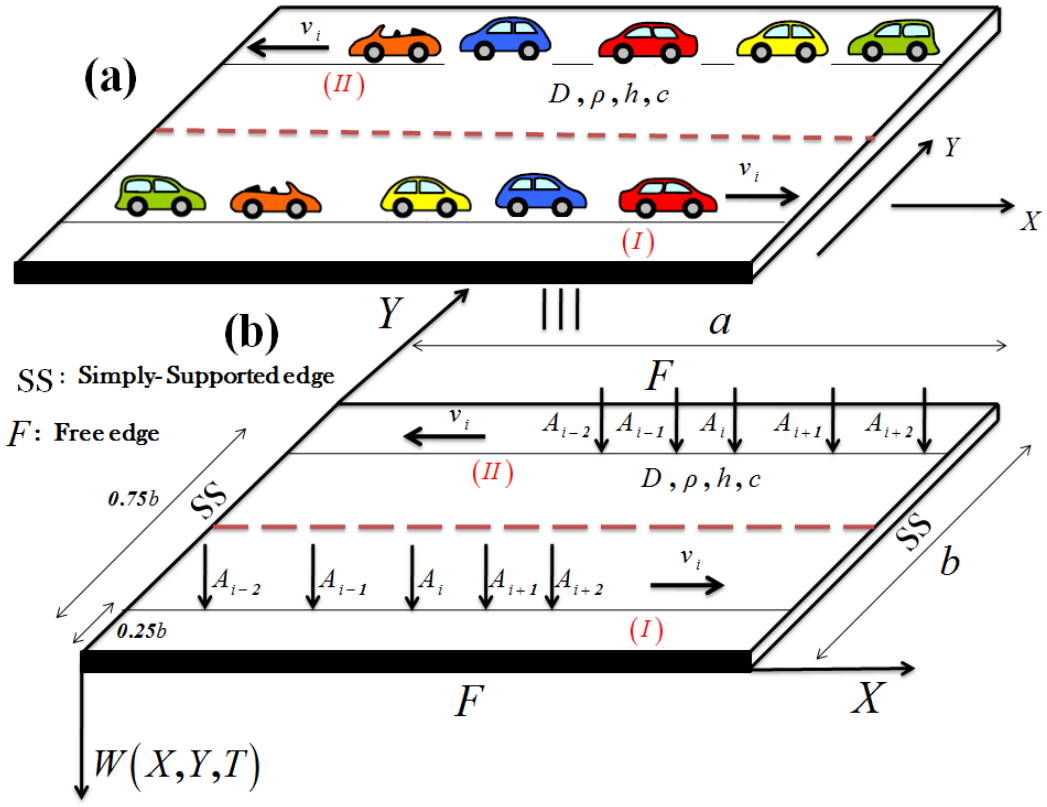

Figure 18: *The general plan of a two lane slab-type bridge model and its loading (a). The simplified scheme of the model (b).*

Such an excitation process is an appropriate model of vehicular traffic loads acting on the bridge. The plate is assumed to behave according to the Kirchhoff's hypothesis [145]. Thus, vibrations of the plate due to these random forces are described by the following equation:

$$\rho h \frac{\partial^2 W}{\partial T^2} + c\frac{\partial W}{\partial T} + D\left[\frac{\partial^4 W}{\partial X^4} + \frac{\partial^4 W}{\partial X^2 \partial Y^2} + \frac{\partial^4 W}{\partial Y^4}\right] = P\left(X, Y, T\right) \tag{120}$$

where $W(X, Y, T)$ denotes vertical deflection of the plate at point X, Y, and time T. $D = Eh^3/12\left(1-\upsilon^2\right)$ is the bending rigidity of the plate, with h, E, υ are the thickness, elastic modulus and Poisson's ratio of the plate, respectively. ρ represents the mass per unit of volume of the plate, c the damping coefficient of the plate and $P\left(X, Y, T\right)$ denotes the load process. In the case of a random train of forces (vehicles) moving in opposite directions in two separate rectilinear paths ($n_l = 2$), the loading process has a form:

$$P\left(X, Y, T\right) = \sum_{j=1}^{n_l} \sum_{i=1}^{N_j(T)} A_{ij}\delta\left[X - X_{ij}\left(T - T_{ij}\right)\right]\delta\left[Y - Y_{0j}\right] \tag{121}$$

where $\delta[...]$ stands for the Dirac delta function, A_{ij} are the weights which are assumed to be random variables, mutually independent and also independent of the instants t_{ij} (arrival times of the moving forces), Y_{0j} is the deterministic y-coordinate that fixes the position of each traffic lane, n_l is the number of traffic lane considered and $N_j(T)$ is the number of forces that acted on the plate from the beginning of observation up to the time T and that describes the Poisson process. $X_{ij}(T-T_{ij})$ is the distance covered by the i^{th} force moving one by one to the time T on the j^{th} traffic lane. It is assumed that one of a random train of forces traverses the plate on the following rectilinear trajectory:

$$\frac{dX_{ij}(T-T_{ij})}{dT} = v_{ij}(T-T_{ij}) = \varepsilon_j v_{0j} + \sigma_{vj}\xi_{ij}(T-T_{ij})$$

$$Y_{0j} = \begin{cases} 0.25b & \text{For the trajectory (I)}, \quad \varepsilon_j = 1 \\ \\ 0.75b & \text{For the trajectory (II)}, \varepsilon_j = -1 \end{cases} \tag{122}$$

$$0 \le X_{ij}(T-T_{ij}) \le a$$

where $v_{ij}(T-T_{ij})$ is the stochastic velocity of the i^th force, that moving in the traffic lane j. v_{0j} presents the mean value of velocity, σ_{vj} its standard deviation and $\xi_{ij}(T-T_{ij})$ the velocity disturbance. The function ε_j is introduced and defined as: $\varepsilon_j = 1$ when the loads are crossing the plate in one of their rectilinear path (trajectory (I) of Fig. 18), and $\varepsilon_j = -1$ for the other line of the loads trajectory (trajectory (II) of Fig. 18). It is assumed that, the force disturbances $\xi_{ij}(T-T_{ij})$ are stationary random processes, here the mutually independent Gaussian white noise processes, i.e.

$$\mathrm{E}[v_{ij}(T-T_{ij})] = v_{0j}, \quad \mathrm{E}[\xi_{ij}(T-T_{ij})] = 0$$

$$\mathrm{E}[\xi_{ij}(T-T_{ij})\,\xi_{kl}(T-T_{ij})] = 0 \quad \text{for } (k,l) \neq (i,j), \tag{123}$$

$$\mathrm{E}[\xi_{ij}(T-T_{ij})\,\xi_{ij}(T-T_{ij}+\tau)] = \Delta_j^2 \delta(\tau)$$

where E[...] denotes the expected value of the quantity in brackets and $\Delta_j = v_{oj}\sigma_{vj}$. In order to improve the accuracy of the numerical calculation, the following dimensionless variables are defined as follows:

$$w = \frac{W}{h}, \; x = \frac{X}{a}, \; y = \frac{Y}{b}, \; t = \omega_0 T; \qquad x \in [0,\,1], \quad y \in [0,\,1] \tag{124}$$

Eq. (120) takes the form:

$$\frac{\partial^2 w}{\partial t^2} + \mu\frac{\partial w}{\partial t} + \frac{\partial^4 w}{\partial x^4} + 2\Big(\frac{a}{b}\Big)^2 \frac{\partial^4 w}{\partial x^2 \partial y^2} + \Big(\frac{a}{b}\Big)^4 \frac{\partial^4 w}{\partial y^4} = P(x,y,t) \tag{125}$$

with

$$\omega_0 = \frac{1}{a^2}\sqrt{\frac{D}{\rho h}},\ \mu = \frac{ca^2}{\sqrt{\rho h D}},\ P(x,y,t) = \frac{a^4}{Dh}P(X,Y,T) \tag{126}$$

Eq. (122) takes the dimensionless form:

$$\begin{gathered}
\frac{dx_{ij}(t-t_{ij})}{dt} = u_{ij}(t-t_{ij}) = \varepsilon_j u_{0j} + \sigma_{vj}\zeta_{ij}(t-t_{ij}) \\
y_{0j} = \begin{cases} 0.25 & \text{For the trajectory (I)},\ \ \varepsilon_j = 1 \\ 0.75 & \text{For the trajectory (II)}, \varepsilon_j = -1 \end{cases} \\
0 \le x_{ij}(t-t_{ij}) \le 1
\end{gathered} \tag{127}$$

where:

$$u_{0j} = \frac{v_{0j}}{a\omega_0},\quad \zeta_{ij} = \frac{\xi_{ij}}{a\omega_0},\ x_{ij} = \frac{X_{ij}}{a},\ y_{0j} = \frac{Y_{0j}}{b}. \tag{128}$$

Since the parameters of the plate are deterministic, let the dynamic influence function $H_j(x,y,t-t_{ij})$ denote the response of the plate at the time t to the moving force when the amplitude $A_{ij}=1$. This function satisfies the following equation:

$$\begin{gathered}
\frac{\partial^2 H_j}{\partial t^2} + \mu\frac{\partial H_j}{\partial t} + \frac{\partial^4 H_j}{\partial x^4} + 2\left(\frac{a}{b}\right)^2\frac{\partial^4 H_j}{\partial x^2\partial y^2} + \left(\frac{a}{b}\right)^4\frac{\partial^4 H_j}{\partial y^4} \\
= \frac{a^3}{Dhb}1.\,\delta\left[x - x_{ij}(t-t_{ij})\right]\delta\left[y - y_{0j}\right]
\end{gathered} \tag{129}$$

and the following boundary (Simply supported one) and initial conditions are considered

$$\begin{gathered}
H_j(x,y,t-t_{ij})|_{x=0} = H_j(x,y,t-t_{ij})|_{x=1} = 0 \\
H_j(x,y,t-t_{ij})|_{y=0} = H_j(x,y,t-t_{ij})|_{y=1} = 0\,, \\
\left.\frac{\partial^2 H_j(x,y,t-t_{ij})}{\partial x^2}\right|_{x=0} = \left.\frac{\partial^2 H_j(x,y,t-t_{ij})}{\partial x^2}\right|_{x=1} = 0\,, \\
\left.\frac{\partial^2 H_j(x,y,t-t_{ij})}{\partial x^2}\right|_{y=0} = \left.\frac{\partial^2 H_j(x,y,t-t_{ij})}{\partial x^2}\right|_{y=1} = 0, \\
\left.H_j(x,y,t-t_{ij})\right|_{t=t_{ij}} = 0\,,\ \left.\frac{\partial H_j(x,y,t-t_{ij})}{\partial t}\right|_{t=t_{ij}} = 0.
\end{gathered} \tag{130}$$

To investigate the probabilistic response of the system let us derive the modal equations. To do so, Galerkin's method is applied. According to this method and by taking into account the boundary conditions of the plate, the solution of the partial differential equation

(129) is assumed to be in the form:

$$H_j\left(x,y,t-t_{ij}\right)=\sum_{n=1}^{\infty}\sum_{m=1}^{\infty}\chi_{n,m}^{(j)}\left(t-t_{ij}\right)\sin\left(n\pi x\right)\sin\left(m\pi y\right) \tag{131}$$

where $\chi_{n,m}^{(j)}\left(t-t_{ij}\right)$ is the generalized coordinates, $\sin\left(n\pi x\right)\sin\left(m\pi y\right)$ is the dimensionless solution of the eigenvalue problem which depends on the boundary conditions of the free oscillations of the plate and (n,m) is the natural mode with n and m nodal lines lying the $x-$ and $y-$directions, respectively. To apply the method, Eq. (131) is inserted into Eq. (129) and the resultant equation is multiplied by the corresponding eigenfunction and then integrated over the surface area of the plate. Thus, the dimensionless modal equation is obtained as:

$$\ddot{\chi}_{n,m}^{(j)}\left(t-t_{ij}\right)+\mu\dot{\chi}_{n,m}^{(j)}\left(t-t_{ij}\right)+\omega_{nm}^{2}\chi_{n,m}^{(j)}\left(t-t_{ij}\right)=\mathit{\Gamma}_{m}^{(j)}\sin\left[n\pi x_{ij}\left(t-t_{ij}\right)\right] \tag{132}$$

where:

$$\mathit{\Gamma}_{m}^{(j)}=1.\frac{4a^{3}\sin\left(m\pi y_{0j}\right)}{Dhb},\quad \omega_{nm}^{2}=\left[\left(n\pi\right)^{2}+\left(\frac{m\pi a}{b}\right)^{2}\right]^{2} \tag{133}$$

According to Eq. (131), we can see that:

$$\mathrm{E}\left[H_j\left(x,y,t-t_{ij}\right)\right]=\sum_{n=1}^{\infty}\sum_{m=1}^{\infty}\mathrm{E}\left[\chi_{n,m}^{(j)}\left(t-t_{ij}\right)\right]\sin\left(n\pi x\right)\sin\left(m\pi y\right)$$

$$\begin{aligned}\mathrm{E}\left[H_j\left(x_1,y_1,t_1-t_{ij}\right)H_j\left(x_2,y_2,t_2-t_{ij}\right)\right]=&\\ \sum_{k=1}^{\infty}\sum_{l=1}^{\infty}\sum_{n=1}^{\infty}\sum_{m=1}^{\infty}&\mathrm{E}\left[\chi_{k,l}^{(j)}\left(t_1-t_{ij}\right)\chi_{n,m}^{(j)}\left(t_2-t_{ij}\right)\right]\times\\ &\sin\left(k\pi x_1\right)\sin\left(l\pi y_1\right)\ \sin\left(n\pi x_2\right)\sin\left(m\pi y_2\right)\end{aligned} \tag{134}$$

III-2-3-2- Effective solution of the stochastic problem analyzed

In this subsection, an analytical approach for obtaining the probabilistic characteristics of the bridge plate response is developed and some numerical results obtained are shown.

In order to directly evaluate these probabilistic characteristics of the system response under random train of moving loads, Eq. (132) needs to be transformed using the Itô integral and the Itô differentiation rule [15, 146]. Before that, let us introduce first the

following state variables

$$\begin{aligned} z_1^{(j)}(n,m,t) &= \chi_{n,m}^{(j)}(t-t_{ij}), \\ z_2^{(j)}(n,m,t) &= \dot{\chi}_{n,m}^{(j)}(t-t_{ij}), \\ z_3^{(j)}(n,m,t) &= \sin\left[n\pi x_{ij}(t-t_{ij})\right], \\ z_4^{(j)}(n,m,t) &= \cos\left[n\pi x_{ij}(t-t_{ij})\right]. \end{aligned} \tag{135}$$

In view of Eq. (135) and according to the Itô Lemma [146], the corresponding stochastic problem for the state variables $z_i^{(j)}$; $(i=1,2,3,4)$ may be written as a following set of Itô equations:

$$\begin{aligned} \mathrm{d}z_1^{(j)}(n,m,t) &= z_2^{(j)}(n,m,t)\,\mathrm{d}t \\ \mathrm{d}z_2^{(j)}(n,m,t) &= \left[-\omega_{nm}^2 z_1^{(j)}(n,m,t) - \mu z_2^{(j)}(n,m,t) + \Gamma_m^{(j)} z_3^{(j)}(n,m,t)\right]\mathrm{d}t \\ \mathrm{d}z_3^{(j)}(n,m,t) &= \left[n\pi\varepsilon_j u_{0j} z_4^{(j)}(n,m,t) - 0.5(n\pi\sigma_{vj})^2 z_3^{(j)}(n,m,t)\right]\mathrm{d}t \\ &\quad + n\pi\sigma_{vj} z_4^{(j)}(n,m,t)\,\mathrm{d}W_{ij}(t) \\ \mathrm{d}z_4^{(j)}(n,m,t) &= \left[-n\pi\varepsilon_j u_{0j} z_3^{(j)}(n,m,t) - 0.5(n\pi\sigma_{vj})^2 z_4^{(j)}(n,m,t)\right]\mathrm{d}t \\ &\quad + n\pi\sigma_{vj} z_3^{(j)}(n,m,t)\,\mathrm{d}W_{ij}(t) \end{aligned} \tag{136}$$

where $W_{ij}(t)$ is a unit Wiener stochastic process. By appropriately applying the mathematical expectation operator, the deterministic equations for various orders of the response moments can be derived. Thus, the dynamic response of the first order probabilistic moment is described by the following set of differential equations

$$\begin{aligned} \frac{\mathrm{d}m_1^{(j)}(n,m,t)}{\mathrm{d}t} &= m_2^{(j)}(n,m,t) \\ \frac{\mathrm{d}m_2^{(j)}(n,m,t)}{\mathrm{d}t} &= -\omega_{nm}^2 m_1^{(j)}(n,m,t) - \mu m_2^{(j)}(n,m,t) + \Gamma_m^{(j)} m_3^{(j)}(n,m,t) \\ \frac{\mathrm{d}m_3^{(j)}(n,m,t)}{\mathrm{d}t} &= n\pi\varepsilon_j u_{0j} m_4^{(j)}(n,m,t) - 0.5(n\pi\sigma_{vj})^2 m_3^{(j)}(n,m,t) \\ \frac{\mathrm{d}m_4^{(j)}(n,m,t)}{\mathrm{d}t} &= -n\pi\varepsilon_j u_{0j} m_3^{(j)}(n,m,t) - 0.5(n\pi\sigma_{vj})^2 m_4^{(j)}(n,m,t) \end{aligned} \tag{137}$$

where $m_i^{(j)}(n,m,t) = \mathrm{E}\left[z_i^{(j)}(n,m,t)\right]$ and the initial conditions (according to Eqs. (130), (131) and (135)) are: $m_1^{(j)}(n,m,0)=0,\ m_2^{(j)}(n,m,0)=0, m_3^{(j)}(n,m,0)=0,\ m_4^{(j)}(n,m,0)=1$.

The differential equations to calculate the second order probabilistic moments are to be obtained, applying the differentiation formula [146] and applying the expectation operator to both sides. Thus, let us introduce the following notations for the second order probabilistic moments of variables $z_i^{(j)}(n,m,t)$

$$\begin{aligned}
m_{2000}^{(j)}(k,l,n,m,t) =& \mathrm{E}\left[z_1^{(j)}(k,l,t)\, z_1^{(j)}(n,m,t)\right] \\
m_{1100}^{(j)}(k,l,n,m,t) =& \mathrm{E}\left[z_1^{(j)}(k,l,t)\, z_2^{(j)}(n,m,t)\right] \\
m_{1010}^{(j)}(k,l,n,m,t) =& \mathrm{E}\left[z_1^{(j)}(k,l,t)\, z_3^{(j)}(n,m,t)\right] \\
m_{1001}^{(j)}(k,l,n,m,t) =& \mathrm{E}\left[z_1^{(j)}(k,l,t)\, z_4^{(j)}(n,m,t)\right] \\
m_{0200}^{(j)}(k,l,n,m,t) =& \mathrm{E}\left[z_2^{(j)}(k,l,t)\, z_2^{(j)}(n,m,t)\right] \\
m_{0110}^{(j)}(k,l,n,m,t) =& \mathrm{E}\left[z_2^{(j)}(k,l,t)\, z_3^{(j)}(n,m,t)\right] \\
m_{0101}^{(j)}(k,l,n,m,t) =& \mathrm{E}\left[z_2^{(j)}(k,l,t)\, z_4^{(j)}(n,m,t)\right] \\
m_{0020}^{(j)}(k,l,n,m,t) =& \mathrm{E}\left[z_3^{(j)}(k,l,t)\, z_3^{(j)}(n,m,t)\right] \\
m_{0011}^{(j)}(k,l,n,m,t) =& \mathrm{E}\left[z_3^{(j)}(k,l,t)\, z_4^{(j)}(n,m,t)\right] \\
m_{0002}^{(j)}(k,l,n,m,t) =& \mathrm{E}\left[z_4^{(j)}(k,l,t)\, z_4^{(j)}(n,m,t)\right]
\end{aligned} \tag{138}$$

After some rigorous algebraic calculations, we then obtain

$$\begin{aligned}
\frac{\mathrm{d}m_{2000}^{(j)}(k,l,n,m,t)}{\mathrm{d}t} &= m_{1100}^{(j)}(k,l,n,m,t) + m_{1100}^{(j)}(n,m,k,l,t) \\
\frac{\mathrm{d}m_{1100}^{(j)}(k,l,n,m,t)}{\mathrm{d}t} &= m_{0200}^{(j)}(k,l,n,m,t) - \omega_{nm}^2 m_{2000}^{(j)}(k,l,n,m,t) - \mu m_{1100}^{(j)}(k,l,n,m,t) \\
&\quad + \Gamma_m^{(j)} m_{1010}^{(j)}(k,l,n,m,t) \\
\frac{\mathrm{d}m_{1010}^{(j)}(k,l,n,m,t)}{\mathrm{d}t} &= m_{0110}^{(j)}(k,l,n,m,t) + n\pi\varepsilon_j u_{0j} m_{1001}^{(j)}(k,l,n,m,t) - 0.5(n\pi\sigma_{vj})^2 m_{1010}^{(j)}(k,l,n,m,t) \\
\frac{\mathrm{d}m_{1001}^{(j)}(k,l,n,m,t)}{\mathrm{d}t} &= m_{0101}^{(j)}(k,l,n,m,t) - n\pi\varepsilon_j u_{0j} m_{1010}^{(j)}(k,l,n,m,t) - 0.5(n\pi\sigma_{vj})^2 m_{1001}^{(j)}(k,l,n,m,t) \\
\frac{\mathrm{d}m_{0200}^{(j)}(k,l,n,m,t)}{\mathrm{d}t} &= -\omega_{kl}^2 m_{1100}^{(j)}(k,l,n,m,t) - \omega_{nm}^2 m_{1100}^{(j)}(n,m,k,l,t) - 2\mu m_{0200}^{(j)}(k,l,n,m,t) \\
&\quad + \Gamma_m^{(j)} m_{0110}^{(j)}(k,l,n,m,t) + \Gamma_l^{(j)} m_{0110}^{(j)}(n,m,k,l,t) \\
\frac{\mathrm{d}m_{0110}^{(j)}(k,l,n,m,t)}{\mathrm{d}t} &= -\omega_{kl}^2 m_{1010}^{(j)}(k,l,n,m,t) - \mu m_{0110}^{(j)}(k,l,n,m,t) + n\pi\varepsilon_j u_{0j} m_{0101}^{(j)}(k,l,n,m,t) \\
&\quad - 0.5(n\pi\sigma_{vj})^2 m_{0110}^{(j)}(k,l,n,m,t) + \Gamma_l^{(j)} m_{0020}^{(j)}(k,l,n,m,t) \\
\frac{\mathrm{d}m_{0101}^{(j)}(k,l,n,m,t)}{\mathrm{d}t} &= -\omega_{kl}^2 m_{1001}^{(j)}(k,l,n,m,t) - \mu m_{0101}^{(j)}(k,l,n,m,t) - n\pi\varepsilon_j u_{0j} m_{0110}^{(j)}(k,l,n,m,t) \\
&\quad - 0.5(n\pi\sigma_{vj})^2 m_{0101}^{(j)}(k,l,n,m,t) + \Gamma_l^{(j)} m_{0011}^{(j)}(k,l,n,m,t) \\
\frac{\mathrm{d}m_{0020}^{(j)}(k,l,n,m,t)}{\mathrm{d}t} &= \pi\varepsilon_j u_{0j}\left[n m_{0011}^{(j)}(k,l,n,m,t) + k m_{0011}^{(j)}(n,m,k,l,t)\right] + nk\pi^2\sigma_{vj}^2 m_{0002}^{(j)}(k,l,n,m,t) \\
&\quad - 0.5\pi^2\sigma_{vj}^2\left[k^2+n^2\right] m_{0020}^{(j)}(k,l,n,m,t) \\
\frac{\mathrm{d}m_{0011}^{(j)}(k,l,n,m,t)}{\mathrm{d}t} &= k\pi\varepsilon_j u_{0j} m_{0002}^{(j)}(k,l,n,m,t) - n\pi\varepsilon_j u_{0j} m_{0020}^{(j)}(k,l,n,m,t) + nk\pi^2\sigma_{vj}^2 m_{0011}^{(j)}(k,l,n,m,t) \\
&\quad - 0.5\pi^2\sigma_{vj}^2\left[k^2+n^2\right] m_{0011}^{(j)}(k,l,n,m,t) \\
\frac{\mathrm{d}m_{0002}^{(j)}(k,l,n,m,t)}{\mathrm{d}t} &= -\pi\varepsilon_j u_{0j}\left[k m_{0011}^{(j)}(k,l,n,m,t) + n m_{0011}^{(j)}(n,m,k,l,t)\right] + nk\pi^2\sigma_{vj}^2 m_{0020}^{(j)}(k,l,n,m,t) \\
&\quad - 0.5\pi^2\sigma_{vj}^2\left[k^2+n^2\right] m_{0002}^{(j)}(k,l,n,m,t)
\end{aligned} \tag{139}$$

For $(k,l) \neq (n,m)$, the above set of differential equations must be completed by adding a duplicate set of equations in which the parameters (k,l) should be replaced by (n,m)

and vice versa. According to Eqs. ((130), (131) and (138)), the initial conditions are:

$$
\begin{aligned}
&m_{2000}^{(j)}(k,l,n,m,0) = m_{2000}^{(j)}(n,m,k,l,0) = 0\\
&m_{0200}^{(j)}(k,l,n,m,0) = m_{0200}^{(j)}(n,m,k,l,0) = 0\\
&m_{0020}^{(j)}(k,l,n,m,0) = m_{0020}^{(j)}(n,m,k,l,0) = 0\\
&m_{0002}^{(j)}(k,l,n,m,0) = m_{0002}^{(j)}(n,m,k,l,0) = 1\\
&m_{1100}^{(j)}(k,l,n,m,0) = m_{1100}^{(j)}(n,m,k,l,0) = 0\\
&m_{1010}^{(j)}(k,l,n,m,0) = m_{1010}^{(j)}(n,m,k,l,0) = 0\\
&m_{1001}^{(j)}(k,l,n,m,0) = m_{1001}^{(j)}(n,m,k,l,0) = 0\\
&m_{0110}^{(j)}(k,l,n,m,0) = m_{0110}^{(j)}(n,m,k,l,0) = 0\\
&m_{0101}^{(j)}(k,l,n,m,0) = m_{0101}^{(j)}(n,m,k,l,0) = 0\\
&m_{0011}^{(j)}(k,l,n,m,0) = m_{0011}^{(j)}(n,m,k,l,0) = 0
\end{aligned}
\tag{140}
$$

For the loading process, the solution of Eq. (125) is a superposition of individual response due to each train of forces moving to each lane. So the plate response may be expressed in the following form:

$$
\begin{aligned}
w(x,y,t) &= \tfrac{a^3}{Dhb}\sum_{j=1}^{n_l}\sum_{i=1}^{N_j(t)} A_{ij}H_j(x,y,t-t_{ij})\\
&= \tfrac{a^3}{Dhb}\sum_{j=1}^{n_l}\int_0^t A_j(\tau)\,H_j(x,y,t-\tau)\,\mathrm{d}N_j(\tau)
\end{aligned}
\tag{141}
$$

By taking into account the features of the Poisson process, we are looking for the expected value of the plate response in the form:

$$
\begin{aligned}
\mathrm{E}[w(x,y,t)] &= \tfrac{a^3}{Dhb}\sum_{j=1}^{n_l}\mathrm{E}[A_j]\int_0^t \mathrm{E}[H_j(x,y,t-\tau_j)]\lambda_j(\tau)\,\wp\{x_j(t-\tau_j)<1\}\,\mathrm{d}\tau_j\\
&= \tfrac{a^3}{Dhb}\sum_{j=1}^{n_l}\mathrm{E}[A_j]\sum_{n=1}^{\infty}\sum_{m=1}^{\infty}\sin(n\pi x)\sin(m\pi y)\times\\
&\int_0^t m_1^{(j)}(n,m,t-\tau_j)\lambda_j(\tau)\,\wp\{x_j(t-\tau_j)<1\}\,\mathrm{d}\tau_j
\end{aligned}
\tag{142}
$$

and the variance of the plate response in the form:

$$\sigma_w^2(x,y,t) = \left(\frac{a^3}{Dhb}\right)^2 \sum_{j=1}^{n_l} \mathrm{E}\left[A_j^2\right] \int_0^t \mathrm{E}\left[H_j^2(x,y,t-\tau_j)\right] \lambda_j(\tau)\, \wp\left\{x_j(t-\tau_j) < 1\right\} \mathrm{d}\tau_j$$

$$= \sum_{j=1}^{n_l} \mathrm{E}\left[A_j^2\right] \sum_{k=1}^{\infty}\sum_{l=1}^{\infty}\sum_{n=1}^{\infty}\sum_{m=1}^{\infty} \sin(k\pi x)\sin(l\pi y)\sin(n\pi x)\sin(m\pi y)$$
$$\times \left(\frac{a^3}{Dhb}\right)^2 \int_0^t m_{2000}^{(j)}(k,l,n,m,t-\tau_j)\lambda_j(\tau)\, \wp\left\{x_j(t-\tau_j) < 1\right\} \mathrm{d}\tau_j \tag{143}$$

where $\lambda_j(\tau)$ is the arrival rate for the j^{th} loads trajectory, $\wp\left\{x_j(t-\tau_j) < 1\right\}$ is the unknown function which describing the fact that the probability that the forces occurring in time τ_j at the beginning of each rectilinear path j of the plate is still acting on to the structure in time t. This function can be evaluated by first looking for the transition probability density function $f(x_{ij}, t-t_{ij})$ for the process $x_{ij}(t-t_{ij})$ (describes by Eq. (127)) which is governed by the following F-P-K equation.

$$\frac{\partial f(x_{ij},t-t_{ij})}{\partial t} + \varepsilon_j u_{0j} \frac{\partial f(x_{ij},t-t_{ij})}{\partial x_{ij}} + \frac{1}{2}\sigma_{vj}^2 \frac{\partial^2 f(x_{ij},t-t_{ij})}{\partial x_{ij}^2} = 0 \tag{144}$$

By using the Fourier transform, the normalization condition and the following formulas,

$$f(x_{ij},t-t_{ij})\Big|_{\,t=\,t_{ij}} = \delta(x_{ij}), \quad f(x_{ij},t-t_{ij})\Big|_{\,x_{ij}=\infty} = 0 \tag{145}$$

the solution of Eq. (144) is given as:

$$f(x_{ij},t-t_{ij}) = \frac{1}{\mu_{ij}}\sqrt{\frac{2}{\pi(t-t_{ij})}}\exp\left[-\frac{(x_{ij}-\varepsilon_j u_{0j}(t-t_{ij}))^2}{2\sigma_{vj}^2(t-t_{ij})}\right]$$
$$\text{For} \quad x_{ij} \geq 0\,, \quad j = 1,2. \tag{146}$$

Thus, the probability $\wp\left\{x_{ij}(t-t_{ij}) < 1\right\}$ that we are looking for takes a form:

$$\wp\left\{x_{ij}(t-t_{ij}) < 1\right\} = \int_0^1 f(x_{ij},t-t_{ij})\,\mathrm{d}x_{ij}$$
$$= \frac{1}{\mu_{ij}\sqrt{2}}\left[\sigma_{vj}\mathrm{Erf}\left(\sqrt{\frac{1}{2\sigma_{vj}^2(t-t_{ij})}} - \varepsilon_j\frac{u_{0j}}{\sigma_{vj}}\sqrt{\frac{(t-t_{ij})}{2}}\right) + \mu_{ij} - \sigma_{vj}\right] \tag{147}$$

In which

$$\mu_{ij} = \sigma_{vj}\left[1 - \mathrm{Erf}\left(-\varepsilon_j\frac{u_{0j}}{\sigma_{vj}}\sqrt{\frac{(t-t_{ij})}{2}}\right)\right] \tag{148}$$

Erf (...) is an error function.

Now, the explicit formulas for the expected value and variance for the dimensionless displacement of a thin rectangular plate subjected to two opposite train of random forces

(vehicles) were derived. In order to have a complete investigation of the dynamic behaviors of the studied system, the numerical analysis will be carried out in which the effects of some main parameters of the moving loads on the probabilistic bridge response will be analysed in the following subsection.

III-2-3-3- Numerical results obtained and their discussion

For the numerical purpose, the case of bridge plate having the following parameters are considered (see Table IV). It is assumed that the vehicles weight had a lognormal distribution with the expected value and the standard deviation equal to $\mathrm{E}[A] = 10^5$ N and $\mathrm{E}[A^2] = 1.2 \times 10^{10}\,\mathrm{N}^2$ ([14]), respectively. In this paper the problem will be confined to the homogeneous case. Therefore, the intensity of the load distribution is assumed to be constant for the simplicity: $\lambda_j(\tau) = \lambda = 0.33/\omega_0$ [15]. In traffic engineering [147], this intensity is related to the average passage speed of the vehicles and inversely. The mean value of the velocity v_{oj} varying from 10 to 50 m/s; the variation coefficient of velocity σ_{vj} varying from 0.01 to 0.3. We assume that $u_0 = u_{01} = u_{02}$. The presents numerical

Table IV: *Properties of the plate studied* [58]

Item	Notation	Value
Length	a	24 m
Width	b	8 m
Thickness	h	1 m
Young's modulus	E	50 GPa
Poisson's ratio	υ	0.3
Mass density	ρ	2400 kg/m^3
damping coefficient	c	0.91 kg/s

analysis is carried out by simulating first the deterministic Eqs. ((137) and (139)) through the RK4 algorithm. Therefore, the expected $\mathrm{E}[w(x, y, t)]$ and the standard deviation $\sigma_w^2(x, y, t)$ of the dimensionless plate displacement at the midspan ($x = 1/2, y = 1/2$) were obtained for different range of the moving loads parameters.

In Fig. 19, the average plate deformation is shown when various numbers of modes are used to analyze the response of the structure. It is quite evident that moving from a single mode (mode (1, 1)) analysis to another one, mode (1,2) the accuracy of the solution drastically increases and an abrupt change in the shape of the plate is observed. This can be explained by the fact that, moving load is commonly expected to excite more modal shape, not only the first mode. Likewise, increasing the number of modes in the analysis to (1,4) apparently decreases the solution.

Fig. 20 illustrates the relations between the normalized average flow intensity λ or the standard deviation of the stochastic velocity and the expected values and variances of a stochastic maximal plate displacement $w(x, y, t)$. It is observed first that as the value of λ increases the expected $\mathrm{E}[w]$ and standard deviation σ_w^2 of a maximal plate deflection

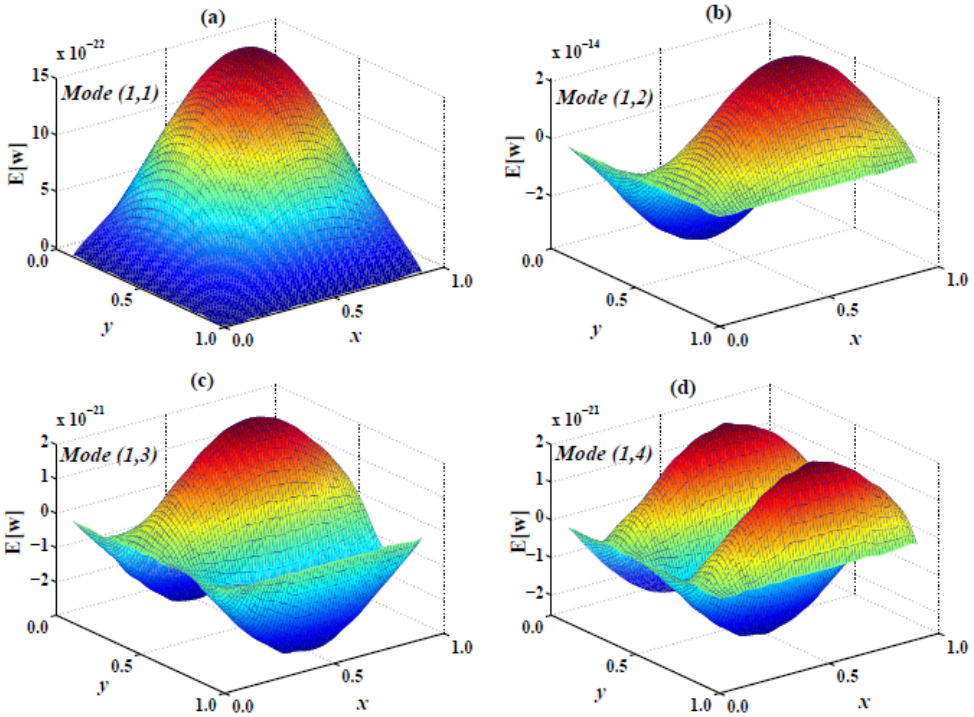

Figure 19: *Average plate deformation when* $\lambda_1 = \lambda_2 = 0.15, \sigma_{v1} = \sigma_{v2} = 0.3, u_{01} = u_{02} = 0.5$. *(a) mode (1,1), (b) mode (1,2), (c) mode (1,3) and (d) mode (1,4). The parameters used are obtained according to Eqs. ((126),(133)) and Table IV.*

merely increase (see Figs. 20(a) and 20(c)). Secondly, the increase of the value of σ_v also increases the expected and standard deviation of a maximal plate deflection (see Figs. 20(b) and 20(d)). The analysis leads us to the conclusion that it is necessary and more important to take into account the stochastic nature of the load velocity in such studies. The influence of the mean velocity on the same probabilistic features of the plate response is also investigated and we show that as the mean velocity increases, the expected value and the variance of the plate response also increase. It is also observed that for a normalized average speed $u_0 = 0.8$ (about 50 m/s), an unstable zone is observed when the standard deviation of the velocity $\sigma_v \in [0.01, 0.11]$. This unstable zone decreases as the mean velocity decreases. Fig. 21 clearly illustrates the influence of randomness velocity on the probabilistic characteristics of the bridge response such as the expected and the variance values. It is observed that the mean deflection of the bridge decreases with the standard deviation of the stochastic velocity σ_v. More interesting, it is also observed that the maximum mean deflection at mid-span bridge is obtained for the vehicle position equal to 0.85 (about 20.4 m) (fig. 21 (a), fig. 21(b)). This last result is different to the one obtained by Nikkhoo et *al.* [58] which demonstrated that the deflection at mid-span of the bridge appears in the middle of the bridge. The difference is probably due to the randomness of the velocity introduced in this work. In fig. 21 (a), fig. 21(c), the effective presence of instability in the plate response is confirmed and well illustrated. It is noted that the expected value and standard deviation of the bridge deflection in the middle of

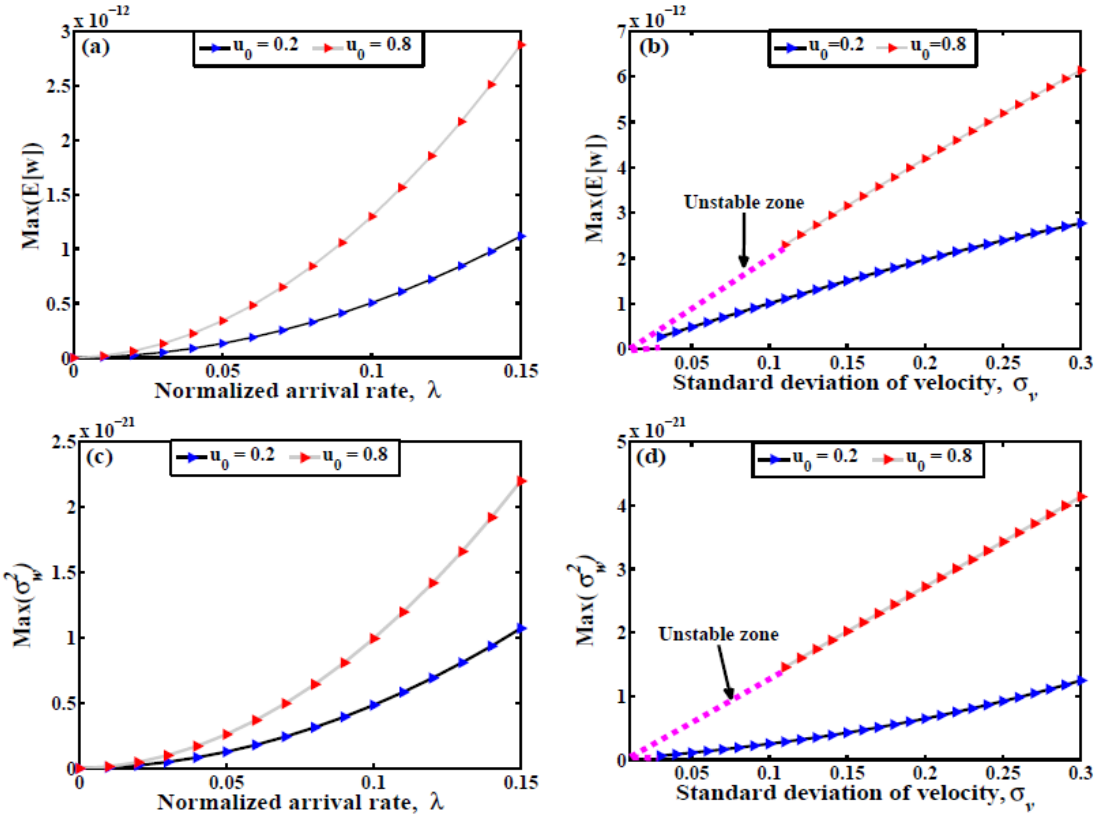

Figure 20: *The maximum expected values and variances of a plate displacement in relation to the normalized average flow intensity* λ *or the standard deviation of the stochastic velocity* σ_v*. (a), (b) expected value, (c), (d) variance. The other parameters used are obtained according to Eqs. ((126),(133)) and Table IV.*

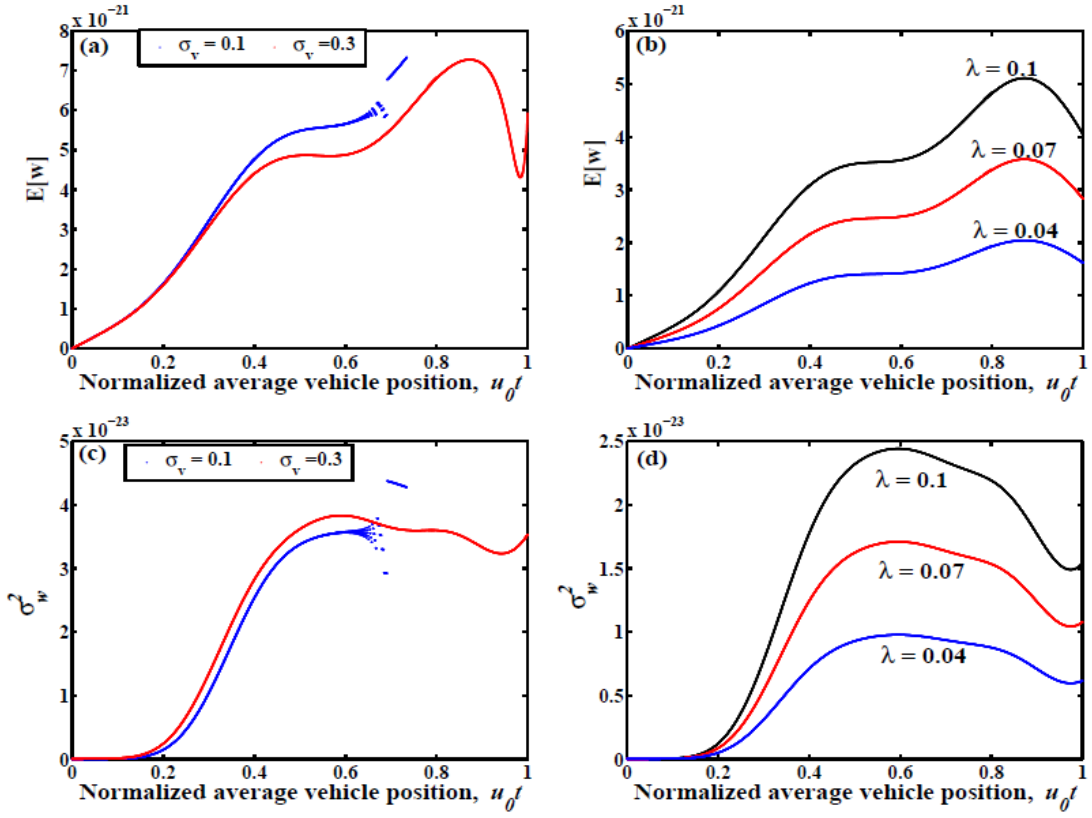

Figure 21: *The expected values and variances of a plate displacement versus the normalized average vehicle position* ($u_0 t$). *(a), (b) expected value, (c), (d) variance. The other parameters used are obtained according to Eqs. ((126),(133)) and Table IV.*

the bridge increases with the number of vehicles (see fig. 21 (b), fig. 21(d)), since that the number of vehicles $N(t)$ is related to the arrival rate λ. This result confirms well the one obtains by Nikkhoo et *al.* [58].

As short conclusion of this part, notice that the bridge safety strongly depend to the randomness of the vehicles velocities. Thus, some bridges may last more than expected or may prematurely destroy because of the effect of the intensity of these velocities.

III-3- On the dynamics of railway track and bridge-bearings systems supporting a moving train and wind action: Fractional derivative model

Recently, dynamical systems with fractional damping have brought the attention of scientists from different research fields with the expectation to describe complex system behavior and/or complex material dynamical responses [148–152]. This approach differs from the linear and nonlinear damping given by a function of velocity [153, 154]. Introducing fractional damping to a dynamical system is made by replacing an integer order derivative with a fractional operator. In this section, this approach is used to model the track structures and the bearings of the railway and girder bridges respectively. Therefore, the railway track and bridge-bearings systems are modeled as the Rayleigh beams on fractional-order viscoelastic foundation.

III-3-1- Rayleigh beams on viscoelastic Pasternak foundation supporting a sequence of equidistant moving loads: Vibratory and chaotic dynamics approaches

III-3-1-1- Mathematical modelling of a beam-foundation model

With reference to Fig. 22, consider a simply supported Rayleigh beam of finite length L, placed on a viscoelastic Pasternak foundation, subjected to a series of lumped loads P with constant interval d moving at the same direction with constant velocity v_0. The loading actions is idealized a real train moving on the bridge. It is assumed that the Pasternak viscoelastic foundation includes a Winkler foundation in conjunction with a shear layer material which is modelled here by using the constitutive equation of Kelvin-Voigt type containing fractional derivative of real order. Fractional hereditary materials involving Kelvin-Voigt units with real order fractional derivatives are analysed in Refs. [155, 156]. The soil is considered to be infinitely extending beyond the beam and the displacement originating from the beam to propagate along it (see refs. [157–159]). The deformed beam can be described by the transverse deflection $w(x,t)$ and the rotation of the cross section

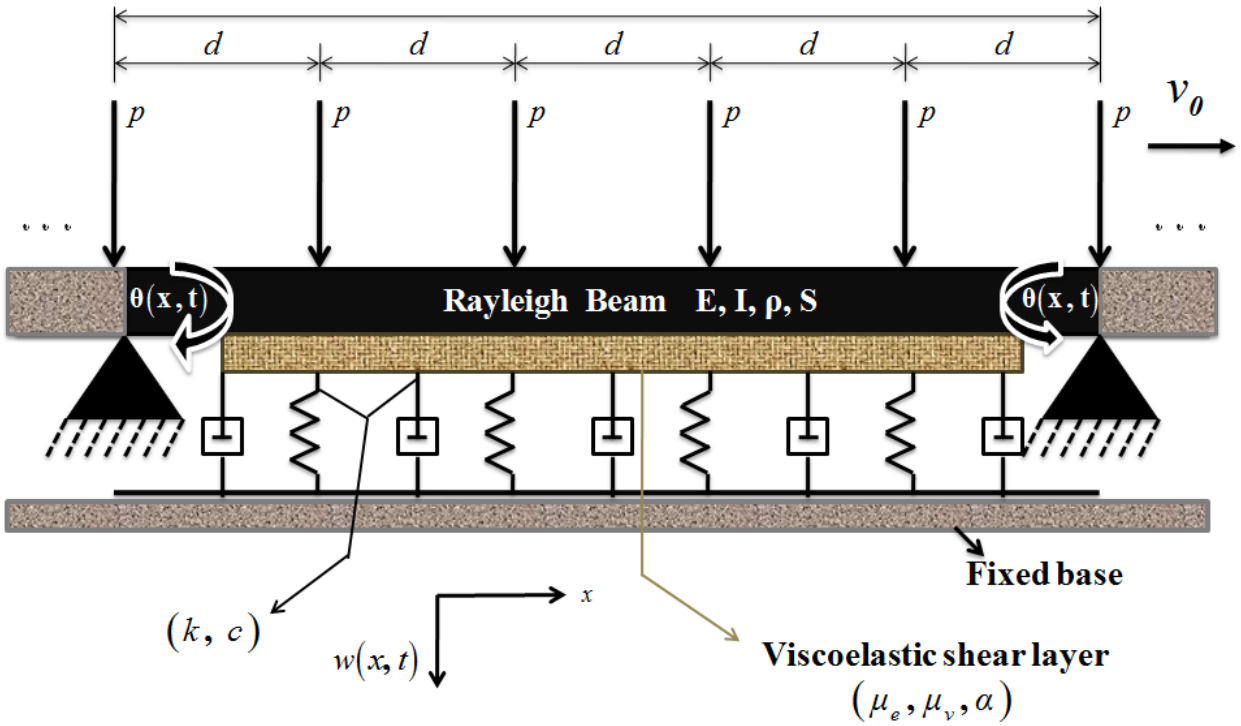

Figure 22: *Sketch of a Rayleigh beam on viscoelastic Pasternak foundation under equidistant moving loads. The gravitational forces are represented by arrows P, whose separations are uniform, for the identical speed* v_0.

of the beam $\theta(x,t)$. Considering the Newton's second law of motion for an infinitesimal element of the beam, the equation of motion for the small deformations $\left(\theta(x,t) \backsimeq \frac{\partial w(x,t)}{\partial x}\right)$ is obtained as:

$$\begin{aligned} &\rho S \frac{\partial^2 w(x,t)}{\partial t^2} + EI \frac{\partial^4 w(x,t)}{\partial x^4} - \frac{3}{2} EI \frac{\partial^2}{\partial x^2}\left[\frac{\partial^2 w(x,t)}{\partial x^2}\left(\frac{\partial w(x,t)}{\partial x}\right)^2\right] \\ &-\rho I \frac{\partial^4 w(x,t)}{\partial x^2 \partial t^2} + Q_F(x,t) = P \sum_{i=0}^{N-1} \varepsilon_i \delta\left[x - x_i(t - t_i)\right] \end{aligned} \tag{149}$$

In which S, E, I, ρ, $w(x,t)$ are cross-sectional area of the beam, the modulus of elasticity, cross-sectional moment of inertia, beam material density and the transversal deflection of the beam element, respectively. $x_i(t - t_i) = v_0(t - id/v_0)$ is the position of the i^{th} force at the time t, $t_i = id/v_0 =$ arriving time of the i^{th} load at the beam, and N is the number of the applied loads. Eq. (1) contains a nonlinear term which may be caused by large curvatures of the beam due to a high deflection [131, 132]. To facilitate a compact representation of the governing equation, a window function ε_i is employed [62]: $\varepsilon_i = 0$ when the loads have left the beam and $\varepsilon_i = 1$ while the loads are crossing the beam. Moreover, $Q_F(x,t)$ is the foundation-beam interaction force (per unit length of the beam's axis) which is obtained (including the new term containing fractional derivative) as [80]:

$$Q_F(x,t) = kw(x,t) + c\frac{\partial w(x,t)}{\partial t} - \left[\mu_e + \mu_v D_t^{\alpha}\right] \frac{\partial^2 w(x,t)}{\partial x^2} \tag{150}$$

In which k and c are foundation stiffness and damping coefficients, μ_e and μ_v are foundation shear elastic and viscosity coefficients. D_t^α is the fractional derivative with order $\alpha \in (0,1)$. There are several definitions for fractional-order derivative, and they are equivalent under some conditions for a wide class of functions. The suitable definition is that of Caputo because it provides initial conditions which physically can be explained [162].

The boundary and initial conditions corresponding to the beam shown in Fig. 22 are given by Eq. (70). For the analytical purpose, it is convenient to assume an expansion of the transversal deflection $w(x,t)$ in a series form as given in Eq. (73). So, after substituting Eq. (150) and Eq. (73) into Eq. (149), multiplying both sides of the resultant equation by the shape function $\sin(n\pi x/L)$, then integrating with respect to the beam axis x over the length L, and at last considering the following dimensionless variables

$$\chi_n = \frac{q_n}{l_r} \;\;,\;\; \tau = \omega_0 t \tag{151}$$

we obtain for the first mode of vibration [160, 161], the dimensionless modal equation (with $n=1$ and $\chi_1 = \chi(\tau)$) given by:

$$\ddot{\chi}(\tau) + 2\xi\dot{\chi}(\tau) + \Omega_0^2\chi(\tau) + \beta\chi^3(\tau) + \lambda D_\tau^\alpha \chi(\tau) = P_0 \sum_{i=0}^{N-1} \varepsilon_i \sin\Omega\left[\tau - i\frac{d\omega_0}{v_0}\right] \tag{152}$$

with

$$\begin{gathered} \Omega = \tfrac{\pi v_0}{L\omega_0}\,,\quad P_0 = \tfrac{2PL^3}{l_r EI\pi^4}\,,\quad \xi = \tfrac{cL^3}{2\pi^2\sqrt{EI\rho[L^2S+I\pi^2]}} \\ \beta = -\tfrac{3}{8}\left(\tfrac{\pi l_r}{L}\right)^2,\;\; \lambda = \eta\omega_0^\alpha\,,\;\; \eta = \tfrac{\mu_v L^2}{EI\pi^2}\,,\;\; \Omega_0^2 = 1 + \tfrac{kL^2+\mu_e\pi^2}{k_{cr}L^2} \end{gathered} \tag{153}$$

and

$$\omega_0 = \frac{\pi^2}{L}\sqrt{\frac{EI}{\rho\left(L^2S + I\pi^2\right)}}\,,\quad l_r = \frac{L}{2},\quad k_{cr} = \frac{EI\pi^4}{L^4}\,,\quad \mu_{ecr} = \frac{k_{cr}L^2}{\pi^2}. \tag{154}$$

According to the Handbook of Mangulis [163],

$$\sum_{n=1}^{m} \sin(n\sigma+\gamma) = \frac{-\sin\gamma + \sin(\gamma+\sigma) - \sin[\gamma+(m+1)\sigma] + \sin(\gamma+m\sigma)}{2(1-\cos\sigma)} \tag{155}$$

By letting $n = i$, $m = N-1$, $n\sigma = -i\frac{\Omega d\omega_0}{V_0}$, $\gamma = \Omega\tau$, and considering the configuration of the system where all the applied loads are crossing the beam ($\varepsilon_i = 1$), the sum of the second member of Eq. (152) is obtained after some trigonometric operations as

$$\begin{aligned} \sum_{i=0}^{N-1} \varepsilon_i \sin\Omega\left[\tau - i\tfrac{d\omega_0}{V_0}\right] &= \sin(\Omega\tau) + \sum_{i=1}^{N-1} \sin\Omega\left[\tau - i\tfrac{d\omega_0}{V_0}\right] \\ &= \tfrac{2\sin\left(\frac{\Omega d\omega_0}{2V_0}\right)\sin\left((N-1)\frac{\Omega d\omega_0}{2V_0}\right)}{1-\cos\left(\frac{\Omega d\omega_0}{V_0}\right)} \sin\left[\Omega\tau - N\tfrac{\Omega d\omega_0}{2V_0}\right] \end{aligned} \tag{156}$$

So Eq. (152) can be rewritten in the alternative form as

$$\ddot{\chi}(\tau)+2\xi\dot{\chi}(\tau)+\Omega_0^2\chi(\tau)+\beta\chi^3(\tau)+\lambda D_\tau^\alpha\chi(\tau)=F_{0N}\sin(\Omega\tau)-G_{0N}\cos(\Omega\tau) \quad (157)$$

where

$$\begin{aligned} F_{0N}&=P_0\left[1+\tfrac{2\sin\tilde{\tau}_0\sin((N-1)\tilde{\tau}_0)}{1-\cos(2\tilde{\tau}_0)}\cos(N\tilde{\tau}_0)\right] \ , \\ G_{0N}&=\tfrac{2P_0\sin\tilde{\tau}_0\sin((N-1)\tilde{\tau}_0)}{1-\cos(2\tilde{\tau}_0)}\sin(N\tilde{\tau}_0)\ ,\ \tilde{\tau}_0=\tfrac{d\pi}{2L}. \end{aligned} \quad (158)$$

From Eq. (157), the dynamics of the beam is that of a Duffing like oscillator with a catastrophic monostable potential since $\beta<0$. This configuration of the potential appears to be more realistic since it may explain best the full dynamics response due to small or high external excitation from a system in engineering science point of view [133].

Noticed that when all the applied loads have left the beam ($\varepsilon_i=0$), the second member of Eq. (152) is now equal to zero. Therefore, for the simplicity, we assume in this case that the dynamic response of the system is also equal to zero ($\chi(\tau)=0$). In the following section, the study of the nonlinear resonance and the stability of the steady states solutions of the considered system will be carried out.

III-3-1-2- Dynamical analysis

In this subsection, a particular attention is focused on the analytical and numerical analysis of the spacing and the velocity of the moving loads, the order of the fractional viscoelastic shear layer material and its strength on the beam response.

We start by using the averaging method [100, 164, 165], which provides an analytical approximate solution and thus permits to detect the effects of the main parameters on the system response. For that aim, let us assume that the solution of Eq. (156) can be written as given in Eq. (89).

Substituting Eq. (89) into Eq. (156), we obtain

$$\begin{cases} \dot{a}=-\frac{1}{\Omega}\left[M_1(a,\theta)+M_2(a,\theta)\right]\sin\theta \\ \\ a\dot{\varphi}=-\frac{1}{\Omega}\left[M_1(a,\theta)+M_2(a,\theta)\right]\cos\theta \end{cases} \quad (159)$$

where

$$\begin{aligned} M_1(a,\theta)&=F_{0N}\sin(\theta-\varphi)-G_{0N}\cos(\theta-\varphi)+a(\Omega^2-\Omega_0^2)\cos\theta \\ &\quad +2\xi a\Omega\sin\theta-\beta a^3\cos^3\theta \\ M_2(a,\psi)&=-\lambda D_\tau^\alpha(a\cos\theta) \\ \Omega\tau&=\theta-\varphi \end{aligned} \quad (160)$$

Then, one could apply the standard averaging method [100, 164, 165] to Eq. (159) in time interval $[0, T]$

$$\begin{cases} \dot{a} = \dot{a}_1 + \dot{a}_2 + \dot{a}_3 \\ \\ a\dot{\varphi} = a\dot{\varphi}_1 + a\dot{\varphi}_2 + a\dot{\varphi}_3 \end{cases} \tag{161}$$

where

$$\begin{aligned} \dot{a}_1 &= \lim_{T\to\infty} \tfrac{1}{T\Omega} \int_0^T - \left[F_{0N}\sin(\theta-\varphi) - G_{0N}\cos(\theta-\varphi) + a\left(\Omega^2 - \Omega_0^2\right)\cos\theta\right]\sin\theta \mathrm{d}\theta \\ \dot{a}_2 &= \lim_{T\to\infty} \tfrac{1}{T\Omega} \int_0^T \left[-2\xi a\Omega \sin^2\theta + \beta a^3 \cos^3\theta \sin\theta\right] \mathrm{d}\theta \\ \dot{a}_3 &= \lim_{T\to\infty} \tfrac{1}{T\Omega} \int_0^T \left[\lambda D_\tau^\alpha \left(a\cos\theta\right)\sin\theta\right] \mathrm{d}\theta \\ a\dot{\varphi}_1 &= \lim_{T\to\infty} \tfrac{1}{T\Omega} \int_0^T - \left[F_{0N}\sin(\theta-\varphi) - G_{0N}\cos(\theta-\varphi) + a\left(\Omega^2 - \Omega_0^2\right)\cos\theta\right]\cos\theta \mathrm{d}\theta \\ a\dot{\varphi}_2 &= \lim_{T\to\infty} \tfrac{1}{T\Omega} \int_0^T \left[-\xi a\Omega \sin 2\theta + \beta a^3 \cos^4\theta\right] \mathrm{d}\theta \\ a\dot{\varphi}_3 &= \lim_{T\to\infty} \tfrac{1}{T\Omega} \int_0^T \left[\lambda D_\tau^\alpha \left(a\cos\theta\right)\cos\theta\right] \mathrm{d}\theta \end{aligned} \tag{162}$$

after some calculation and according to Eqs. (15), (16a) and (16b), we obtain

$$\begin{aligned} \dot{a}_1 &= \tfrac{1}{2\Omega}\left[G_{0N}\sin\varphi - F_{0N}\cos\varphi\right] \\ a\dot{\varphi}_1 &= \tfrac{1}{2\Omega}\left[G_{0N}\cos\varphi + F_{0N}\sin\varphi - a\left(\Omega^2 - \Omega_0^2\right)\right] \\ \dot{a}_2 &= -\xi a \\ a\dot{\varphi}_2 &= \tfrac{3\beta}{8\Omega} a^3 \\ \dot{a}_3 &= -\tfrac{\lambda a}{2}\Omega^{\alpha-1}\sin\left(\tfrac{\alpha\pi}{2}\right) \\ a\dot{\varphi}_3 &= \tfrac{\lambda a}{2}\Omega^{\alpha-1}\cos\left(\tfrac{\alpha\pi}{2}\right) \end{aligned} \tag{163}$$

Accordingly, Eq. (161) becomes

$$\begin{cases} \dot{a} = -\xi a - \tfrac{\lambda a}{2}\Omega^{\alpha-1}\sin\left(\tfrac{\alpha\pi}{2}\right) + \tfrac{1}{2\Omega}\left[G_{0N}\sin\varphi - F_{0N}\cos\varphi\right] \\ \\ a\dot{\varphi} = \tfrac{1}{\Omega}\left[-\tfrac{a\left(\Omega^2-\Omega_0^2\right)}{2} + \tfrac{3\beta}{8}a^3\right] + \tfrac{\lambda a}{2}\Omega^{\alpha-1}\cos\left(\tfrac{\alpha\pi}{2}\right) \\ \qquad\qquad + \tfrac{1}{2\Omega}\left[G_{0N}\cos\varphi + F_{0N}\sin\varphi\right] \end{cases} \tag{164}$$

(a) Steady state solutions and its stability analysis

Now, we study the steady state solution, which is more important and meaningful in vibration engineering. By putting $a = A_0, \varphi = \Phi_0$ and $\dot{a} = 0$, $\dot{\varphi} = 0$, and After eliminating Φ_0 from Eq. (164), we find that the amplitude A_0 of the oscillatory state satisfies the following nonlinear equation:

$$\frac{9}{16}\beta^2 A_0^6 - \frac{3}{2}\beta\Theta_1(\alpha) A_0^4 + \left[\Theta_1^2(\alpha) + \Theta_2^2(\alpha)\right] A_0^2 = F_{0N}^2 + G_{0N}^2 \tag{165}$$

with

$$\begin{aligned}\Theta_1(\alpha) &= (\Omega^2 - \Omega_0^2) - \lambda\Omega^\alpha \cos\left(\tfrac{\alpha\pi}{2}\right) \\ \Theta_2(\alpha) &= 2\Omega\xi + \lambda\Omega^\alpha \sin\left(\tfrac{\alpha\pi}{2}\right)\end{aligned} \tag{166}$$

This equation has more than one steady state solution for some parameters. An interesting observation is the dependence of the oscillations amplitude upon the beam parameters (natural frequency Ω_0^2 and nonlinear component β), the loads traffic (loads weights intensity P_0, loads number N, spacing loads d and driving frequency Ω) and of the foundation parameters (damping ξ, the order of the fractional derivative α and its strength λ).

Next, we study the stability of the steady state solution by using the method of Andronov and Witt [166]. Let $a = A_0 + \Delta_a, \quad \varphi = \Phi_0 + \Delta_\varphi$ and substituting them into Eq. (164) yields

$$\begin{cases} \frac{\mathrm{d}\Delta_a}{\mathrm{d}\tau} = -\frac{\Theta_2(\alpha)}{2\Omega}\Delta_a + \frac{A_0}{2\Omega}\left[\Theta_1(\alpha) - \frac{3\beta}{4}A_0^2\right]\Delta_\varphi \\ \frac{\mathrm{d}\Delta_\varphi}{\mathrm{d}\tau} = \frac{1}{2\Omega A_0}\left[\frac{9\beta}{4}A_0^2 - \Theta_1(\alpha)\right]\Delta_a - \frac{\Theta_2(\alpha)}{2\Omega}\Delta_\varphi \end{cases} \tag{167}$$

where $\Theta_1(\alpha)$ and $\Theta_2(\alpha)$ are given by Eq. (166). The stability of the steady state solution is determined by the eigenvalues of the corresponding Jacobian matrix of Eq. (167). The corresponding eigenvalues Λ are the roots of

$$\Lambda^2 + \frac{\Theta_2(\alpha)}{\Omega}\Lambda + \left(\frac{\Theta_2(\alpha)}{2\Omega}\right)^2 + \frac{1}{4\Omega}\left[\frac{3\beta}{4}A_0^2 - \Theta_1(\alpha)\right] \times \left[\frac{9\beta}{4}A_0^2 - \Theta_1(\alpha)\right] = 0 \tag{168}$$

Since $0 < \alpha \leq 1$, then $\Theta_2(\alpha) > 0$ and the instability condition for the steady-state solution is found by using the Routh-Hurwitz criterion [103, 167] as

$$\left(\frac{\Theta_2(\alpha)}{2\Omega}\right)^2 + \frac{1}{4\Omega}\left[\frac{3\beta}{4}A_0^2 - \Theta_1(\alpha)\right] \times \left[\frac{9\beta}{4}A_0^2 - \Theta_1(\alpha)\right] < 0 \tag{169}$$

This condition keeps the real parts of the eigenvalues positive. The asymptotically stable solution may occur in the opposite case.

(b) Numerical analysis

The physical and geometrical properties of the beam are listed in Table V.

In order to verify the precision of the analytical solutions, we first solve numerically Eq. (156) using the Newton-Leipnik algorithm [114, 162] that considering the Grünwald-Letnikov definition of the fractional order derivative (Eq. (63)).

Table V: *Properties of the Beam, Foundation and Moving load* [51, 144]

Item	Notation	Value
Beam		
Length	L	628.1 m
Young's modulus (steel)	E	200 MPa
Cross-sectional area	S	4.8 m^2
Mass density	ρ	7850 kg/m^3
Moment of inertia	I	12 m^4
Foundation		
Stiffness	k	202.66 N/m^2
Viscous damping	c	192.0 $N.S/m^2$
Shear viscosity coefficient	μ_v	5×10^6N.S
Shear stiffness coefficient	μ_e	5×10^5N
Moving load		
Load	P	350 kN
Mean velocity	v_0	30 m/s

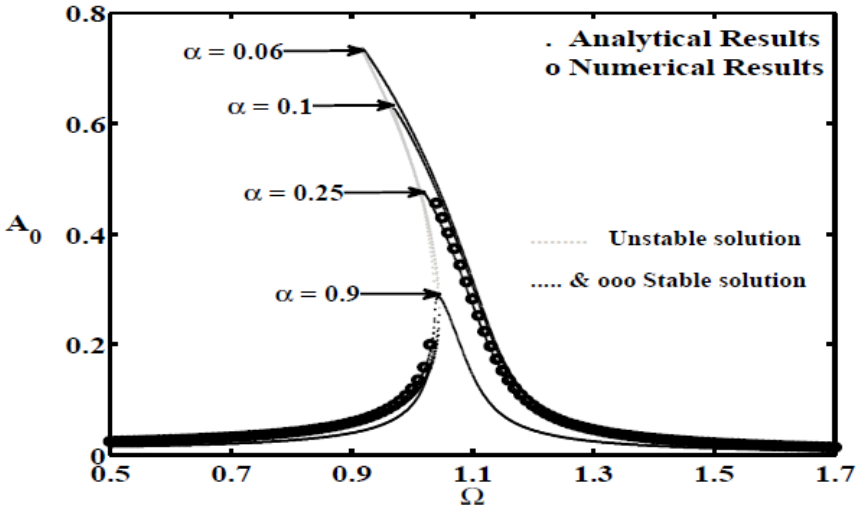

Figure 23: *Amplitude response of the system A_0 as function of the driven frequency Ω for different values of the fractional-order α. $N = 16$, $d = L/(N-1)$*

Second, we display in some figures the effects of the main parameters of the proposed model. For example, Fig. 23 shows the effects of the order of the derivative on the amplitude of vibration of the beam. This graph also shows a comparison between the results from the mathematical analysis (curve with dotted line) and the results obtained from numerical simulation of Eq. (156) (curve with circles for $\alpha = 0.25$) using the definition of Eq. (63). The match between the results shows a good level of precision of the approximation made in obtaining Eq. (165). This figure also reveals that as the order of the derivative increases, the resonant amplitude of the beam vibration decreases. Similar results were obtained by Shen et al. [165] who analyzed the periodic vibration of a Duffing oscillator with additional fractional damping and showed that increasing the order of the derivative (damping term) results in a decrease of the amplitude of vibration. For small

order derivative, the bending degree of the curves becomes severe, which leads to multiple amplitude solutions and the appearance of the unstable solution.

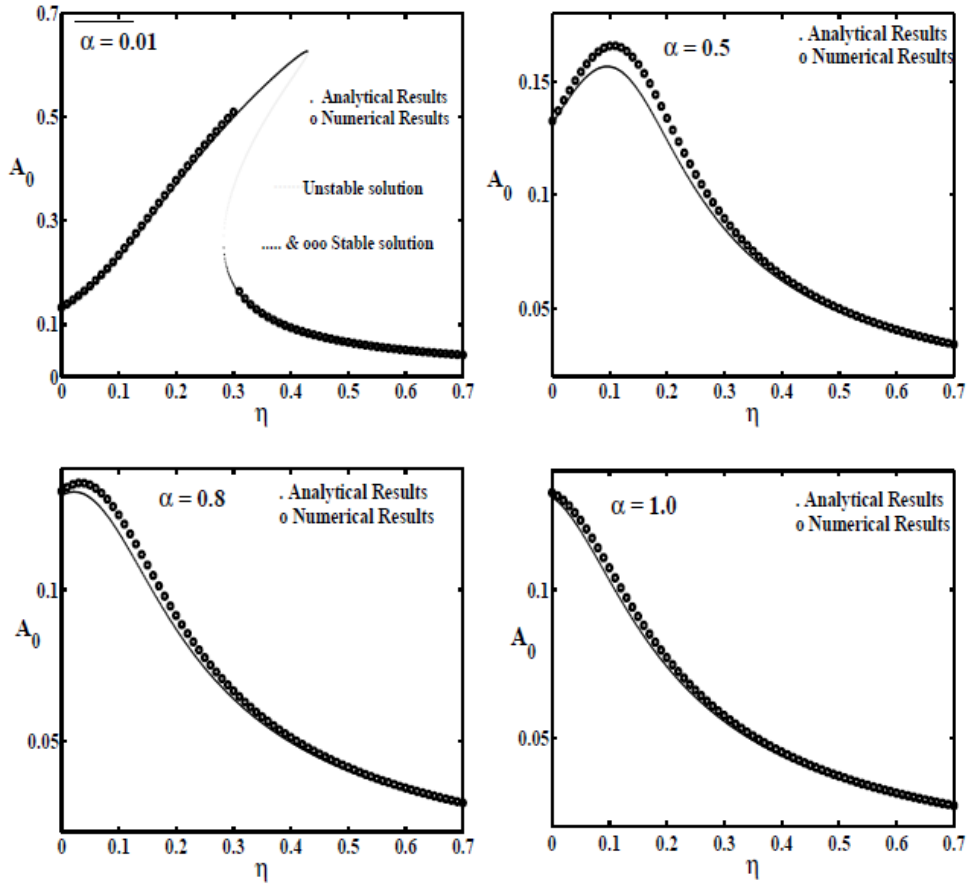

Figure 24: *The steady-state amplitude of the beam A_0 as function of the shear viscosity coefficient η for several order of the derivative. $N = 16$, $\Omega = 1.14$, $d = L/(N-1)$*

In Fig. 24, we have plotted the evolution of the amplitude of vibration of the beam A_0 as a function of the shear viscosity coefficient η for several orders of the derivative. It clearly shows that the system is more stable for the highest order of the derivative. The multivalued solution appears for small order and disappears progressively as the order increases.

Fig. 25 shows how an increase in the number of the moving loads affects the amplitude of vibration of the beam. It is observed that as the value of N increases, the amplitude of vibration at the resonant state merely increases. Second, the effect of spacing loads is investigated. It is found that when the moving loads are uniformly distributed upon all the length of the structure, it vibrates the least possible.

The so-called force-response curve is depicted in Fig. 26. Here, multiple and up to three coexisting solutions (the dotted and circles lines correspond to stable and unstable branches, respectively) are observed. In particular, there are three coexisting solutions for $P_{01} < P_0 < P_{02}$, and exactly one solution branch outside this region of bistability. The stable (dotted line) and unstable (circles line) branches merge at $P_0 = P_{01}$ and $P_0 = P_{02}$.

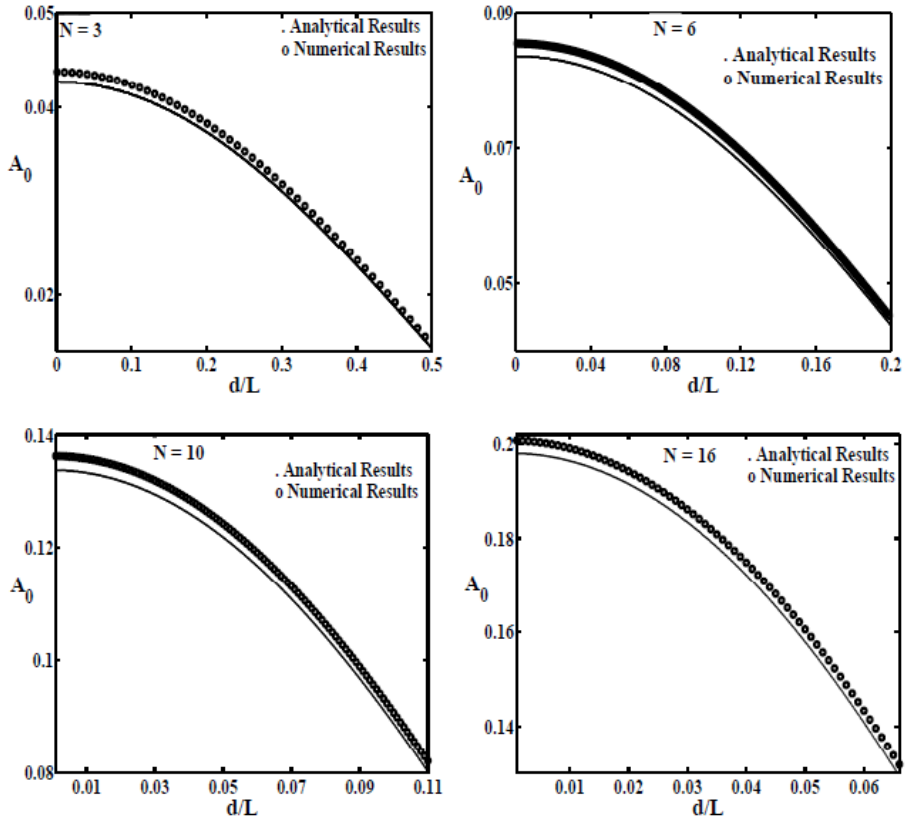

Figure 25: *Vibration amplitude of the beam A_0 for different values of the loads number N versus the dimensionless spacing loads d/L. $\alpha = 0.8$, $\Omega = 1.14$.*

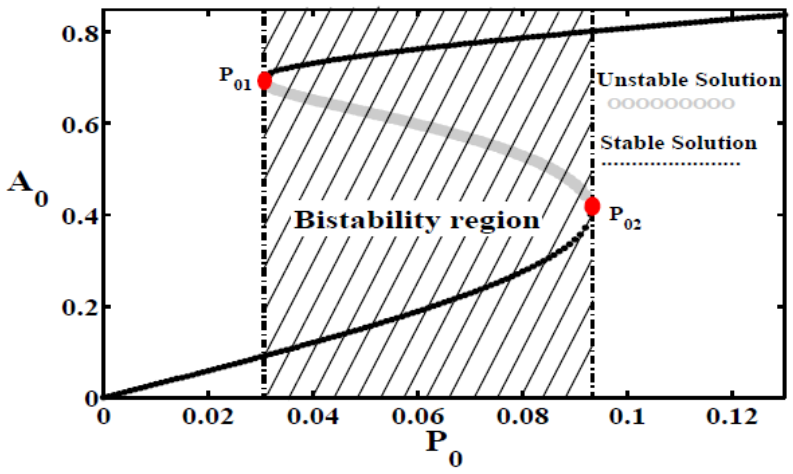

Figure 26: *Force-response curve for $\alpha = 0.8$, $\Omega = 0.9$, $N = 3$, $d = L/(N-1)$.*

For the practical convenience, it is important to note that, the bistability region (hatched zone of Fig. 26) gives the range of dangerous weight of the moving loads for the beam safety.

In this subsection, we have studied the effects of some main parameters such as α, η, N and d on the periodic solution of the system. The following subsection will investigate the peculiar effects of fractional order of the derivative and the shear viscosity coefficient on the possible appearance of the horseshoes chaos by using the Melnikov theory.

III-3-1-3- A chaotic dynamic approach for the system response

In the present subsection, we apply the Melnikov method [91, 108, 110] to detect analytically the effects of the fractional order of the derivative and the shear viscosity coefficient on the threshold condition for the inhibition of smale horseshoes chaos in the system and on the fractal basin boundaries. Many researchers have begun to investigate the chaotic dynamics of fractional-order systems [164,168]. A peculiar attention is put on the work of Oumbé *et al.* [164] who, based to the Melnikov method, demonstrated that the order and strength of the fractional viscoelastic property of the flexible material can be effectively used to control chaos in a system. Our main objective in this subsection is to use the same method to demonstrate that the order of the fractional viscoelastic shear layer material can be used either to control chaos in the beam system, or to cause chaos.

To perform the Melnikov analysis, we introduce the small parameter ε into the differential Eq. (156) and rewrite the governing system as

$$\frac{\mathrm{dU}}{\mathrm{d}\tau} = \mathrm{F}\left[\mathrm{U}\right] + \varepsilon \mathrm{G}\left[\mathrm{U}, \tau\right] \tag{170}$$

where the vector fields U, F and G are given by

$$\begin{gathered} \mathrm{U} = \begin{bmatrix} \chi \\ \\ y = \dot{\chi} \end{bmatrix}, \quad \mathrm{F} = \begin{bmatrix} y \\ \\ -\Omega_0^2 \chi - \beta \chi^3 \end{bmatrix} \\ \mathrm{G} = \begin{bmatrix} 0 \\ \\ -2\xi^* y - \lambda^* D_\tau^\alpha \chi + F_{0N}^* \sin \Omega\tau - G_{0N}^* \cos \Omega\tau \end{bmatrix} \end{gathered} \tag{171}$$

with $\xi = \varepsilon\xi^*$, $\lambda = \varepsilon\lambda^*$, $F_{0N} = \varepsilon F_{0N}^*$, $G_{0N} = \varepsilon G_{0N}^*$ and ε the perturbation parameter. But the stars (*) are removed in the following for simplicity.

For $\varepsilon = 0$, the system of Eq. (170) is the Hamiltonian system with Hamiltonian function

$$H\left(\chi, y\right) = \frac{1}{2} y^2 + \frac{1}{2} \Omega_0^2 \chi^2 + \frac{\beta}{4} \chi^4 \tag{172}$$

Since $\beta < 0$, the system has three equilibrium points that are a center point $\chi_{es} = (0, 0)$ and two saddle points $\chi_{eu\pm} = \left(\pm\sqrt{-\frac{\Omega_0^2}{\beta}}, 0\right)$. Since phase trajectories cannot cross the center, the unperturbed system shows a stable periodic motion. These trajectories are shown in Fig. 27. The saddle points surrounding the center are connected by heteroclinic orbits Eq. (113)

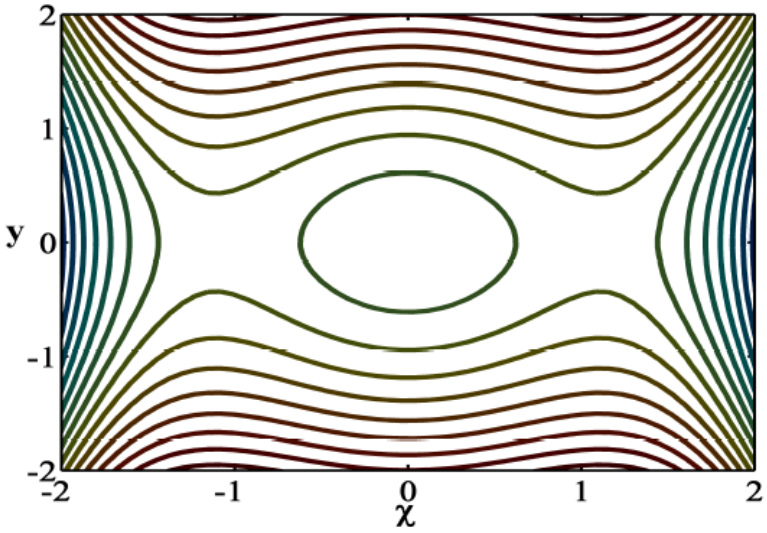

Figure 27: *Phase space trajectories.*

The Melnikov theory defines the condition for the appearance of the so-called transverse intersection points between the perturbed and the unperturbed separatrix or the appearance of the fractality on the basin of attraction. This theory can be applied in the case of Eq. (170) by using formula given by Wiggins [91] as follows

$$\begin{aligned} M_D(\tau_0) &= \int_{-\infty}^{+\infty} F\left[U_{het}(\tau)\right] \wedge G\left[U_{het}(\tau), \tau + \tau_0\right] \mathrm{d}\tau \\ &= -2\xi \int_{-\infty}^{+\infty} y_{het}^2(\tau)\,\mathrm{d}\tau - \lambda \int_{-\infty}^{+\infty} y_{het}(\tau) D_\tau^\alpha\left[\chi_{het}(\tau)\right]\,\mathrm{d}\tau + \\ F_{0N} &\int_{-\infty}^{+\infty} y_{het}(\tau)\sin\Omega(\tau+\tau_0)\,\mathrm{d}\tau \quad - G_{0N}\int_{-\infty}^{+\infty} y_{het}(\tau)\cos\Omega(\tau+\tau_0)\,\mathrm{d}\tau \end{aligned} \tag{173}$$

When the Melnikov function has simple zero point, the stable manifold and the unstable manifold intersect transversally, chaos in the sense of Smale horseshoe transform occurs. So let $M_D(\tau_0) = 0$, one concludes that horsehoes chaos appears when

$$P_0 \geq P_{0cr} = \left| \frac{2\xi\Omega_0 I_1 - \lambda\sqrt{2} I_\alpha}{\frac{\sqrt{-2\beta}}{\Omega_0} I_2 \left[1 + \frac{2\sin\tilde{\tau}_0 \sin((N-1)\tilde{\tau}_0)}{1-\cos(2\tilde{\tau}_0)} . \left(\cos(N\tilde{\tau}_0) + \sin(N\tilde{\tau}_0)\right)\right]} \right| \tag{174}$$

where

$$
\begin{aligned}
I_1 &= \frac{4\sqrt{2}}{3\Omega_0} \\
I_2 &= \frac{2\pi\Omega}{\Omega_0^2.\sinh\left[\frac{\Omega\pi}{\Omega_0\sqrt{2}}\right]} \\
I_\alpha &= \int_{-\infty}^{+\infty} \sec h^2\left[\frac{\Omega_0}{\sqrt{2}}\tau\right] D_\tau^\alpha\left[\tanh\left[\frac{\Omega_0}{\sqrt{2}}\tau\right]\right] \mathrm{d}\tau
\end{aligned}
\tag{175}
$$

The integral I_α is evaluated by using the numerical formulas for the right and left side

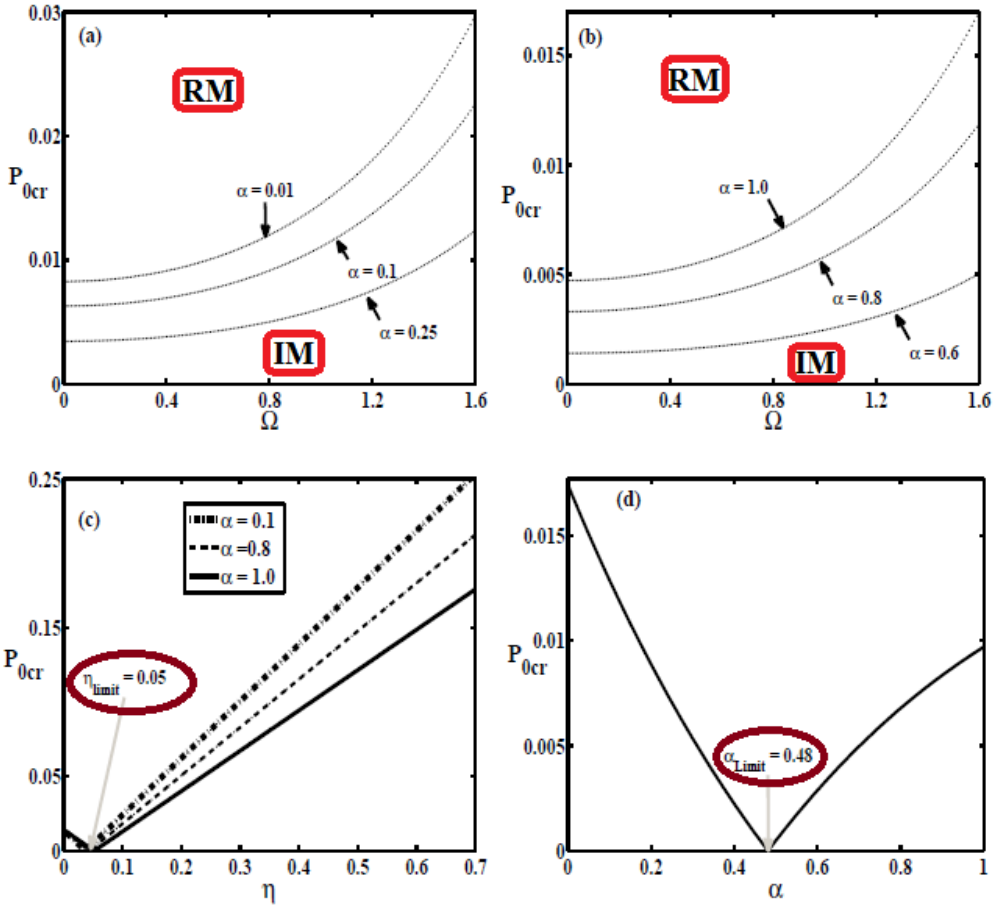

Figure 28: *Critical weight P_{0cr} for the appearance or disappearance of horseshoes chaos as a function of the system parameters. $N = 6$, $d = L/(N-1)$.*

of the fractional derivative [114, 164]. Here P_{0cr} is the threshold amplitude for the onset of horseshoes chaos in the system. This threshold condition is plotted in Fig. 28 as a function of the driving frequency Ω for different values of the fractional order α (Figs. 28(a) and 28(b)), as function of the viscosity coefficient η (Fig. 28(c)) and as function of the fractional order (Fig. 28(d)). We observe that the area below the curves (dotted line) indicates the region for regular solutions while above them the corresponding solutions have sensitivity to initial conditions, chaotic transient and fractal basin boundaries. The graph also shows that increasing the order of derivative contributes first to lower the threshold boundary for onset of chaos and then enlarges the possible chaotic domain (Fig. 28(a)), and second to rise it (reduction of the chaotic domain) (Fig. 28(b)). This

observation is well illustrated in Fig. 28(d) where we demonstrate that for $0 < \alpha < 0.48$, the threshold decreases and for $0.48 < \alpha < 1$, it increases. The same investigations are made on the case of Fig. 28(c).

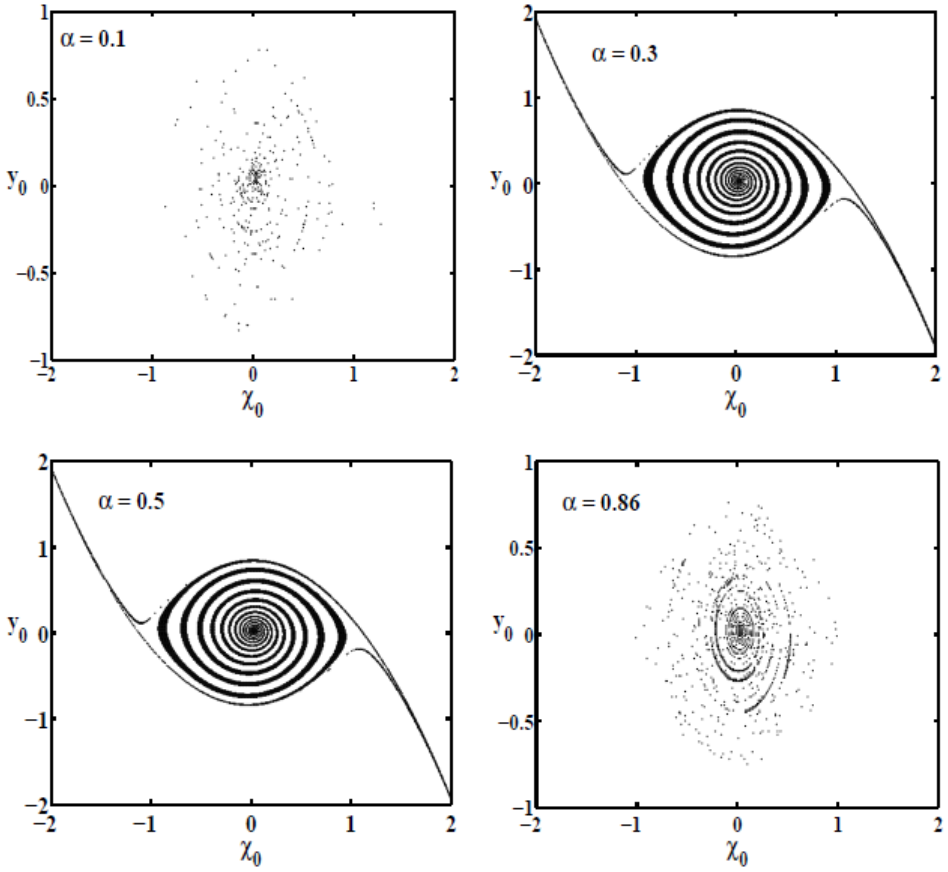

Figure 29: *Basins of attraction showing the confirmation of the analytical prediction for* $N = 6$, $\Omega = 1.14$, $P_0 = 0.02$, $d = L/(N-1)$.

To validate the accuracy of the proposed analytical predictions, we solve numerically Eq. (156) using the Newton-Leipnik method [114,162] to display the shape of the basin of attraction. A particular characteristic of the Melnikov chaos is the fractality of the basin of attraction and the resulting unpredictability due to the dependence on the initial conditions. Moreover, Awrejcewicz *et al.* [169] proved a dependence on the fractal structure of a basin of attraction on the occurrence of heteroclinic or homoclinic bifurcation taking as an example the Duffing oscillator. To check the effects of the fractional order α on the performance of our system, Fig. 8 is plotted and the metamorphoses of the basin of attraction around the central equilibrium point $(0, 0)$ are observed. It is clear that the fractal structure of the basin appears for the lowest ($\alpha = 0.1$) and highest ($\alpha = 0.86$) values of the fractional order. While the regular shape is observed for the intermediate values. These observations had already been predicted by the previously analytical developments.

In this subsection, we have studied the effects of fractional order of the derivative and the shear viscosity coefficient on the possible appearance or disappearance of the horseshoes chaos in the beam system. The results obtained here give more precision

about the effect of the fractional order on the beam stability investigated previously in subsection. It is shown how the extreme values (lowest and highest values) of the fractional order have negative effects on the system stability and positive for the intermediate values. Thus, proper selection of this fractional order can be contributed to control chaos in a system or to cause chaos. These results also explain well why it was necessary to introduce the fractional nature of the shear layer material in the model of a viscoelastic Pasternak foundation.

As short conclusion for this part, we have demonstrated firstly that, as the order of the derivative increases, the resonant amplitude of the beam vibration decreases and, when the moving loads are uniform distributed upon all the length of the structure, it vibrates the least possible. Secondly, proper selection of the shear layer of the foundation that having fractional order viscoelastic material can be contributed to suppression of chaos in a system.

III-3-2- Vibration analysis of Rayleigh beams laying on fractional-order viscoelastic bearings subject to moving loads and stochastic wind

III-3-2-1- Beam model description and equations of motion

Consider a beam of finite length L, laying on the bearings having fractional-order viscoelastic materials, subjected to combined loads of stochastic wind and moving vehicles, as shown in Fig. 30. The beam is modelled by using a Rayleigh beam theory [124] with geometric nonlinearities [102,132] (to take into account the high deflection and the assumed negligible longitudinal displacement). It is assumed that the vehicles can be modelled by several point forces P of constant intervals d moving along the bridge deck in the same direction with constant velocity v. It is also assumed that the distance between two bearings x_0 is equal to the one between one bearing and one beam end. No wind loading on the vehicles is considered since the vehicles are moving inside the bridge beam, but the effect of the wind load is applied downward to the beam axis with an attack angle α $\left(\tan(\alpha) = \frac{\dot{w}}{U}\right)$, where $w = w(x,t)$ is the deflection of the beam and U the wind flow velocity. When this angle changes or varies, the resulting divergent vibration or galloping may occur in the beam structure. The beam oscillates due to the lift force (mean force in the direction normal to U) and drag force (mean force in the direction of U). The

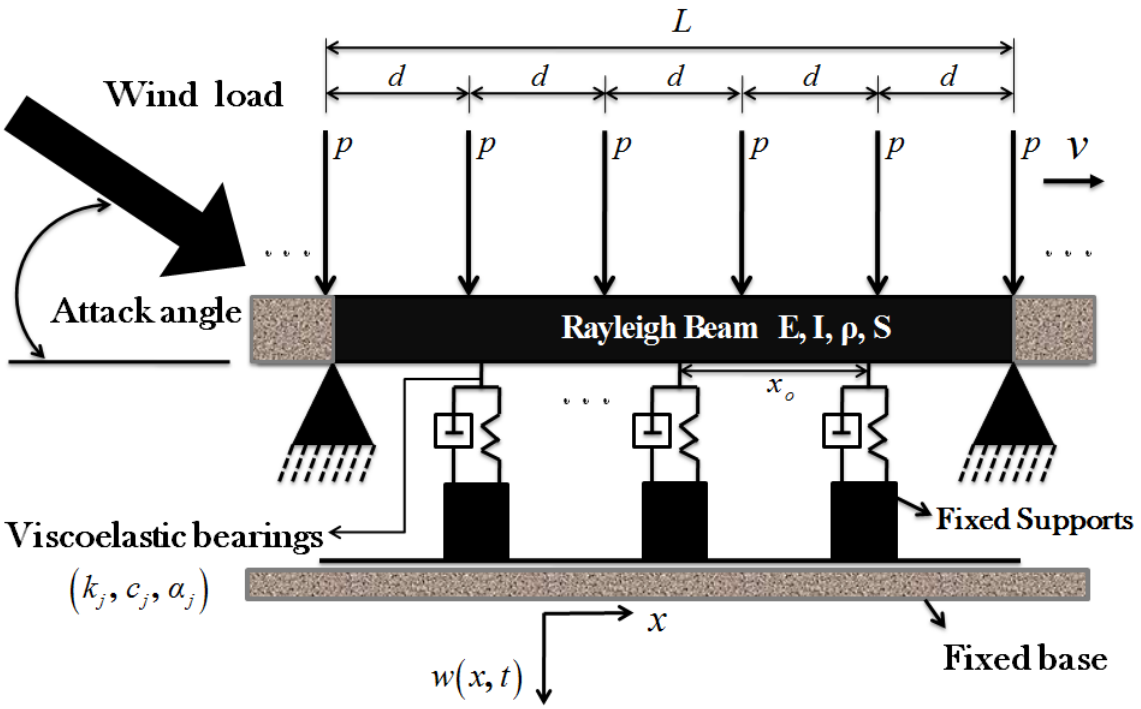

Figure 30: *Scheme of the analysed Rayleigh beam, resting on viscoelastic bearings (characterized by the parameters k_j, c_j and α_j). Loads are represented by equally spaced forces of identical intensity P moving at speed v. The load effect of the wind blowing at a speed U is also schematically represented as a force on the side of the beam.*

dynamic equation of motion for small deformations is obtained as [132]

$$\begin{aligned}&\rho S\tfrac{\partial^2 w(x,t)}{\partial t^2}+EI\tfrac{\partial^4 w(x,t)}{\partial x^4}-\tfrac{3}{2}EI\tfrac{\partial^2}{\partial x^2}\left[\tfrac{\partial^2 w(x,t)}{\partial x^2}\left(\tfrac{\partial w(x,t)}{\partial x}\right)^2\right]-\rho I\tfrac{\partial^4 w(x,t)}{\partial x^2\partial t^2}+\mu\tfrac{\partial w(x,t)}{\partial t}\\&-\tfrac{ES}{2L}\tfrac{\partial^2 w(x,t)}{\partial x^2}\int_0^L\left(\tfrac{\partial w(x,t)}{\partial x}\right)^2\mathrm{d}x+\sum_{j=1}^{N_P}\left(k_j+c_jD_t^{\alpha_j}\right)w(x,t)\,\delta\left[x-\tfrac{jL}{N_P+1}\right]=F_{ad}(x,t)\\&+P\sum_{i=0}^{N-1}\varepsilon_i\delta\left[x-x_i(t-t_i)\right]\end{aligned}\tag{176}$$

Here S, E, I, ρ, μ, $w(x,t)$ are the cross-sectional area of the beam, the modulus of elasticity, the cross-sectional moment of inertia, the beam material density, the damping coefficient of the beam and the beam transversal deflection at point x and time t, respectively. The terms k_j and c_j are the stiffness and damping coefficients of the $j-th$ bearings, respectively. The coordinate $x_i(t-t_i)=v(t-id/v)$ represents the position of the $i-th$ force at the time t, $t_i=id/v=$ the arriving time of the $i-th$ load at the beam, N_v is the number of the applied loads, N_P is the number of bearings. Eq. (176) contains two nonlinear terms which take into account the geometric nonlinearities due to a high deflection [132] and the inplane tension of the beam [102, 132]. This model is seem to be more realistic (from a bridge-system point of view) since it may explain best the transition from elastic to plastic deformation leading to rupture of the bridge under the action of high loads. ε_i is a window function [62]. In this model of moving load, the inertia of the vehicles is altogether neglected. $D_t^{\alpha_j}$ is the fractional derivative with order

$\alpha_j \in (0,1)$. The term $F_{ad}(x,t)$ is the major component of the aerodynamic force (vertical component) obtained according to Refs. [1, 170, 171] and gives by:

$$F_{ad}(x,t) = \frac{1}{2}\rho_a b U^2 \left[A_0 + \frac{A_1}{U}\frac{\partial w(x,t)}{\partial t} + \frac{A_2}{U^2}\left(\frac{\partial w(x,t)}{\partial t}\right)^2 \right], \tag{177}$$

where A_j (j = 0, 1, 2) are the aerodynamic coefficients ($A_0 = 0.0297$, $A_1 = 0.9298$, $A_2 =$ -0.2400) [170], ρ_a is the air mass density, b is the beam width. U is the wind velocity which can be decomposed as $U = \bar{u} + u(t)$, where $\bar{u}$ is a constant (average) part representing the steady component and $u(t)$ is a time varying part representing the turbulence. It is assumed in this study that the turbulence part is small compared to the steady one ($\bar{u} \gg u(t)$) and Consequently, a third order Taylor expansion of $(\bar{u} + u(t))^{-k} (k = 1, 2)$ is taken.

For the beam in Fig. 30, the displacement and flexure moment vanish at the beam ends, and the associated boundary conditions are given by Eq. (70). To investigate the dynamics of the system let us derive the modal equations. To this end, we apply the Galerkin's method by assuming that the solution of the partial differential Eq. (176) is given by Eq. (73). According to Refs. [160, 172], the Galerkin's decomposition method can be truncated to the fundamental mode of vibration ($n = 1$). Therefore, the single one-dimensional modal equation is obtained after substituting Eq. (177) and Eq. (73) into Eq. (176), and considering the following dimensionless variables,

$$\chi_n = \frac{q_n}{l_r}, \quad \tau = \omega_0 t, \quad \xi = \frac{u}{u_c}, \tag{178}$$

as

$$\begin{aligned} \ddot{\chi}(\tau) + (2\lambda - \vartheta_1)\dot{\chi}(\tau) + \chi(\tau) + \beta\chi^3(\tau) + \eta \sum_{j=1}^{N_p} \left(k_j + c_j \omega_0^{\alpha_j} D_\tau^{\alpha_j}\right)\chi(\tau) \sin^2\left(\frac{j\pi}{N_p+1}\right) \\ = \vartheta_2 \dot{\chi}^2(\tau) + \vartheta_0 + (\theta_0 + \theta_1 \dot{\chi}(\tau))\,\xi(\tau) + f_0 \sum_{i=0}^{N_v-1} \varepsilon_i \sin\Omega\left[\tau - i\frac{d\omega_0}{v}\right] \end{aligned} \tag{179}$$

with

$$\begin{aligned} &\Omega = \tfrac{\pi v}{L\omega_0}, \quad f_0 = \tfrac{2PL^3}{l_r EI\pi^4}, \quad \eta = \tfrac{2L^3}{EI\pi^4}, \quad \beta = \tfrac{l_r^2}{4}\left[\tfrac{S}{I} - \tfrac{3}{2}\left(\tfrac{\pi}{L}\right)^2\right], \\ &\vartheta_1 = \tfrac{\rho_a b L^3 A_1 \bar{u}}{2\pi^2\sqrt{EI\rho[L^2S+I\pi^2]}}, \quad \vartheta_0 = \tfrac{2\rho_a b A_0 \bar{u}^2 L^4}{EI l_r \pi^5}, \quad \vartheta_2 = \tfrac{4\rho_a b L^2 A_2 l_r}{3\rho[L^2S+I\pi^2]}, \\ &\theta_0 = \tfrac{2\bar{u}\rho_a b L^4 u_c A_0}{EI l_r \pi^6}, \quad \theta_1 = \tfrac{\rho_a b L^3 A_1 u_c}{2\pi^2\sqrt{EI\rho[L^2S+I\pi^2]}}, \quad \lambda = \tfrac{\mu L^3}{2\pi^2\sqrt{EI\rho[L^2S+I\pi^2]}}. \end{aligned} \tag{180}$$

and

$$\omega_0 = \frac{\pi^2}{L}\sqrt{\frac{EI}{\rho(L^2S + I\pi^2)}}, \quad l_r = \frac{L}{2}. \tag{181}$$

Considering the configuration of the system where the load is crossing the beam ($\varepsilon_i = 1$), the sum of the second member of Eq. (179) can be simplified according to the Handbook of Mangulis [163]. Thus, Eq. (179) can be rewritten as

$$\begin{aligned}\ddot{\chi}(\tau) + (2\lambda - \vartheta_1)\dot{\chi}(\tau) + \chi(\tau) + \beta\chi^3(\tau) + \eta\sum_{j=1}^{N_p}\left(k_j + c_j\omega_0^{\alpha_j}D_\tau^{\alpha_j}\right)\chi(\tau)\sin^2\left(\tfrac{j\pi}{N_p+1}\right) \\ = \vartheta_2\dot{\chi}^2(\tau) + \vartheta_0 + (\theta_0 + \theta_1\dot{\chi}(\tau))\,\xi(\tau) + F_{0N}\sin(\Omega\tau) - G_{0N}\cos(\Omega\tau)\end{aligned} \tag{182}$$

where

$$\begin{aligned}F_{0N} &= f_0\left[1 + \tfrac{2\sin\tilde{\tau}_0\sin((N_v-1)\tilde{\tau}_0)}{1-\cos(2\tilde{\tau}_0)}\cos(N_v\tilde{\tau}_0)\right] \quad , \quad \tilde{\tau}_0 = \tfrac{d\pi}{2L}, \\ G_{0N} &= \tfrac{2f_0\sin\tilde{\tau}_0\sin((N_v-1)\tilde{\tau}_0)}{1-\cos(2\tilde{\tau}_0)}\sin(N_v\tilde{\tau}_0).\end{aligned} \tag{183}$$

III-3-2-2- Beam model analysis and approximated analytical solutions

This subsection deals with the analytical investigation of the system response and on the derivation of the response of the steady-state vibration of the beam system to moving loads and wind actions. Here we use the stochastic averaging method [96, 98, 99] for the analysis of the resulting dynamic systems with fractional derivative, random noise and harmonic excitation (Eq. (182)). To this end, the solution of the modal Eq. (182) is sought in the form

$$\chi(\tau) = a_0 + a(\tau)\cos\psi, \quad \dot{\chi}(\tau) = -\Omega a(\tau)\sin\psi, \quad \psi = \Omega\tau + \phi(\tau). \tag{184}$$

where a_0 is the constant mean amplitude of the beam, $a(\tau)$ and ψ the slow-varying amplitude and generalized phase respectively. Substituting Eq. (184) into Eq. (182) one obtains:

$$\begin{cases}\dot{a} = -\frac{1}{\Omega}\left[M_1(a,\psi) + M_2(a,\psi)\right]\sin\psi \\ \\ a\dot{\phi} = -\frac{1}{\Omega}\left[M_1(a,\psi) + M_2(a,\psi)\right]\cos\psi\end{cases} \tag{185}$$

where

$$\begin{aligned}&M_1(a,\psi) = F_{0N}\sin(\psi-\phi) - G_{0N}\cos(\psi-\phi) + (2\lambda-\vartheta_1)\,a\Omega\sin\psi a - \tfrac{1}{4}\beta a^3\cos 3\psi \\ &-\left[1 + \eta\sum_{j=1}^{N_p}k_j\sin^2\left(\tfrac{j\pi}{N_p+1}\right) + 3\beta a_0^2 + \tfrac{3}{4}\beta a^2 - \Omega^2\right]\cos\psi + \tfrac{a^2}{2}\left[\vartheta_2\Omega^2 - 3\beta a_0\right]\cos 2\psi, \\ &M_2(a,\psi) = -\eta\sum_{j=1}^{N_p}c_j\omega_0^{\alpha_j}\sin^2\left(\tfrac{j\pi}{N_p+1}\right)D_\tau^{\alpha_j}(a\cos\psi) + (\theta_0 - \theta_1\Omega a\sin\psi)\,\xi(\tau).\end{aligned} \tag{186}$$

and a_0 satisfies the following non-linear equation:

$$\beta a_0^3 + \left[1 + \frac{3}{2}\beta a^2 + \eta\sum_{j=1}^{N_p}k_j\sin^2\left(\frac{j\pi}{N_p+1}\right)\right]a_0 = \vartheta_0 - \frac{1}{2}\vartheta_2\Omega^2a^2 \tag{187}$$

To apply the stochastic averaging method [96,98,99], we average over the period $T = 2\pi/\Omega$ in the case of periodic function ($M_1(a,\psi)$), or $T = \infty$ in the case of aperiodic one ($M_2(a,\psi)$). The method gives the following pair of first order differential equations for the amplitude $a(\tau)$ and the phase $\phi(\tau)$:

$$\begin{aligned}\dot{a} = &-(2\lambda - \vartheta_1)\tfrac{a}{2} - \tfrac{1}{2}\eta a \sum_{j=1}^{N_p} c_j \omega_0^{\alpha_j} \Omega^{\alpha_j - 1} \sin^2\left(\tfrac{j\pi}{N_p+1}\right) \sin\left(\tfrac{\alpha_j \pi}{2}\right) + \tfrac{1}{2\Omega}\left[G_{0N}\sin\phi - F_{0N}\cos\phi\right] \\ &+ \tfrac{\pi\theta_1^2 a}{8}\left[3S_\xi(2\Omega) + 2S_\xi(0)\right] + \tfrac{\pi\theta_0^2}{2\Omega^2 a} S_\xi(\Omega) + \sqrt{\tfrac{\pi\theta_0^2}{\Omega^2} S_\xi(\Omega) + \tfrac{\pi\theta_1^2 a^2}{4}\left[S_\xi(2\Omega) + 2S_\xi(0)\right]}\,\xi_1(\tau)\end{aligned} \tag{188}$$

and

$$\begin{aligned}a\dot{\phi} = &\tfrac{a}{2\Omega}\left[1 + 3\beta a_0^2 - \Omega^2 + \tfrac{3}{4}\beta a^2 + \eta \sum_{j=1}^{N_p}\left(k_j + c_j \omega_0^{\alpha_j}\Omega^{\alpha_j}\cos\left(\tfrac{\alpha_j\pi}{2}\right)\right)\sin^2\left(\tfrac{j\pi}{N_p+1}\right)\right] \\ &+ \tfrac{1}{2\Omega}\left[G_{0N}\cos\phi + F_{0N}\sin\phi\right] - \tfrac{\pi\theta_1^2 a}{4}\Psi_\xi(2\Omega) + \sqrt{\tfrac{\pi\theta_0^2}{\Omega^2}S_\xi(\Omega) + \tfrac{\pi\theta_1^2 a^2}{4}S_\xi(2\Omega)}\;\xi_2(\tau).\end{aligned} \tag{189}$$

Here $S_\xi(\Omega)$ and $\Psi_\xi(\Omega)$ are the cosine and sine power spectral density function, respectively [146]:

$$\begin{aligned}&S_\xi(\Omega) = \int_{-\infty}^{+\infty} R(\zeta)\cos(\Omega\tau)\,\mathrm{d}\zeta = 2\int_0^{+\infty} R(\zeta)\cos(\Omega\tau)\,\mathrm{d}\zeta = 2\int_{-\infty}^{0} R(\zeta)\cos(\Omega\tau)\,\mathrm{d}\zeta, \\ &\Psi_\xi(\Omega) = 2\int_0^{+\infty} R(\zeta)\sin(\Omega\tau)\,\mathrm{d}\zeta = -2\int_{-\infty}^{0} R(\zeta)\sin(\Omega\tau)\,\mathrm{d}\zeta, \\ &\int_{-\infty}^{+\infty} R(\zeta)\sin(\Omega\tau)\,\mathrm{d}\zeta = 0\;; \quad R(\zeta) = \mathrm{E}\left[\xi(\tau)\,\xi(\tau+\zeta)\right].\end{aligned} \tag{190}$$

The spectral density function of the bounded noise can be used to approximate the Dryden and Von Karman spectra of wind turbulence with a suitable choice the parameters of the model [146, 173]. For this aim, the random processes of bounded variation with multiple spectrum peaks [174] is used in this work to take into account the turbulent component of the wind flow $\xi(\tau)$. This component can be expressed as [174]

$$\xi(\tau) = \sum_{i=1}^{m} \sigma_i \cos\left[\omega_i \tau + \gamma_i B_i(\tau) + \theta_i\right], \tag{191}$$

where σ_i and γ_i are positive constants, $B_i(\tau)$ are mutually independent unit Wiener process, and θ_i are mutually independent random variables uniformly distributed in $[0, 2\pi]$. The sum $\xi(\tau)$ is a stationary random process in wide sense, with zero mean and spectral density:

$$\Phi_\xi(\omega) = \sum_{i=1}^{m} \frac{\sigma_i^2 \gamma_i^2 \left(\omega^2 + \omega_i^2 + \gamma_i^4/4\right)}{4\pi\left[\left(\omega^2 - \omega_i^2 - \gamma_i^4/4\right)^2 + \gamma_i^2\omega^2\right]}. \tag{192}$$

(a) Analytical estimate of the beam response under moving loads only

We first consider system (182) with only deterministic moving loads ($F_{ad}(x,t)=0$) neglecting wind effects on the beam. If $\vartheta_1=\theta_0=\theta_1=0$, Eqs. (188) and (189) become:

$$\dot{a}=-\lambda a-\tfrac{1}{2}\eta a\sum_{j=1}^{N_p}c_j\omega_0^{\alpha_j}\Omega^{\alpha_j-1}\sin^2\left(\tfrac{j\pi}{N_p+1}\right)\sin\left(\tfrac{\pi\alpha_j}{2}\right)+\tfrac{1}{2\Omega}\left[G_{0N}\sin\phi-F_{0N}\cos\phi\right] \quad (193)$$

and

$$\begin{aligned}a\dot{\phi} &= \frac{a}{2\Omega}\left[1-\Omega^2+3\beta a_0^2+\frac{3}{4}\beta a^2+\eta\sum_{j=1}^{N_p}\left(k_j+c_j\omega_0^{\alpha_j}\Omega^{\alpha_j}\cos\left(\frac{\pi\alpha_j}{2}\right)\right)\sin^2\left(\frac{j\pi}{N_p+1}\right)\right]\\ &+ \frac{1}{2\Omega}\left[G_{0N}\cos\phi+F_{0N}\sin\phi\right] \quad (194)\end{aligned}$$

By substituting $a=A,\phi=\Phi$ and $\dot{a}=0,\ \dot{\phi}=0$ in Eqs. (193) and (194), algebraic manipulations give for the steady state vibrations of the system response A the following nonlinear equation:

$$\frac{9}{16}\beta^2A^6-\frac{3}{2}\beta\Theta_1(\alpha_j)A^4+\left[\Theta_1^2(\alpha_j)+\Theta_2^2(\alpha_j)\right]A^2=F_{0N}^2+G_{0N}^2, \quad (195)$$

with

$$\begin{aligned}\Theta_1(\alpha_j)&=\Omega^2-1-3\beta a_0^2-\eta\sum_{j=1}^{N_p}\left(k_j+c_j\omega_0^{\alpha_j}\Omega^{\alpha_j}\cos\left(\tfrac{\pi\alpha_j}{2}\right)\right)\sin^2\left(\tfrac{j\pi}{N_p+1}\right),\\ \Theta_2(\alpha_j)&=2\Omega\lambda+\eta\sum_{j=1}^{N_p}c_j\omega_0^{\alpha_j}\Omega^{\alpha_j}\sin\left(\tfrac{\pi\alpha_j}{2}\right)\sin^2\left(\tfrac{j\pi}{N_p+1}\right).\end{aligned} \quad (196)$$

The stability of the steady-state vibration of the system response is investigated by using the method of Andronov and Witt [166] associated to the Routh-Hurwitz criterion [167]. Thus, the steady-state response is asymptotically stable if Eq. (197a) is satisfied and unstable if Eq. (197b) is satisfied:

$$\left(\frac{\Theta_2(\alpha_j)}{2\Omega}\right)^2+\frac{1}{4\Omega}\left[\frac{3\beta}{4}A^2-\Theta_1(\alpha_j)\right]\times\left[\frac{9\beta}{4}A^2-\Theta_1(\alpha_j)\right]>0 \quad (197a)$$

$$\left(\frac{\Theta_2(\alpha_j)}{2\Omega}\right)^2+\frac{1}{4\Omega}\left[\frac{3\beta}{4}A^2-\Theta_1(\alpha_j)\right]\times\left[\frac{9\beta}{4}A^2-\Theta_1(\alpha_j)\right]<0 \quad (197b)$$

The trivial solution of Eq. (187) is $a_0=0$.

(b) Analytical estimate of the beam response under stochastic wind loads only

Here, we analyze system (182) with only the aerodynamic force ($F_{ad}(x,t)\neq 0$) that takes into account the additive and parametric stochastic wind effects. If the effect of the

moving load on the beam is neglected, $F_{0N} = G_{0N} = 0$, Eqs. (188) and (189) become:

$$\mathrm{d}a = \left\{ -\tfrac{1}{2}\eta a \sum_{j=1}^{N_p} c_j \omega_0^{\alpha_j} \Omega^{\alpha_j - 1} \sin^2\left(\tfrac{j\pi}{N_p+1}\right) \sin\left(\tfrac{\alpha_j \pi}{2}\right) + \tfrac{\pi\theta_1^2 a}{8}\left[3S_\xi(2\Omega) + 2S_\xi(0)\right] \right\} \mathrm{d}\tau$$

$$+ \left\{ -(2\lambda - \vartheta_1)\tfrac{a}{2} + \tfrac{\pi\theta_0^2}{2\Omega^2 a} S_\xi(\Omega) \right\} \mathrm{d}\tau \; + \sqrt{\tfrac{\pi\theta_0^2}{\Omega^2} S_\xi(\Omega) + \tfrac{\pi\theta_1^2 a^2}{4}\left[S_\xi(2\Omega) + 2S_\xi(0)\right]}\, \mathrm{d}W_1(\tau). \tag{198}$$

and

$$\begin{aligned} \mathrm{d}\phi &= \frac{1}{2\Omega}\left\{ 1 + 3\beta a_0^2 - \Omega^2 + \frac{3}{4}\beta a^2 + \eta \sum_{j=1}^{N_p} \left(k_j + c_j \omega_0^{\alpha_j} \Omega^{\alpha_j} \cos\left(\frac{\alpha_j \pi}{2}\right)\right) \sin^2\left(\frac{j\pi}{N_p+1}\right) \right\} \mathrm{d}\tau \\ &- \frac{\pi\theta_1^2}{4}\Psi_\xi(2\Omega)\,\mathrm{d}\tau \; + \sqrt{\frac{\pi\theta_0^2}{\Omega^2 a^2} S_\xi(\Omega) + \frac{\pi\theta_1^2 a^2}{4} S_\xi(2\Omega)}\; \mathrm{d}W_2(\tau). \end{aligned} \tag{199}$$

Here $W_1(\tau)$ and $W_2(\tau)$ are independent normalized sources of Gaussian white noise. the differential equation for $a(\tau)$ does not rely on $\phi(\tau)$; thus, a probability density function $P(a,\tau)$ for $a(\tau)$ can be derived. The associated F-P-K equation for $P(a,\tau)$ is

$$\begin{aligned} \tfrac{\partial P(a,\tau)}{\partial \tau} = &-\tfrac{\partial}{\partial a}\left[\left(-(2\lambda - \vartheta_1)\tfrac{a}{2} - \tfrac{1}{2}\eta a \sum_{j=1}^{N_p} c_j \omega_0^{\alpha_j} \Omega^{\alpha_j - 1} \sin^2\left(\tfrac{j\pi}{N_p+1}\right) \sin\left(\tfrac{\alpha_j \pi}{2}\right) \right) P(a,\tau) \right] \\ &-\tfrac{\partial}{\partial a}\left[\tfrac{\pi\theta_0^2}{2\Omega^2 a} S_\xi(\Omega) + \tfrac{\pi\theta_1^2 a}{8}\left[3S_\xi(2\Omega) + 2S_\xi(0)\right] P(a,\tau) \right] \\ &+\tfrac{1}{2}\left(\tfrac{\pi\theta_0^2}{\Omega^2} S_\xi(\Omega) + \tfrac{\pi\theta_1^2 a^2}{4}\left[S_\xi(2\Omega) + 2S_\xi(0)\right] \right) \tfrac{\partial^2 P(a,\tau)}{\partial a^2} \end{aligned} \tag{200}$$

In the stationary case, $\frac{\partial P(a,\tau)}{\partial \tau} = 0$, the solution of Eq. (200) is:

$$P_s(a) = Na\left(\Gamma_0 + a^2 \Gamma_1\right)^{-(Q+1)} \tag{201}$$

where

$$\begin{aligned} &\Gamma_0 = \tfrac{\pi\theta_0^2}{\Omega^2} S_\xi(\Omega), \;\; \Gamma_1 = \tfrac{\pi\theta_1^2}{4}\left[S_\xi(2\Omega) + 2S_\xi(0)\right], \;\; Q = \tfrac{\Gamma_1 - 2\Gamma_2}{2\Gamma_1}, \\ &\Gamma_2 = -\tfrac{1}{2}(2\lambda - \vartheta_1) - \tfrac{1}{2}\eta \sum_{j=1}^{N_p} c_j \omega_0^{\alpha_j} \Omega^{\alpha_j - 1} \sin^2\left(\tfrac{j\pi}{N_p+1}\right) \sin\left(\tfrac{\pi\alpha_j}{2}\right) + \tfrac{\pi\theta_1^2}{8}\left[3S_\xi(2\Omega) + 2S_\xi(0)\right]. \end{aligned} \tag{202}$$

Above N is a normalization constant that guarantees $\int_0^\infty P_s(a)\,\mathrm{d}a = 1$.

(c) Analytical estimate of the beam responses under moving vehicles and stochastic wind loads

We finally consider the dynamic performances of the beam system subject to the stochastic wind and moving loads. Thus, for the special case of $\beta = \theta_1 = 0$ (considering only the additive effects of the wind turbulence and linear bridge responses for the

analytical purposes), the previous Eqs. (188) and (189) is reduced to:

$$\begin{aligned} \mathrm{d}a &= \left[-\left(2\lambda-\vartheta_1\right)\frac{a}{2}-\frac{1}{2}\eta a\sum_{j=1}^{N_p}c_j\omega_0^{\alpha_j}\Omega^{\alpha_j-1}\sin^2\left(\frac{j\pi}{N_p+1}\right)\sin\left(\frac{\alpha_j\pi}{2}\right)+\frac{\Gamma_0}{a}\right]\mathrm{d}\tau \\ &+ \frac{1}{2\Omega}\left[G_{0N}\sin\phi-F_{0N}\cos\phi\right]\mathrm{d}\tau+\sqrt{\Gamma_0}\mathrm{d}W_1\left(\tau\right). \end{aligned} \tag{203}$$

and

$$\begin{aligned} \mathrm{d}\phi &= \frac{1}{2\Omega}\left[1-\Omega^2+\eta\sum_{j=1}^{N_p}\left(k_j+c_j\omega_0^{\alpha_j}\Omega^{\alpha_j}\cos\left(\frac{\alpha_j\pi}{2}\right)\right)\sin^2\left(\frac{j\pi}{N_p+1}\right)\right]\mathrm{d}\tau \\ &+ \frac{1}{2\Omega a}\left[G_{0N}\cos\phi+F_{0N}\sin\phi\right]\mathrm{d}\tau+\frac{1}{a}\sqrt{\Gamma_0}\,\mathrm{d}W_2\left(\tau\right). \end{aligned} \tag{204}$$

The averaged F-P-K equation associated with the previous Itô Eqs. (203) and (204) is

$$\begin{aligned} \frac{\partial P\left(a,\phi,\tau\right)}{\partial\tau} &= -\frac{\partial}{\partial a}\left(\bar{a}_1P\left(a,\phi,\tau\right)\right)-\frac{\partial}{\partial\phi}\left(\bar{a}_2P\left(a,\phi,\tau\right)\right)+\frac{1}{2}\frac{\partial^2}{\partial a^2}\left(\bar{b}_{11}P\left(a,\phi,\tau\right)\right) \\ &+ \frac{1}{2}\frac{\partial^2}{\partial\phi^2}\left(\bar{b}_{22}P\left(a,\phi,\tau\right)\right) \end{aligned} \tag{205}$$

where

$$\begin{aligned} &\bar{a}_1=-\left(2\lambda-\vartheta_1\right)\tfrac{a}{2}-\tfrac{1}{2}\eta a\sum_{j=1}^{N_p}c_j\omega_0^{\alpha_j}\Omega^{\alpha_j-1}\sin^2\left(\tfrac{j\pi}{N_p+1}\right)\sin\left(\tfrac{\alpha_j\pi}{2}\right)+\tfrac{1}{2\Omega}\left[G_{0N}\sin\phi-F_{0N}\cos\phi\right]+\tfrac{\Gamma_0}{a} \\ &\bar{a}_2=\tfrac{1}{2\Omega}\left[1-\Omega^2+\eta\sum_{j=1}^{N_p}\left(k_j+c_j\omega_0^{\alpha_j}\Omega^{\alpha_j}\cos\left(\tfrac{\alpha_j\pi}{2}\right)\right)\sin^2\left(\tfrac{j\pi}{N_p+1}\right)+\tfrac{1}{a}\left[G_{0N}\cos\phi+F_{0N}\sin\phi\right]\right] \\ &\bar{b}_{11}=\Gamma_0 \\ &\bar{b}_{22}=\tfrac{\Gamma_0}{a^2} \end{aligned} \tag{206}$$

Applying the solution procedure proposed by Huang *et al.* [107], one obtains the following exact stationary solution

$$P_s\left(a,\phi\right)=N^{'}a\exp\left\{\frac{\Gamma_2^{'}}{\Gamma_0}a^2-\frac{a}{\Omega\left(\Gamma_0^2+d_0^2\right)}\left[\left(d_0G_{0N}+F_{0N}\Gamma_0\right)\cos\phi+\left(d_0F_{0N}-G_{0N}\Gamma_0\right)\sin\phi\right]\right\} \tag{207}$$

where $N^{'}$ is a normalization constant and

$$\begin{aligned} &\Gamma_2^{'}=-\tfrac{1}{2}\left(2\lambda-\vartheta_1\right)-\tfrac{\eta}{2}\sum_{j=1}^{N_p}c_j\omega_0^{\alpha_j}\Omega^{\alpha_j-1}\sin^2\left(\tfrac{j\pi}{N_p+1}\right)\sin\left(\tfrac{\alpha_j\pi}{2}\right),\ d_0=-\tfrac{\Gamma_0\Gamma_3}{\Gamma_2^{'}} \\ &\Gamma_3=\tfrac{1}{2\Omega}\left[1-\Omega^2+\eta\sum_{j=1}^{N_p}\left(k_j+c_j\omega_0^{\alpha_j}\Omega^{\alpha_j}\cos\left(\tfrac{\alpha_j\pi}{2}\right)\right)\sin^2\left(\tfrac{j\pi}{N_p+1}\right)\right] \end{aligned} \tag{208}$$

Eq. (207) illustrates the main result of this part: the dependence of stationary probability distributions of the oscillations amplitude of the beam upon the parameters (damping λ and natural frequency $\Omega_0=1$); the moving loads(loads weights intensity f_0, number N_v,

spacing load d and driving frequency Ω), of the wind loads (deterministic ϑ_1 and turbulent θ_0 part) and the bearings parameters (stiffness k_j, damping c_j, fractional-order α_j and number of bearings N_p).

III-3-2-3- Numerical analysis and discussion of the results

For numerical purposes we consider the case of beam, bearings and aerodynamic force having the parameters of Table VI and the following one: ($L = 100\,\mathrm{m},\ b = 6\,\mathrm{m},\ \mu = 192\,\mathrm{Ns/m^2},\ P = 1500\,\mathrm{kN},\ v = 60\,\mathrm{m/s}$) assumed here to extend the work done by others researchers and in order to make the qualitative effects studied visible. It is assumed that all the bearings have the same viscoelastic property ($c_j = c_0,\ k_j = k_0,\ \alpha_j = \alpha$ with $j = 1, 2, ..., N_p$). In this work, the case of a two-peak spectral density ($m = 2$) is used. Thus, the parameters of Eq. (192) are chosen to approach the well-know Dryden wind spectrum [173] given by $\omega_1 = 0.5,\ \omega_2 = 1.0,\ \gamma_1 = \gamma_2 = 0.5,\ \sigma_1 = \sigma_2 = 0.4$.

Table VI: *Properties of the Beam, bearings and aerodynamic force* [70, 170, 175]

Item	Notation	Value
Beam		
Young's modulus	E	29.43 MPa
Cross-sectional area	S	0.004 $\mathrm{m^2}$
Mass density	ρ	7850.0 $\mathrm{kg/m^3}$
Moment of inertia	I	3.81 $\mathrm{m^4}$
viscoelastic bearings		
Stiffness	k_0	138.6 $\mathrm{N/m^2}$
Viscous damping	c_0	1732.50 $\mathrm{Ns/m^2}$
Aerodynamic force		
Air mass density	ρ_a	1.25 $\mathrm{kg/m^3}$
Critical wind velocity	u_c	30.0 m/s
Mean wind velocity	$\bar{u}$	21.0 m/s

The dimensionless parameters of Eq. (182) are thus calculated as per Eq. (180) and shown in Table VII

Table VII: *Numerical values of the dimensionless parameters (defined in Eq. (182) and elsewhere)*

Parameter	Value	Parameter	Value
Ω	0.04	ϑ_0	0.1×10^{-4}
f_0	0.005	ϑ_2	-1.8
η	1.0×10^{-7}	θ_0	0.000005
β	-0.2	θ_1	0.03
ϑ_1	0.02	λ	0.03
ω_0	41.4	l_r	50.0

Numerical results are also presented to verify the accuracy of the analytical solution, Eq. (184). The numerical solutions is obtained using the model or the adjusted model of the Newton-Leipnik algorithm [114,162] to simulate the resulting fractional system or the stochastic-fractional system, respectively.

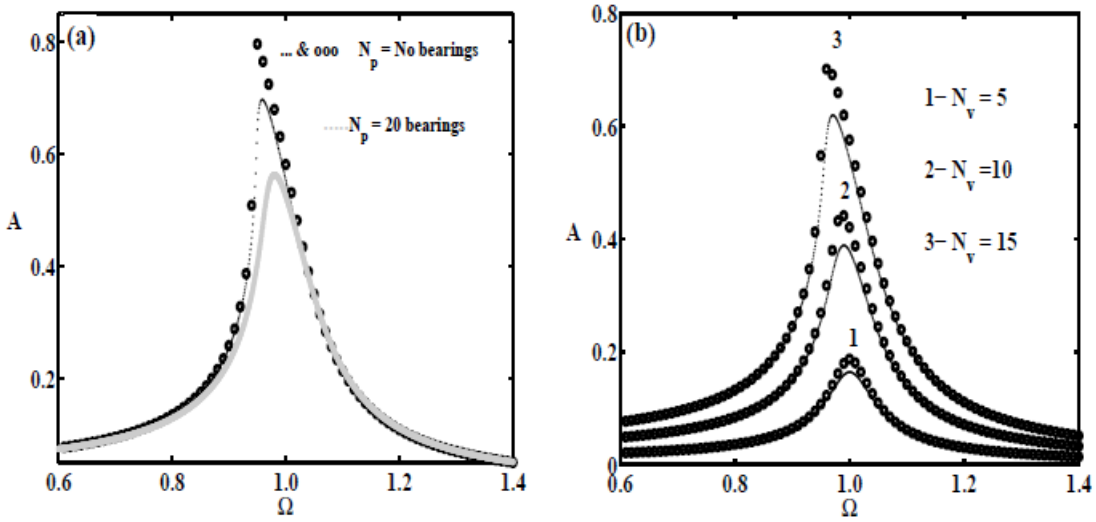

Figure 31: *The steady-state vibration amplitude of the beam as a function of the parameter Ω, see Eq. (182). (a) The effect of the number of the bearings for fixed number of moving loads, $N_v = 15$; (b) The effect of the number of moving loads N_v for fixed number of bearings $N_p = 10$. The dotted line represents the analytical results as per Eq. (195), while the curves with circles are the numerical results obtained simulating Eq. (182). The simulation parameters are $\alpha = 0.5$, $\vartheta_0 = \vartheta_1 = \vartheta_2 = \theta_0 = \theta_1 = 0$ (no stochastic terms). The other parameters are given in Table VII.*

Fig. 31 shows both the effects of the number of bearings, Fig. 31 (a), and of the moving loads, Fig. 31 (b), on the steady-state amplitude A and frequency Ω (that is related to the vehicles speed, as per Eq. (182)) of the beam system. The data reported in Fig. 31 (a) demonstrate that, as the number of bearings increases, the resonant amplitude of the bridge beam decreases and the resonance frequency of the system increases. Thus, it is evident that the number of bearings plays an important role for the beam stability. The second graph, Fig. 31 (b), shows how an increase in the number of the moving loads affects the amplitude and the frequency of the beam. It is observed that as the value of N_v increases, the amplitude of vibration at the resonant state merely increases. It is well know that, the frequency response is important in engineering, for through the frequency response curve one can determine the resonance frequency. For example in Fig. 31 (b) the resonance frequency occurs near $\Omega = 1$.

In Fig. 32 we report the effect of the fractional-order α, on the steady-state vibration amplitude of the beam A versus the dimensionless piers stiffness coefficient $k_0^{'}$, as per the analytical prediction of Eq. (195) compared to the numerical simulations of Eq. (182). The system response is more stable for the higher order of the derivative. The multivalued solution only appears for the smallest order and suddenly disappears as the derivative

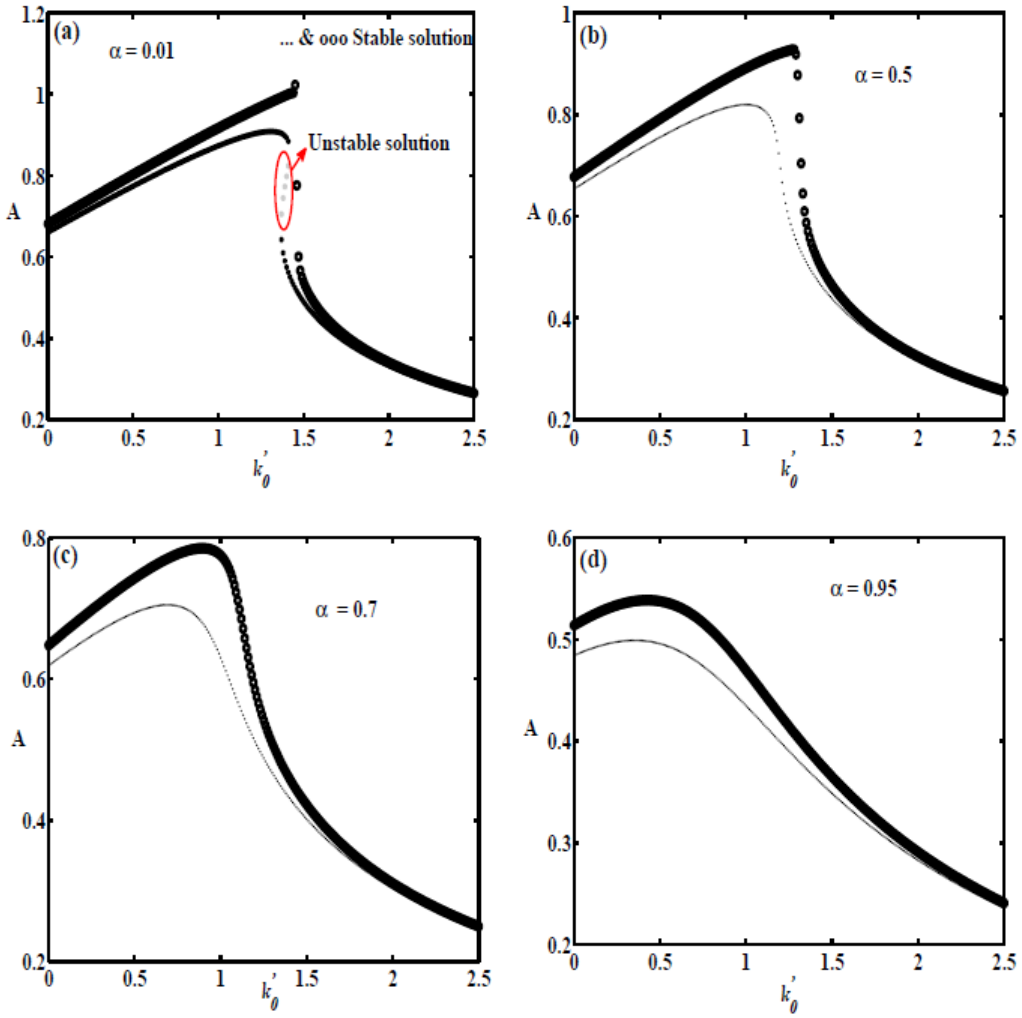

Figure 32: *Amplitude of the oscillation resonance induced by the dimensionless stiffness parameter* $k_0^{'}$ (k_0/k_m) *for different fractional-order values (the parameter* k_m *is a reference stiffness coefficient). The dotted line represents the analytical results as per Eq. (195), while the curves with circles are the numerical results obtained simulating Eq. (182). The simulation parameters are:* $N_v = 20$, $N_p = 10$, $\Omega = 1.0$, $\vartheta_0 = \vartheta_1 = \vartheta_2 = \theta_0 = \theta_1 = 0$ *(no stochastic terms). The other parameters are given in Table VII.*

order increases. The resonance (a peak of the amplitude) appears as the parameter k_0' increases, see Fig. 32 (a), Fig. 32 (b), Fig. 32 (c) and Fig. 32 (d). Shortly, the resonance of the beam system strongly depends upon the stiffness and viscosity (that is, the order of the derivative) of the bearings. For the investigated parameters, it is found that the numerical results are in good agreement with the analytical predictions.

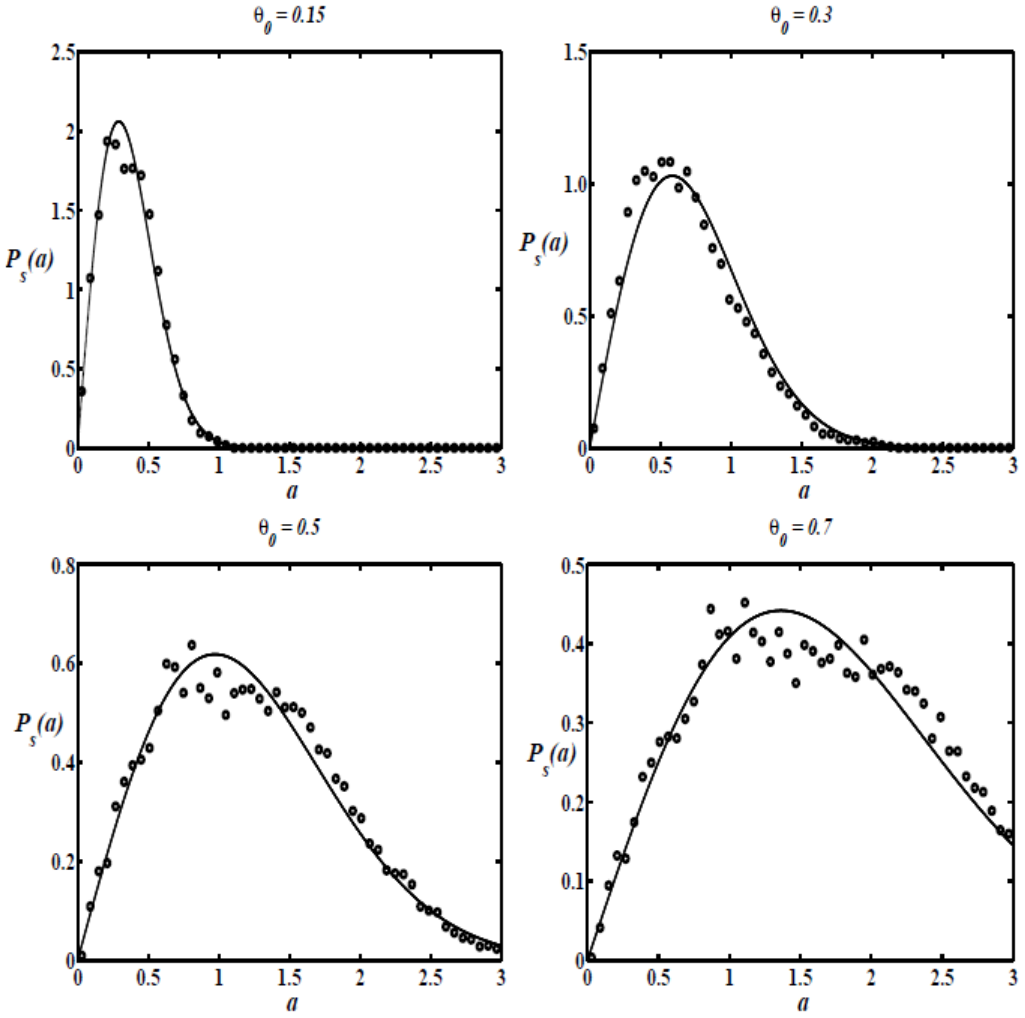

Figure 33: *Effect of the wind turbulence on the stationary probability distributions of the oscillations amplitude of the beam. The dotted line represents the analytical results as per Eq. (201), while the curves with circles are the numerical results obtained simulating Eq. (182). The simulation parameters are:* $\Omega = 0.75$, $\alpha = 0.5$, $N_p = 10$, $\theta_1 = 0.1$, $f_0 = 0$. *The other parameters are given in Table VII.*

The consequences of the stochastic effects, as modelled by the random term ξ in Eq. (181), have been investigated in Figs. 33,34. The consequences of the additive wind turbulence θ_0 on the probabilistic responses of the beam is plot in Fig. 34, as the stationary probability density function of the oscillations amplitude of the beam $P_s(a)$ versus the amplitude a curve, where we also report the numerical solutions of Eq. (182). The distribution, as per Eq. (207), has only one peak that corresponds to a larger amplitude. The main feature of this analysis of the role of the wind is that as the additive

wind turbulence parameter θ_0 increases, the value of the peak decreases and progressively shifts towards larger amplitude values. Surprisingly, it implies that the additive wind turbulence decreases the chance for the bridge beam to reach the resonant amplitude (i.e., the most probable position to find the maximum amplitude of the bridge beam oscillations).

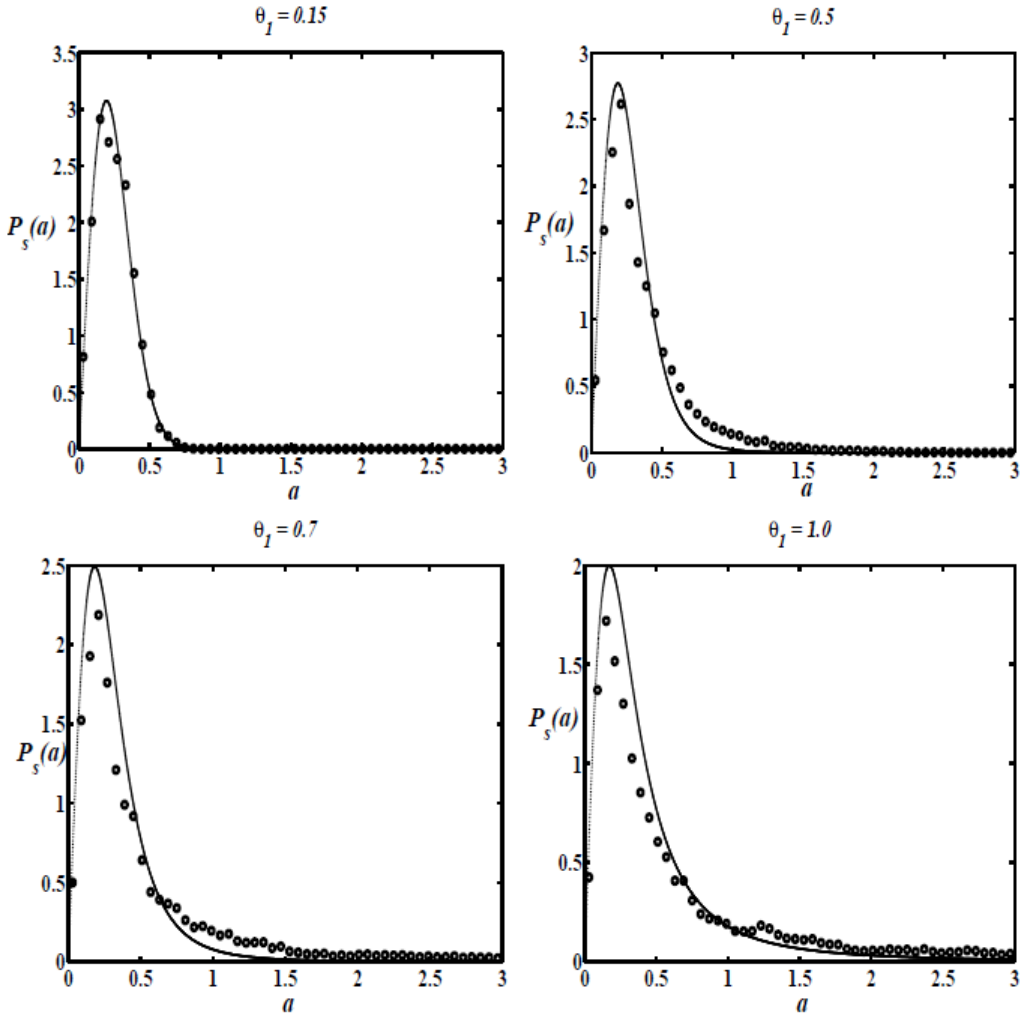

Figure 34: *Effect of the wind turbulence on the stationary probability distributions of the oscillations amplitude of the beam. The dotted line represents the analytical results as per Eq. (201), while the curves with circles are the numerical results obtained simulating the full Eq. (182). The simulation parameters are:* $\Omega = 0.75$, $\alpha = 0.5$, $N_p = 10$, $\theta_0 = 0.1$, $f_0 = 0$. *The other parameters are given in Table VII.*

Also for the parameter θ_1 that governs the wind turbulence effects, see Eq. (184), the stationary probability density function of the oscillations amplitude of the beam is investigated, see Fig. 34. In this case the amplitude distribution has only one maximum situated in the vicinity of $a_m = 0.2$. As θ_1 increases, the peak value of the probability density function slightly decreases and stays located practically in the same position. The agreement between numerical and analytical results is fairly good in both cases of Figs. 33 and 34.

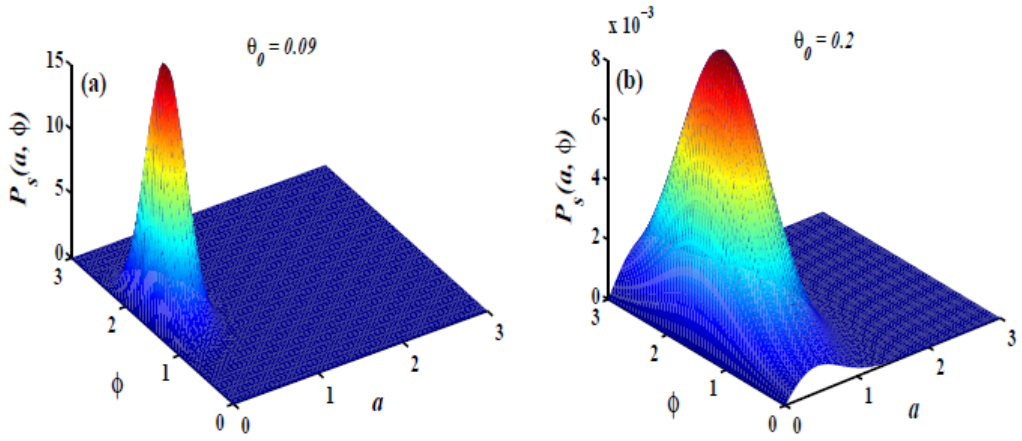

Figure 35: *The analytical result of the stationary probability distribution function versus the amplitude a and the phase ϕ for (a) $\theta_0 = 0.09$ and (b) $\theta_0 = 0.2$. The constant N' is found numerically to ensure normalization. The simulation parameters are: $\alpha = 0.5$, $N_v = 10$, $N_p = 10$, $\Omega = 1$, $\vartheta_1 = 0.02$, $f_0 = 0.005$.*

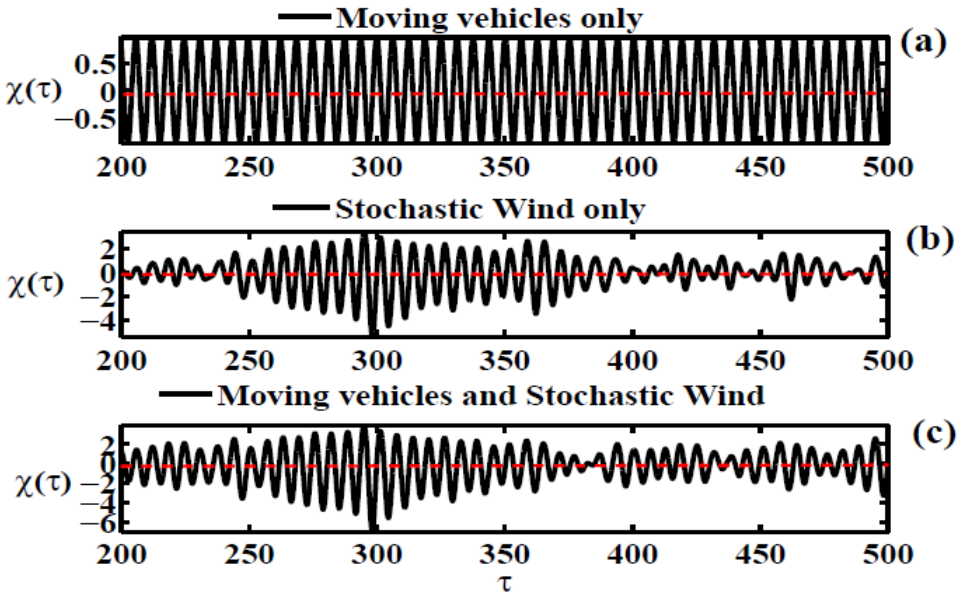

Figure 36: *Time dependent response of the beam considering (a) only moving vehicles, (b) only stochastic wind effects, (c) both vehicles and stochastic wind loads. The simulation parameters are: $\vartheta_0 = 0.00011$, $\vartheta_1 = 0.02$, $\vartheta_2 = -0.092$, $\theta_0 = 0.7$, $\theta_1 = 0.15$, $f_0 = 0.005$, $N_v = 20$, $N_p = 5$, $\Omega = 1$, $\alpha = 0.5$, $\lambda = 0.03$, $\beta = 0$.*

The analytical prediction of Eq. (207) for the three-dimensional curve of the stationary probability distribution function versus the amplitude a and the phase ϕ are plotted in Fig. 35. The graphs confirm the effect of the additive wind turbulence parameter θ_0 on the probabilistic response of the beam. The remarkable peak of the graphs shows the most probable position to find the maximum vibration of the beam system. This peak strongly depends on the wind turbulence parameters.

To visualize the beam oscillations, in Fig. 36, the time dependent beam vertical displacement dynamic response is investigated for three conditions. First, in Fig. 36 (a) we report the oscillations under the influence of the vehicles. As the vehicles in this model move deterministically, the resulting oscillations are periodic and the maximum peak value of the dimensionless vertical displacement of the beam does not exceed 1.0. However, when the stochastic term associated to wind loads is included, even without the presence of moving loads, the maximum peak value of the dimensionless vertical displacement of the beam increases, up to about 2.25 as shown in Fig. 36 (b). In this condition, the fluctuations dominate and the oscillations alternate quite periods of small oscillations to sizeable oscillations with large fluctuations. Finally, the simultaneous presence of both moving and stochastic wind loads cause a remarkable additional increase of the dimensionless vertical displacement response, as shown in Fig. 36 (c).

III-4- Conclusion

In this chapter, we have investigated the dynamical behaviors of some models of bridges subject to moving loads and stochastic wind. The results obtained have been presented and discussed.

Firstly, an analytic approach to the dynamics of a Rayleigh beam under the effect of loads moving with stochastic speed has been considered. By way of short summary, we have retrieved what is the effect of the load random velocities on the behavior of the mean amplitude of the beam versus the parameters. Some nonlinear dependences are new but not fully unexpected: the number of vehicles changes the resonant velocity (Fig. 5). More interesting is the unexpected influence of the load, that is not just nonlinear, but reentrant (Fig. 7). To single out what we regard as the most relevant finding, we have focused on the non-monotonic effect of the noise intensity, Fig. 6, that discloses an unexpected beneficial role of noise intensity on the bridge stability. The analytic approach has been also checked with numerical simulations and the fairly good agreement between the two approaches has been found.

Secondly, we have identified the horseshoes chaos in a semi-harp model of cable-stayed bridge subjected to train of forces moving with stochastic velocity. We have found that the intensity of the random component of the loads velocity causes an increase of the threshold for the onset of chaos in the model and then increases the chances to have a

regular behavior of the bridge; after a maximum a further increase of the noise causes a decrease of the threshold and then enlarges the possible chaotic domain in parameter space.

Thirdly, an evaluation approach to obtain the probabilistic characteristics of a two lane slab-type-bridge response due to traffic flow has been investigated. Mathematical formulation of the problem has been done and base to stochastic analysis, the effects of some traffic parameters on the expected value and on the standard deviation of the bridge deflection response have been investigated.

Fourthly, we have presented an analytical and numerical solution for the dynamic response of a Rayleigh beam resting on viscoelastic Pasternak foundations considering the shear layer as viscoelastic material having fractional-order property and subjected to the passing of series of equidistant moving loads with constant velocity. The analysis leads us to the conclusion that, as the order of the derivative increases, the resonant amplitude of the beam vibration decreases and, when the moving loads are uniform distributed upon all the length of the structure, it vibrates the least possible. Also, a proper selection of the shear layer of the foundation that having fractional order viscoelastic material can be contributed to suppression of chaos in a system.

Finally, We have investigated the effects of both moving loads and stochastic wind on the steady-state vibration of a beam laying on bearings that are characterized by a fractional-order viscoelastic material. The main conclusion is that the resonance phenomenon and the stability in the beam system strongly depends on the stiffness and fractional-order of the derivative term of the viscous properties of the bearings. In fact, the resonance phenomenon appears as the stiffness of the bearings increases. Another interesting conclusion is that the additive and parametric wind turbulence decreases the chance for the beam to quickly reach the amplitude resonance.

General Conclusion

This dissertation has dealt with an analysis of the vibratory and chaotic dynamics of bridges under the action of moving vehicles, trains, and stochastic wind loads. The studied structures include girder bridges, railway bridges, slab bridges and cable-stayed bridges. Each moving vehicle has been modelled as a simple load moving with a stochastic velocity while a train has been idealised as multiple moving vehicles with regular uniform intervals. Specific analytical and numerical analysis methods have been formulated to evaluate the response of various models of excited bridge. The Rayleigh beam theory and the Kirchhoff thin-plate theory have been used to model bridges. The main results obtained in this work are summarized as follows:

In the first chapter, an overview on some key factors involved in the dynamic interaction between the bridge and service loads including roads traffic, train traffic and wind actions has been presented. We have also briefly presented a state-of-art review of research based on this topic and the problems that we have solved in this dissertation.

Generally, the whole excited bridge system is modelled with a PDE that is reduced to a one-dimensional system applying the Galerkin's method. Therefore, in the second chapter the general background of the approximate response methods for this reduced mathematical system has been presented. More precisely, five analytical techniques including the classical stochastic averaging technique to approach the nonlinear SDEs, Melnikov's method to predict Smale horseshoe type chaos, Fourier transform and theory of residues to characterize the probabilistic features of the nonlinear SDEs, Routh-Hurwitz criterion to give the decision on the stability of the non-trivial steady-states solutions of the nonlinear ODEs, and the Itô differential rule associated with the averaging method to approximate solutions for statistical moments have been presented. Four numerical methods have been presented: the SRK4 algorithm to integrate the nonlinear SDEs, the RK4 for the ODEs, the Newton-Leipnik and the A-B-M predictor-corrector schemes to integrate the nonlinear FDEs, the bisection method to solve complex or non-trivial polynomial equations.

The third chapter has been devoted to the dynamical behavior of some models of bridges subject to moving loads and stochastic wind. Five models have been studied and the main results obtained have been presented and discussed. In the first set of results, the problem of the nonlinear response of a Rayleigh beam to the passage of a sequence of forces moving with stochastic velocity has been considered. On the basis of the Fourier transform and of the theory of residues, we have demonstrated that the effect of the load random velocities is highly nonlinear, leading to a nonmonotonic behavior of the mean amplitude versus the intensity of the stochastic term and of the load weight. The analytic approach has been also checked with numerical simulations and we have observed a fairly good agreement. In the second set of results, a chaotic dynamic approach to analyse the nonlinear response of a semi-harp model of cable-stayed bridge loaded by a sequence of moving forces with stochastic velocity has been investigated. On the basis of the stochastic Melnikov method, we have demonstrated that the intensity of the random

component of the loads velocity can be contributed to the enlargement of the possible chaotic domain of the system, and increases the chances of a regular behavior of the system. Also, the presence of cables in cable-stayed bridges system increases the degree of safety and can paradoxically contribute to destabilization. In the third set of results, to increase the realism of the studies, we have includes an evaluation approach to obtain the probabilistic characteristics of a two lane slab-type-bridge response due to traffic flow employing a two lane slab-type-bridge modelled by a Simply Supported thin rectangular plate with two separate rectilinear paths. The traffic flow has been considered as two opposite series of vehicles of random weights arriving at the bridge at random times that constitute the Poisson stochastic process, with stochastic velocities. The effects of the standard deviation of the stochastic velocity and of the arrival rate of the vehicles on the expected values and the variance of the bridge deflection response have been investigated. In the fourth set of results, the standard averaging method has been used to provide an analytical explanation of the effects of spacing loads, load velocity, and order of the fractional viscoelastic property of shear layer material on the vibration amplitude of the beam. We have demonstrated that when the moving loads are uniformly distributed upon all the length of the structure, the vibrations are the least. Moreover, as the order of the derivative increases, the resonant amplitude of the beam vibration decreases. Also, by means of the Melnikov technique, we have pointed out the critical weight of moving loads and of the order of the fractional derivative above which the system becomes unstable. Finally, both effects of moving loads and stochastic wind on the steady-state vibration of a Rayleigh beam laying on bearings having fractional order viscoelastic material have been also investigated in this work. We have found that as the number of bearings increase, the resonant amplitude of the beam decreases and shifts towards larger frequency values. The latter result implies that the installation of these kinds of devices at the supports of the bridges can contribute to reduce the vibration of the bridge. Further, as the additive wind turbulence parameter increases, the peak value of the probability density function of the beam response decreases and shifts towards larger amplitude values. The increase of the parametric wind turbulence slightly lowers the peak value of the probability density function, that remains approximately located in the same position. Surprisingly, the shift implies that the additive and parametric wind turbulence contribute to decrease the chance for the bridge to reach the resonance of the amplitude oscillations.

In this thesis, some of the results have opened interesting perspectives for future investigations. For example, it would be interesting to complete the present study by also investigating the case of suspension bridges that are leading to long span technology today. It might also be interesting to extend this work to include the higher coupled modes which have been neglected. Since the bridge deck is assumed to be an elastic structure, it could exhibit hyteristic phenomenon due to their memory effect. So, it could be interesting to find suitable models for this effect to increase the realism.

Appendix A: Derivation of the governing equation of a Rayleigh beam Eq. (69)

In this appendix, we introduce a governing equation of a Rayleigh beam model describing the dynamical behavior of a bridge structure. We start the development by reviewing the basic assumptions from undergraduate strength materials concerning the bending of the beam.

These assumptions read:

- The beam is prismatic and has a straight cendroidal axis (which we will label the x-axis),
- the beam's cross-section has an axis symmetry (which we will label the y-axis),
- all th transverse loadings act in the plane of symmetry ($x - y$ plane),
- plane sections perpendicular to the cendroidal axis remain plane after deformation,
- the material is elastic, isotropic and homogeneous,
- transverse deflections is small.
- the motion is translational in the y-direction and rotational,
- the geometric nonlinearity is taken into account.

The physical situation is drawn schematically in Fig. 37 [124]. We denote the internal bending moment by M, the internal shear force by Q and the external distributed loading by $f(x,t)$.

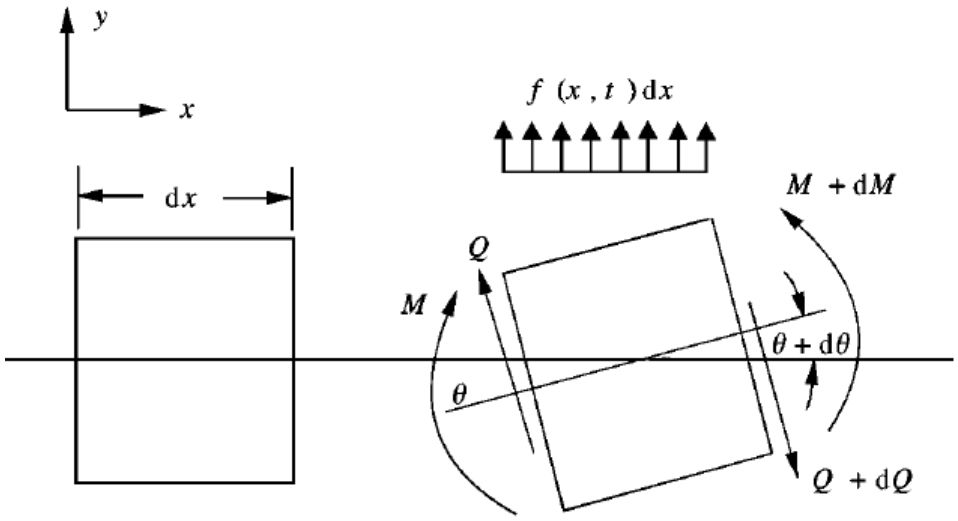

Figure 37: *An incremental beam element.*

To deal with the modelling, let us consider the dynamic equilibrium of a beam element of length dx; $w = w(x,t)$ and $\theta = \theta(x,t)$ be the transversal displacement and the angle of rotation of the beam element respectively.

With these assumptions, setting the vertical forces on the element equal to the mass times acceleration gives:

$$\begin{aligned}\sum F_y &= \rho A \mathrm{d}x \frac{\partial^2 w}{\partial t^2} \\ &= -\left(Q + \mathrm{d}Q\right)\cos\left(\theta + \mathrm{d}\theta\right) + Q\cos\theta + f\left(x,t\right)\mathrm{d}x\end{aligned} \tag{209}$$

where θ can be approximated as $\partial w/\partial x$, and $\mathrm{d}Q$ and $\mathrm{d}\theta$ represent $\left(\partial Q/\partial x\right)\mathrm{d}x$ and $\left(\partial\theta/\partial x\right)\mathrm{d}x$ respectively. Expanding $\cos\left(\theta+\mathrm{d}\theta\right)$ about θ using a Taylor series expansion and using the small angle assumption ($\theta^2 \ll 1$), we obtain

$$-\frac{\partial Q}{\partial x} = \rho A \frac{\partial^2 w}{\partial t^2} - f\left(x,t\right) \tag{210}$$

Similarly, taking the sum of the moments about the center of the beam element, we obtain

$$\frac{\partial M}{\partial x} - Q = \rho I \frac{\partial^3 w}{\partial t^2 \partial x} \tag{211}$$

Taking the first derivative of Eq. (211) with respect to x, and subtracting Eq. (210) from it, we obtain

$$\frac{\partial^2 M}{\partial x^2} = \rho I \frac{\partial^4 w}{\partial t^2 \partial x^2} - \rho A \frac{\partial^2 w}{\partial t^2} + f\left(x,t\right) \tag{212}$$

From the geometry of the deformation, and using Hooke's law $\sigma_x = E\varepsilon_x$, one can show that (see reference [132]):

$$\begin{aligned} M = \frac{EI}{R} &= EI\frac{\frac{\partial^2 w}{\partial x^2}}{\left[1+\left(\frac{\partial w}{\partial x}\right)^2\right]^{\frac{3}{2}}} \approx EI\frac{\partial^2 w}{\partial x^2}\left[1 - \tfrac{3}{2}\left(\tfrac{\partial w}{\partial x}\right)^2\right] + O\left(\left(\tfrac{\partial w}{\partial x}\right)^2\right) \\ &\approx EI\frac{\partial^2 w}{\partial x^2} - \tfrac{3}{2}EI\left[\frac{\partial^2 w}{\partial x^2}\left(\tfrac{\partial w}{\partial x}\right)^2\right] + O\left(\left(\tfrac{\partial w}{\partial x}\right)^2\right)\end{aligned} \tag{213}$$

where the Taylor expansion of the inverse of the radius of curvature $\left(\frac{1}{R}\right)$ up to the second order is carried out. Finally taking into account the dissipation term ($C\frac{\partial w}{\partial t}$), putting Eq. (212) and Eq. (213) together gives the desired result (Eq. (69) of the thesis)

$$\rho A\frac{\partial^2 w}{\partial t^2} - \rho I\frac{\partial^4 w}{\partial t^2 \partial x^2} + C\frac{\partial w}{\partial t} + EI\frac{\partial^2}{\partial x^2}\left[\frac{\partial^2 w}{\partial x^2}\left(1 - \frac{3}{2}\left(\frac{\partial w}{\partial x}\right)^2\right)\right] = f\left(x,t\right) \tag{214}$$

where

$$f\left(x,t\right) = P\sum_{i=1}^{N_v}\varepsilon_i \delta\left[x - x_i\left(t - t_i\right)\right] \tag{215}$$

Bibliography

[1] E. Simiu and R. H. Scanlan, **Wind effects on structures: Fundamentals and Applications to Design**. *John Wiley & Sons Publication*, (1996).

[2] C. G. Bucher and Y. K. Lin, **Stochastic stability of bridges considering coupled modes**. *J. Eng. Mech. ASCE* 114, pp. 2055-2071 (1988).

[3] C. C. Tung, **Random response of highway bridges to vehicle loads**. *J. Eng. Mech. Div. ASCE* 93, pp. 79-94 (1967).

[4] C. C. Tung, **Life expectancy of highway bridges to vehicle loads**. *J. Eng. Mech. Div. ASCE* 95, pp. 1417-1428 (1969).

[5] C. C. Tung, **Response of highway bridges to renewal traffic loads**. *J. Eng. Mech. Div. ASCE* 95, pp. 41-57 (1969).

[6] R. Sieniawska and P. Śniady, **First passage problem of the beam under a random stream of moving forces**. *J. Sound Vib.* 136, pp. 177-185 (1990).

[7] R. Sieniawska and P. Śniady, **Life expectancy of highway bridges due to traffic load**. *J. Sound Vib.* 140, pp. 31-38 (1990).

[8] Y. B. Yang, J. D. Yau, Y. S. Wu, **Vehicle-bridge interaction dynamics: with applications to high-speed railways**. *World Scientific Publishing* Singapore, (2004).

[9] Y. L. Xu, H. Xia and Q.S. Yan QS, **Dynamic response of suspension bridge to high wind and running train**. *J. Bridge Eng.* 8, pp. 46-55 (1988).

[10] Y. L. Xu and W. H. Guo, **Dynamic analysis of coupled road vehicle and cable-stayed bridge system under turbulent wind**. *Eng. Struct.* 25, pp. 473-486 (2003).

[11] S. R. Chen and J. Wu, **Dynamic performance simulation of long-span bridge under combined loads of stochastic traffic and wind**. *J. Bridge Eng.* 3, pp. 219-230 (2010).

[12] W. Zhang, C. S. Cai, F. Pan, **Fatigue Reliability Assessment for Long-Span Bridges under Combined Dynamic Loads from Winds and Vehicles**. *J. Bridge Eng.* 8, pp. 735-747 (2013).

[13] Y. Zhou and S. Chen, **Dynamic Simulation of a Long-Span Bridge-Traffic System Subjected to Combined Service and Extreme Loads**. *J. Struct. Eng.* pp. 04014215 (2014).

[14] D. Bryja and P. Śniady, **Spatially coupled vibrations of a suspension bridge under random Highway traffic**. *Earthq. Eng. Struct. Dyn.* 20, pp. 995-1010 (1991).

[15] P. Śniady, S. Biernat, R. Sieniawska, S. Zukowski, **Vibrations of the beam due to a load moving with stochastic velocity**. *Prob. Eng. Mech.* 16, pp. 53-59 (2001).

[16] R. Karoumi, **Response of Cable-Stayed and Suspension Bridges to Moving Vehicles, Analysis methods and practical modelling techniques**. *Ph.D. Dissertation, Royal Institute of Technology* SE-10044 Stockholm, Sweden, (1996).

[17] L. Frýba, **Dynamics of Railway Bridges**. *Thomas Telford* London, (1996).

[18] H. Xia, N. Zhang, W. W. Guo, **Analysis of resonance mechanism and conditions of train-bridge system**. *J. Sound Vib.* 297, pp. 810-822 (2006).

[19] C. O'Connor and T. H. T. Chan, **Dynamic wheel loads from bridge strains**. *J. Struct. Eng. ASCE* 114, pp. 1703-1723 (1988).

[20] E. A. Sekhniashvili, I. E. Byus and Y. S. Sarkisov, **Work of girder bridge structures under dynamic loads**. *Beton zhelezobeton* 11, pp. 491-494 (1961).

[21] D. Dinev, **Analytical solution of beam on elastic foundation by singularity functions**. *Eng. Mech.* 19, pp. 381-392 (2012).

[22] E. Winkler, **Die Lehre von der Elastizitat und Festigkeit**. *Dominicus* Prague, (1867).

[23] M. M. Filonenko-Borodich, **A very simple model of an elastic foundation capable of spreading the load**. *Sbornik Moskovkovo Elektro Instituta*, (1945).

[24] M. Hetenyi, **Beams on elastic foundation**. *University of Michigan Press*, (1946).

[25] P. L. Pasternak, **On a new method of analysis of an elastic foundation by means of two foundation constants**. *Gosudarstvennoe Izdatelstvo Literaturi po Stroitelstvu i Architekture* Moskva, (1954).

[26] A. D. Kerr, **A study of a new foundation model**. *Acta Mech.* 1, pp. 135-147 (1965).

[27] E. Reissner, **Deflection of plates on viscoelastic foundation**. *J. Appl. Mech.* 25, pp. 144-145 (1958).

[28] V. Z. Vlasov and U. N. Leontiev, **Beams, Plates and Shells on Elastic Foundations**. *Izrael Program for Scientic Translations* Jerusalem, (1966).

[29] R. Willis, **Appendix to the Report of the Commissioners Appointed to Inquire into the Application of Iron to Railway Structures**. *H. M. Stationary Office* London, (1849).

[30] J. Biggs, **Introduction to structural dynamics**. *McGraw-Hill* New York, (1964).

[31] L. Frýba, **Vibration of solids and structures under moving loads**. *Thomas Telford* London, (1999).

[32] L. Frýba, **Non-stationary response of a beam to a moving random force**. *J. Sound Vib.* 46, pp. 323-338 (1976).

[33] J. K. Knowles, **On the dynamic response of a beam to randomly moving load**. *J. Appl. Mech. Int. ASME* 35, pp. 1-6 (1968).

[34] J. D. Robson, **An Introduction to Random Vibration**. *Edinburgh University Press* Amsterdam, (1964).

[35] V. V. Bolotin, **Statistical Methods in Structural Mechanics**. *2nd ed., Stroiizdat* Moscow, (1965).

[36] R. Iwankiewicz and P. Śniady, **Vibration of a beam under a random stream of moving forces**. *J. Struct. Mech. ASCE* 12, pp. 13-26 (1984).

[37] P. Śniady, **Vibration of a beam due to a random stream of moving forces with random velocity**. *J. Sound Vib.* 97, pp. 23-33 (1984).

[38] H. S. Zibdeh, **Stochastic vibration of an elastic beam due to random moving loads and deterministic axial forces**. *Eng. Struct.* 17, pp. 530-535 (1995).

[39] T. P. Chang, **Deterministic and random vibration of an axially loaded Timoshenko beam resting on an elastic foundation**. *J. Sound Vib.* 178, pp. 55-66 (1994).

[40] A. Argento, H. L. Morano, R. A. Scott, **Accelerating load on a rotating beam**. *J. Sound Vib.* 116, pp. 397-403 (1994).

[41] H. S. Zibdeh and H. S. Juma, **Dynamic response of a rotating beam subjected to a random moving load**. *J Sound Vib.* 223, pp. 741-758 (1999).

[42] S. S. Rao, **Reliability-based design**. *McGraw-Hill* New York, (2009).

[43] Y. K. Lin, G. Q. Cai, **Probabilistic structural dynamic, advanced theory and applications**. *McGraw Hill Professional Publishing* New York, (2004).

[44] A. M. Abdel-Ghaffar, A. S. Nazmy, **3-D Nonlinear Seismic Behaviour of Cable-Stayed Bridges**. *J. Struct. Eng. ASCE* 117, pp. 3456-3476 (1991).

[45] D. Bruno, V. Colotti, **Vibration Analysis of Cable-Stayed Bridges**. *Struct. Eng.* 4, pp. 23-28 (1994).

[46] R. Karoumi, **Aerodynamic Stability, Wind Forces on Suspension and Cable-Stayed Bridges**. *TRITA-BKN Report No. 11, Dept. of Struct. Eng.* Stockholm, (1994).

[47] S. G. Meisenholder, P. Weidlinger, **Dynamic interaction aspects of cable-stayed guideways for high speed ground transportation**. *J. Dyn. Systems Meas. Control ASME* 74, pp. 180-192 (1974).

[48] F. Yang, A. Fonder, **Dynamic response of cable-stayed bridges under moving loads**. *J. Eng. Mech. ASCE* 214, pp. 741-747 (1998).

[49] F. T. K. Au, J. J. Wang, Y. K. Cheung, **Impact study of cable-stayed bridge under railway traffic using various models**. *J. Sound Vib.* 240, pp. 447-465 (2001).

[50] J. D. Yau and Y. B. Yang, **Dynamic interaction of cable stayed bridges with moving high speed trains**. *Proceedings of the Eighth East Asia-Pacific Conference on Structural Engineering and Construction* Singapore, December 6-8 (2001).

[51] J. D. Yau and Y. B. Yang, **Vibration reduction for cable-stayed bridges traveled by high-speed trains**. *Finite Elem. Anal. Des.* 40, pp. 341-359 (2004).

[52] M. Zaman, M. R. Taheri and A. Khanna, **Dynamic response of cable-stayed bridges to moving vehicles using the structural impedance method**. *Appl. Math. Mod.* 20, pp. 875-889 (1996).

[53] M. Rasoul, **Dynamic Analysis of Cable-Stayed Bridges**. *Ph.D. Dissertation* Purdue University, (1981).

[54] A. Hirai and M. Ito, **Response of suspension bridges to moving vehicles**. *J. Fac. Eng., University of Tokyo* 29, pp. 1- 52 (1967).

[55] Y. Yasoshima, Y. Matsumoto and T. Nishioka, **Studies on the running stability of railway vehicles on suspension bridges**. *J. Fac. Eng., University of Tokyo* 36, pp. 99- 232 (1981).

[56] P. K. Chatterjee, T. K. Datta and C. S. Surana, **Vibration of suspension bridges under vehicular movement**. *J. Struct. Eng.* 120, pp. 681-703 (1994).

[57] D. Bryja and P. Śniady, **Spatially coupled vibrations of a suspension bridge under random highway traffic**. *Earthq. Eng. Struct. Dyn.* 20, pp. 999- 1010 (1991).

[58] A. Nikkhoo, F. R. Rofooei, **Parametric study of the dynamic response of thin rectangular plates traversed by a moving mass**. *Acta Mech.* 223, pp. 15-27 (2012).

[59] J.-J. Wu, **Vibration analyses of an inclined flat plate subjected to moving loads**. *J. Sound Vib.* 299, pp. 373-387 (2007).

[60] J. Vaseghi Amiri, A. Nikkhoo, M. R. Davoodi, M. Ebrahimzadeh Hassanabadi, **Vibration analysis of a Mindlin elastic plate under a moving mass excitation by eigenfunction expansion method**. *Thin Wall. Struct.* 62, pp. 53-64 (2013).

[61] X. Q. Zhu, S. S. Law, **Dynamic Behavior of Orthotropic Rectangular Plates under Moving Loads**. *J. Eng. Mech.* 129, pp. 79-87 (2007).

[62] A. Nikkhoo, M. Ebrahimzadeh Hassanabadi, S. Eftekhar Azamc, J. Vaseghi Amiri, **Vibration of a thin rectangular plate subjected to series of moving inertial loads**. *Mech. Res. Commun.* 55, pp. 105-113 (2014).

[63] A. Rystwej, P. Śniady, **Dynamic response of an infinite beam and plate to a stochastic train of moving forces**. *J. Sound Vib.* 299, pp. 1033-1048 (2007).

[64] M. Li, T. Qian, Y. Zhong, H. Zhong, **Dynamic response of the rectangular plate subjected to moving loads with variable velocity**. *J. Eng. Mech.* 140, pp. 06014001 (2007).

[65] R. T. Wang and T. Y. Lin, **Vibration of multi-span Mindlin plates to a moving load**. *Journal of the Chinese Institute of Engineers, Series A* 19, pp. 467-477 (1996).

[66] R. T. Wang and T. Y. Lin, **Random vibration of multi-span Mindlin plate due to moving load**. *Journal of the Chinese Institute of Engineers, Series A* 21, pp. 347-356 (1998).

[67] Nurkan yagiz and L. sakman, **Vibrations of a rectangular bridge as an isotropic plate under a traveling full vehicle model**. *J. Vib. Control* 12, pp. 83-98 (2006).

[68] P. Paul and S. Talukdar, **Nonstationary response of orthotropic bridge deck to moving vehicle**. *Adv. Struct. Eng.* 10.1007/978-81-322-2193-7, pp. 1367-1376 (2015).

[69] V. K. Garg and R. V. Dukkipati, **Dynamics of railway vehicle systems**. *Academic press* Toronto, (1984).

[70] Y. B. Yang, J. D. Yau and L. C. Hsu, **Vibration of simple beams due to trains moving at high speeds**. *Eng. Struct.* 19, pp. 936-944 (1997).

[71] Y. S. Wu, Y. B. Yang and J. D. Yau, **Three-dimensional analysis of train-rail-bridge interaction problems**. *Vehicle Syst. Dyn.* 36, pp. 1-35 (2001).

[72] Y. S. Wu, **Dynamic interaction of train-rail-bridge system under normal and seismic conditions**. *Ph.D. Dissertation, National Taiwan University* Taipei, (2000).

[73] Y. B. Yang and Y. S. Wu, **Dynamic stability of trains moving over bridges shaken by earthquakes**. *J. Sound Vib.* 258, pp. 65-94 (2002).

[74] P. Museros, M. L. Romero, A. Poy and E. Alarcón, **Advances in the analysis of short span railway bridges for high-speed lines**. *Comp. & Struct.* 80, pp. 2121-2132 (2002).

[75] V. V. Bolotin, **The Dynamic Stability of Elastic Systems**. *Holden-Day, Inc.* U.S.A, (1964).

[76] C. R. Steele, **The finite beam with a moving load**. *J. Appl. Mech.* 34, pp. 111-118 (1967).

[77] C. R. Steele, **The Timoshenko beam with a moving load**. *J. Appl. Mech.* 35, pp. 481-488 (1968).

[78] S. I. Suzuki, **Dynamic behaviour of a finite beam subjected to travelling loads with acceleration**. *J. Sound Vib.* 55, pp. 65-70 (1977).

[79] M. H. Kargarnovin, D. Younesian, **Dynamics of Timoshenko beams on Pasternak foundation under moving load**. *Mech. Res. Commun.* 31, pp. 713-723 (2004).

[80] D. Younesian, M. H. Kargarnovin, **Response of the beams on random Pasternak foundations subjected to harmonic moving loads**. *J. Mech. Sci. Tech.* 23, pp. 3013-3023 (2009).

[81] Y. Li, S. Qiang, H. Liao, Y. L. Xu, **Dynamics of wind-rail vehicle-bridge systems**. *J. Wind Eng. Ind. Aerodyn.* 93, pp. 483-507 (2005).

[82] J. D. Yau, Y. S. Wu and Y. B. Yang, **Impact response of bridges with elastic bearings to moving loads**. *J. Sound Vib.* 248, pp. 9-30 (2001).

[83] Y. B. Yang, C. L. Lin, J. D. Yau and D. W. Chang, **Mechanism of resonance and cancellation for train-induced vibrations on bridges with elastic bearings**. *J. Sound Vib.* 269, pp. 345-360 (2004).

[84] X. Q. Zhu, S. S. Law, **Moving load identification on multi-span continuous bridges with elastic bearings**. *Mech. Syst. Signal Process.* 20, pp. 1759-1782 (2006).

[85] S. Naguleswaran, **Transverse vibration of an Euler-Bernoulli uniform beam on up to five resilient supports including ends**. *J. Sound Vib.* 261, pp. 372-384 (2003).

[86] G. Barone, M. Di Paola, F. Lo Iacono, G. Navarra, **Viscoelastic bearings with fractional constitutive law for fractional tuned mass dampers**. *J. Sound Vib.* 344, pp. 18-27 (2015).

[87] P. Śniady, R. Sieniawska, S. Zukowski, **Influence of some load and structural parameters on the vibrations of a bridge beam**. *Arch. Civ. Eng.* 44, pp. 19-39 (1998).

[88] D. Bryja and P. Śniady, **Stochastic non-linear vibrations of highway suspension bridge under inertial sprung moving load**. *J. Sound Vib.* 216, pp. 507-526 (1998).

[89] E. Simiu, M. Frey, **Melnikov processes and noise-induced exits from a well**. *J. Eng. Mech.* 122, pp. 263-270 (1996).

[90] M. Frey, E. Simiu, **Noise-induced chaos and phase space flux**. *Physica D* 63, pp. 321-340 (1993).

[91] S. Wiggins, **Introduction to Applied Nonlinear Dynamical Systems and Chaos**. *Springer Verlag* New York, (1990).

[92] G. Yao, F.-M. Li, **Chaotic motion of a composite laminated plate with geometric nonlinearity in subsonic flow**. *Int. J. Non-Linear Mech.* 50, pp. 81-90 (2013).

[93] R. Tchoukuegno, B.R. Nana Nbendjo, P. Woafo, **Linear feedback and parametric controls of vibrations and chaotic escape in a ϕ^6 potential**. *Int. J. Non-Linear Mech.* 38, pp. 531-541 (2013).

[94] M. Franaszek, E. Simiu, **Noise-induced Snap-through of a Buckled Column with continuously distributed mass: A chaotic dynamics approach**. *Int. J. Non-Linear Mech.* 31, pp. 861-869 (1996).

[95] W.-M. Zhang, O. Tabata, T. Tsuchiya, G. Meng, **Noise-induced chaos in the electrostatically actuated MEMS resonators**. *Phys. Lett. A* 375, pp. 2903-2910 (2011).

[96] R. L. Stratonovich, **Topics in the Theory of Random Noise II**. *Gordon and Breach* New York, (1963).

[97] R. L. Stratonovich, **Topics in the Theory of Random Noise I**. *Gordon and Breach* New York, (1963).

[98] J. B. Roberts and P. D. Spanos, **Stochastic averaging: An approximate method of solving random vibration problems**. *Int. J. Non-Linear Mech.* 21, pp. 111-134 (1986).

[99] B. Vladimir, **Method of Averaging for Differential Equations on an Infinite Interval: Theory and Applications**. *Taylor & Francis Group* New York, (2007).

[100] L. Chen, W. Zhu, **Stochastic jump and bifurcation of duffing oscillator with fractional derivative damping under combined harmonic and white noise excitations**. *Int. J. Non-Linear Mech.* 46, pp. 1324-1329 (2011).

[101] A. Leung, Z. Guo, **Forward residue harmonic balance for autonomous and non-autonomous systems with fractional derivative damping**. *Commun. Nonlinear Sci. Numer. Simul.* 16, pp. 2169-2183 (2011).

[102] A. H. Nayfeh, D. T. Mook, **Nonlinear oscillations**. *Wiley-Interscience* New York, (1979).

[103] C. Hayashi, **Nonlinear oscillations in physical systems**. *McGraw-Hill* New York, (1964).

[104] N. N. Bogoliubov and Y. A. Mitropolsky, **Asymptotic Methods in the Theory of Nonlinear Oscillations**. *Gordon and Breach* New York, (1961).

[105] M. Schreiber, **Differential Forms**. *Springer-Verlag* New York, (1977).

[106] C. Von Westenholz, **Differential Forms in Mathematical Physics**. *North-Holland* Amsterdam, (1981).

[107] Z. L. Huang and W. P. Zhu, **Exact stationary solutions of averaged equations of stochastically and harmonically excited MDOF quasi-linear systems with internal and or external resonances**. *J. Sound Vib.* 204, pp. 249-258 (1997).

[108] V. K. Melnikov, **On the stability of the center for time periodic perturbations**. *Trans. Moscow Math.* 12, pp. 1-57 (1963).

[109] P. Holmes, **A nonlinear oscillator with a strange attractor**. *Philos. Trans. R. Soc* A292, pp. 419-418 (1979).

[110] J. Guckenheimer and P. Holmes, **Nonlinear Oscillations, Dynamical Systems, and Bifurcations of Vector Fields**. *Springer-Verlag* New York, (1983).

[111] P. Ravi Agarwal, Kanishka Perera, Sandra Pinelas, **An Introduction to Complex Analysis**. *Springer* New York, (2011).

[112] C. P. Simon and L. Blume, **Mathematics for economists**. *W.W. Norton and company* New York, (1994).

[113] W. H. Press, S. A. Teukolsky, W. T. Vetterling, and B. P. Flannery, **Numerical Recipes: The Art of Scientific Computing**. *Cambridge University Press* ISBN 0521880688, August (2007).

[114] I. Petráš, **Fractional-order Nonlinear Systems: Modeling, Analysis and Simulation**. *Higher Education Press* Beijing, (2011).

[115] W. Deng, **Short memory principle and a predictor-corrector approach for fractional differential equations**. *J. Comput. Appl. Math.* 206, pp. 174-188 (2007).

[116] K. Diethelm, N. J. Ford, D. Freed, **A predictor-corrector approach for the numerical solution of fractional differential equations**. *Nonlinear Dyn.* 29, pp. 3-22 (2002).

[117] G. S. Ngueteu Mbouna and P. Woafo, **Dynamics and synchronization analysis of coupled fractional-order nonlinear electromechanical systems**. *Mech. Res. Commun.* 46, pp. 20-25 (2012).

[118] N. J. Kasdin, **Runge-Kutta Algorithm for the Numerical Integration of Stochastic Differential Equations**. *J. Guid. Control Dyn.* 18, pp. 114-120 (1995).

[119] Y. K. Lin and G. Q. Cai, **Probabilistic structural dynamics: advanced theory and applications**. *McGraw-Hill* New York, (1995).

[120] D. E. Knuth, **The Art of Computer Programming**. *Addison-Wesley* New York, (1969).

[121] I. Podlubny, **Fractional Differential Equations**. *Academic Press* San Diego, (1999).

[122] I. Petráš, **Chaos in the fractional-order Volta's system: modeling and simulation**. *Nonlinear Dyn.* 57, pp. 157-170 (2009).

[123] H. Ouyang, **Moving load dynamic problems: a tutorial (with a brief overview)**. *Mech. Syst. Signal Process.* 25, pp. 2039-2060 (2011).

[124] S. M. Han, H. Benaroya, T. Wei, **Dynamics of transversely vibration beams using four engineering theories**. *J. Sound Vib.* 225, pp. 935-988 (1999).

[125] L. M. Anague Tabejieu, B. R. Nana Nbendjo, G. Filatrella, P. Waofo, **Amplitude stochastic response of Rayleigh beams to randomly moving loads**. *Nonlinear Dyn.* (In Press, DOI: 10.1007/s11071-017-3492-3) (2017).

[126] L. M. Anague Tabejieu, B. R. Nana Nbendjo, U. Dorka, **Identification of horseshoes chaos in a cable-stayed bridge subjected to randomly moving loads**. *Int. J. Non-Linear Mech.* 85, pp. 62-69 (2016).

[127] L. M. Anague Tabejieu and B. R. Nana Nbendjo, **Probabilistic evaluation approach for analysing the dynamics response of a two lane slab-type-bridge due to traffic flow**. (Submitted for publication).

[128] L. M. Anague Tabejieu, B. R. Nana Nbendjo, P. Waofo, **On the dynamics of Rayleigh beams resting on fractional-order viscoelastic Pasternak foundations**. *Chaos Solitons and Fract.* 93, pp. 39-47 (2016).

[129] L. M. Anague Tabejieu, B. R. Nana Nbendjo, G. Filatrella, **First mode vibration analysis of Rayleigh beams laying on fractional-order viscoelastic bearings subject to moving loads and stochastic wind**. (Submitted for publication).

[130] D. G. Fertis, **Nonlinear Structural Engineering: With Unique Theories and Methods to Solve Effectively Complex Nonlinear Problems**. *Springer* New York, (2007).

[131] G. T. Oumbé Tékam, E. B. Tchawou Tchuisseu, C. A. Kitio Kwuimy, P. Woafo, **Analysis of an electromechanical energy harvester system with geometric and ferroresonant nonlinearities**. *Nonlinear Dyn.* 76, pp. 1561-1568 (2014).

[132] I. Kovacic, M. J. Brennan, **The Duffing Equation: Nonlinear Oscillators and their Behaviour**. *Wiley* New York, (2011).

[133] B. R. Nana Nbendjo, P. Woafo, **Modelling of the dynamics of Euler's beam by ϕ^6 potential**. *Mech. Res. Commun.* 38, pp. 542-545 (2011).

[134] G. Filatrella, B. A. Malomed, S. Pagano, **Noise-induced dephasing of an ac-driven Josephson junction**. *Phys. Rev. E* 65, pp. 051116-1-7 (2002).

[135] R. V. Bobryk, A. Chrzeszczyk, **Transitions induced by bounded noise**. *Physica A* 358, pp. 263-272 (2005).

[136] S. Datta, J. Bhattacharjee, **Effect of stochastic forcing on the Duffing oscillator**. *Phys. Lett. A* 283, pp. 323-326 (2001).

[137] D. Li, W. Xu, X. Yue, Y. Lei, **Bounded noise enhanced stability and resonant activation**. *Nonlinear Dyn.* 70, pp. 2237-2245 (2012).

[138] A. C. Chamgoué, R. Yamapi, P. Woafo, **Bifurcations in a birhythmic biological system with time-delayed noise**. *Nonlinear Dyn.* 73, pp. 2157-2173 (2013).

[139] L. Gammaitoni, P. Hänggi, P. Jung, F. Marchesoni, **Stochastic Resonance**. *Rev. Mod. Phys.* 70, pp. 223-287 (1998).

[140] T. Wellens, V. Shatokhin, A. Buchleitner, **Stochastic Resonance**. *Rep. Prog. Phys.* 67, pp. 45-105 (2004).

[141] B. Ando, S. Graziani, **Adding noise to improve measurement**. *IEEE Instru. Meas. Mag.* 4, pp. 24-31 (2001).

[142] M. McDonnell, D. Abbott, **What is stochastic resonance? Definitions, misconceptions, debates, and its relevance to biology**. *PLOS Comput. Biol.* 5, pp. e1000348 (2011).

[143] P. Addesso, G. Filatrella, V. Pierro, **Characterization of escape times of Josephson junctions for signal detection**. *Phys. Rev. E* 85, pp. 016708 (2012).

[144] R. Karoumi, **Some modeling aspects in the nonlinear finite element analysis of cable supported bridges**. *Comput. Struct.* 71, pp. 397-412 (1999).

[145] S. P. Timoshenko, **Theory of Plates and Shells**. *Wiley* New York, (1959).

[146] W.-C. Xie, **Dynamic stability of structures**. *Cambridge university press* New York, (2006).

[147] R. J. Salter, **Highway Trafic Analysis and Design**. *Macmillan* London, (1976).

[148] R. S. Barbosa, J. A. T. Machado, B. M. Vinagre, A. J. Calderon, **Analysis of the Van der Pol oscillator containing derivatives of fractional order**. *J. Vib. Control* 13, pp. 1291-1301 (2007).

[149] X. Gao, J. Yu, **Chaos in the fractional order periodically forced complex Duffing's systems**. *Chaos, Solitons and Fract.* 24, pp. 1097-1104 (2005).

[150] J. A. T. Machado, M. F. Silva, R. S. Barbosa, I. S. Jesus, C. M. Reis, M. G. Marcos, A. F. Galhano, **Some applications of fractional calculus in engineering**. *Math. Prob. Eng.* 24, pp. 639801 (2010).

[151] R. E. Mikens, K. O. Oyedeji, S. A. Rucker, **Analysis of the simple harmonic oscillator with fractional damping**. *J. Sound Vib.* 268, pp. 842 (2003).

[152] J. Padovan, T. Sawicki, **Nonlinear vibration of fractionally damped systems**. *Nonlinear Dyn.* 16, pp. 321-336 (1998).

[153] M. Borowiec, G. Litak, A. Syta, **Vibration of the Duffing oscillator: effect of fractional damping**. *Shock Vib.* 14, pp. 29-36 (2007).

[154] Y. A. Rossikhin, M. V. Shitikova, **Application of fractional calculus for dynamic problems of solid mechanics: novel trends and recent results**. *Appl. Mech. Rev.* 63, pp. 010801 (2010).

[155] M. D. Paola, F. P. Pinnola, M. Zingales, **A discrete mechanical model of fractional hereditary materials**. *Meccanica* 48, pp. 1573-1586 (2013).

[156] L. B. Eldred, W. P. Baker, A. N. Palazotto, **Kelvin-Voigt vs Fractional Derivative Model as Constitutive Relations for Viscoelastic Materials**. *AIAA J* 33, pp. 547-550 (1995).

[157] A. Nobili, **Variational approach to beams resting on two-parameter tensionless elastic foundations**. *J. Appl. Mech.* 79, pp. 021010 (2012).

[158] A. Nobili, E. Radi, L. Lanzoni, **A cracked infinite Kirchhoff plate supported by a two parameter elastic foundation**. *J. Eur. Ceram. Soc.* 34, pp. 2737-2744 (2014).

[159] L. Lanzoni, A. Nobili, E. Radi, A. Sorzia, **Axisymmetric loading of an elastic-plastic plate on a general two-parameter foundation**. *J. Mech. Mater. Struct.* 10, pp. 459-479 (2015).

[160] C. A. Kitio Kwuimy, B. R. Nana Nbendjo, P. Woafo, **Optimization of electromechanical control of beam dynamics: Analytical method and finite differences simulation**. *J. Sound Vib.* 296, pp. 180-193 (2006).

[161] D. Liu, W. Xu, Y. Xu, **Stochastic response of an axially moving viscoelastic beam with fractional order constitutive relation and random excitations**. *Acta Mech. Sin.* 29, pp. 443-451 (2013).

[162] L. Debnath, **Recent applications of fractional calculus to science and engineering**. *Int. J. Math. Math. Sci.* 54, pp. 3413-3442 (2003).

[163] V. Mangulis, **Handbook of Series for Scientists and Engineers**. *Academic Press* New York, (1965).

[164] G. T. Oumbé Tékam, C. A. Kitio Kwuimy, P. Woafo, **Analysis of tristable energy harvesting system having fractional order viscoelastic material**. *Chaos: Interdiscip. J. Nonlinear Sci.* 25, pp. 013112 (2015).

[165] Y. Shen, Yang, H. Xing, H. Ma, **Primary resonance of Duffing oscillator with two kinds of fractional-order derivatives**. *Int. J. Non-Linear Mech.* 47, pp. 975-983 (2012).

[166] A. A. Andronov, A. Witt, **Towards mathematical theory of capture**. *Archiv fur Electrotechnik* 24, pp. 99-110 (1930).

[167] J. Awrejcewicz, V. A. Krysko, **Introduction to Asymptotic Methods**. *Chapmanand Hall, CRC Press* New York, (2006).

[168] S. Takougang Kingni, B. Nana, G. S. Ngueuteu Mbouna, P. Woafo, J. Danckaert, **Bursting oscillations in a 3D system with asymmetrically distributed equilibria: Mechanism, electronic implementation and fractional derivation effect**. *Chaos, Solitons and Fract.* 71, pp. 29-40 (2015).

[169] J. Awrejcewicz J and M. Holiske, **Smooth and Nonsmooth High Dimensional Chaos and the Melnikov Type Methods**. *World Scientific* Singapore, (2007).

[170] A. Luongo, D. Zulli, **Parametric, external and self-excitation of a tower under turbulent wind flow**. *J. Sound Vib.* 330, pp. 3057-3069 (2011).

[171] W. T. Van Horssen, **An asymptotic theory for a class of initial-boundary value problems for weakly nonlinear wave equations with an application to a model of the galloping oscillations of overhead transmission lines**. *SIAM J. Appl. Math.* 48, pp. 1227-1243 (1988).

[172] S. Timoshenko and J. M. Gere, **Theory of Elastic Stability**. *McGraw-Hill* New York, (1961).

[173] Y. K. Lin and Q. C. Li, **New stochastic theory for bridge stability in turbulence flow**. *J. Eng. Mech.* 119, pp. 113-127 (1993).

[174] G. Q. Cai, C. Wu, **Modeling of bounded stochastic processes**. *Prob. Eng. Mech.* 19, pp. 197-203 (2004).

[175] M. H. Kargarnovin, D. Younesian, D. J. Thompson, C. J. C. Jones, **Response of beams on nonlinear viscoelastic foundations to harmonic moving loads**. *Comput. Struct.* 83, pp. 1865-1877 (2005).

Publication list of the author during PhD study period

Published in international journals

1. **L. M. Anague Tabejieu**, B. R. Nana Nbendjo, G. Filatrella, P. Woafo, Amplitude stochastic response of Rayleigh beams to randomly moving loads. *Nonlinear Dyn. 89*, PP. 925-937, (2017).

2. **L. M. Anague Tabejieu**, B. R. Nana Nbendjo, P. Woafo, On the dynamics of Rayleigh beams resting on fractional-order viscoelastic Pasternak foundations. *Chaos, Solitons and Fract. 93*, pp. 39-47, (2016).

3. **L. M. Anague Tabejieu**, B.R. Nana Nbendjo, U. Dorka, Identification of horse-shoes chaos in a cable-stayed bridge subjected to randomly moving loads. *Int. J. Non-Linear Mech. 85*, pp. 62-69, (2016).

Collection of the published papers

Amplitude stochastic response of Rayleigh beams to randomly moving loads

L. M. Anague Tabejieu, B. R. Nana Nbendjo, G. Filatrella & P. Woafo

Nonlinear Dynamics
An International Journal of Nonlinear Dynamics and Chaos in Engineering Systems

ISSN 0924-090X
Volume 89
Number 2

Nonlinear Dyn (2017) 89:925-937
DOI 10.1007/s11071-017-3492-3

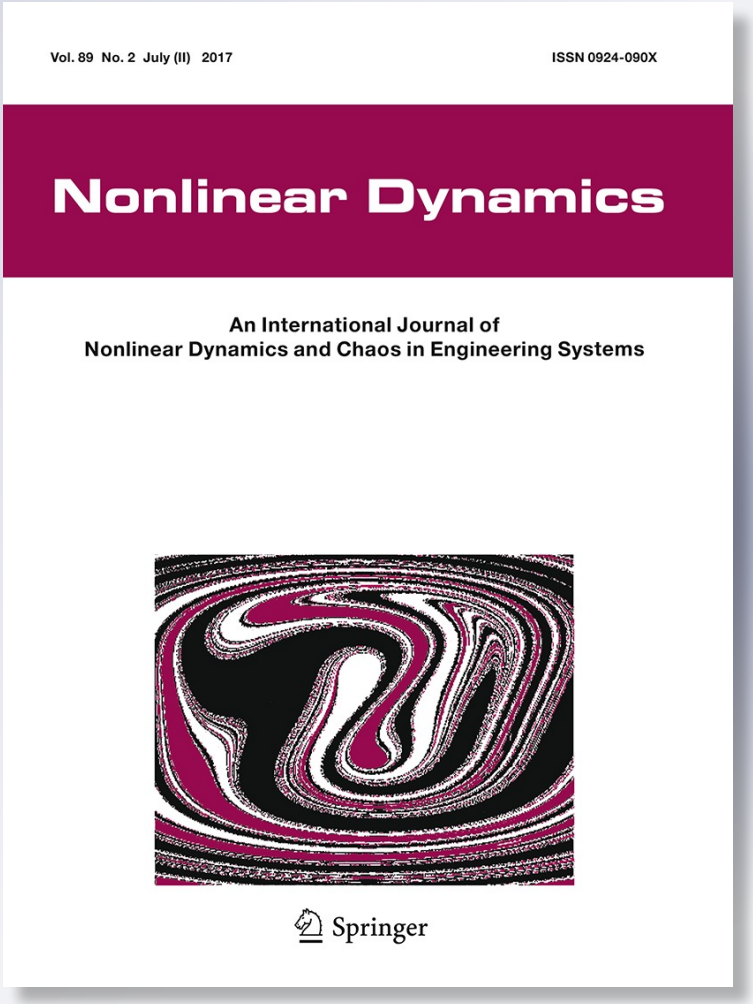

Springer

Chaos, Solitons and Fractals 93 (2016) 39–47

Contents lists available at ScienceDirect

Chaos, Solitons and Fractals

Nonlinear Science, and Nonequilibrium and Complex Phenomena

journal homepage: www.elsevier.com/locate/chaos

On the dynamics of Rayleigh beams resting on fractional-order viscoelastic Pasternak foundations subjected to moving loads

L.M. Anague Tabejieu, B.R. Nana Nbendjo*, P. Woafo

Laboratory of Modelling and Simulation in Engineering, Biomimetics and Prototypes, Faculty of Science, University of Yaoundé I, P.O. Box 812, Yaoundé, Cameroon

ARTICLE INFO

Article history:
Received 30 May 2016
Revised 22 July 2016
Accepted 1 October 2016

Keywords:
Fractional-order derivative
Rayleigh beams
Pasternak foundation
Moving loads
Horseshoes chaos
Beam stability

ABSTRACT

The standard averaging method is used to provide an analytical explanation on the effects of spacing loads, load velocity, order of the fractional viscoelastic property of shear layer material on the amplitude of the beam. The geometric nonlinearity is taken into account in the model. The analysis shows that, when the moving loads are uniformly distributed upon all the length of the structure, it vibrates the least possible. Moreover, as the order of the derivative increases, the resonant amplitude of the beam vibration decreases. In other hand, by means of Melnikov technique, a necessary condition for onset of horseshoes chaos resulting from heteroclinic bifurcation is derived analytically. We point out the critical weight of moving loads and order of the fractional derivative above which the system becomes unstable.

1. Introduction

Many structures, such as bridges, runways, rails, roadways, pipelines, etc., can be modelled as a beam structure on a viscoelastic foundation. In the analysis of vibration of beams resting on viscoelastic foundation under a moving load, the beam can be modelled as an Euler–Bernoulli beam [1–4], or as a Rayleigh beam [5] or as a Timoshenko beam [6–8] and the viscoelastic foundation as a Winkler model [9–11] or a Pasternak model [12–14].

The extensive research in this field is summarized in review articles by Fryba [15], Wang et al. [16], and Beskou and Theodorakopoulos [17]. Amongst those investigations, Kargarnovin and Younesian [13,14] used the first order perturbation method to analyse the response of an infinite Timoshenko beam on the viscoelastic foundation under a moving load. To simulate the behaviour of the foundation, Pasternak viscoelastic model was used. This model includes a Kelvin foundation in conjunction with a shear viscous layer [14] or with a shear elastic layer [13]. These studies clearly show that the shear layer material of the foundation can have viscoelastic physical properties.

In the context of the bridges behaviour, it is well known that, this layer of material (part ranging between the bridge deck and the foundation) is constituted by some viscoelastic materials such as elastomer. Therefore, the long memory effects of this viscoelastic materials must be considered through a fractional-order derivative concept. For this aim, we focus in this work on the analytical and numerical analysis of Rayleigh beams subject to uniform moving loads resting on Pasternak foundations considering the shear layer as fractional-order viscoelastic material. Atanackovic et al. [18,19] considered the vibrations of an elastic rod loaded by axial force of constant intensity and positioned on a foundation having fractional order viscoelastic physical properties. The viscoelastic foundation is modelled by using the constitutive equation of Kelvin–Voigt type containing fractional derivatives of real and complex order [18], or by using Zener model of fractional derivatives [19].

The aim of this work is to explore analytically and numerically, the effects of loads number and their spacing, the load velocity, the order of the fractional viscoelastic shear layer material of the Pasternak foundation and its strength on the amplitude of vibration of the beam, and especially the order of the fractional viscoelastic property of the shear layer on the appearance or disappearance of horseshoes chaos through the Melnikov criteria [20–23].

The paper is organized as follows. Section 2 deals with the derivation of the physical system and their model-building, some mathematical development and the equivalent modal equation of this system. In Section 3, analytical and numerical method (the averaging method [24–27] and Newton–Leipnik methods [28,29] respectively) are used to analyse the effects of the main parameters of the system on the steady-state amplitude and the stability of the beam system. Section 4 deals with the influence of order

* Corresponding author.
E-mail addresses: rnana@uy1.uninet.cm, nananbendjo@yahoo.com (B.R. Nana Nbendjo).

http://dx.doi.org/10.1016/j.chaos.2016.10.001
0960-0779/

International Journal of Non-Linear Mechanics 85 (2016) 62–69

Contents lists available at ScienceDirect

International Journal of Non-Linear Mechanics

journal homepage: www.elsevier.com/locate/nlm

Identification of horseshoes chaos in a cable-stayed bridge subjected to randomly moving loads

L.M. Anague Tabejieu [a], B.R. Nana Nbendjo [a,b,*], U. Dorka [b]

[a] Laboratory of Modelling and Simulation in Engineering, Biomimetics and Prototypes, Faculty of Science, University of Yaounde I, P.O. Box 812, Yaounde, Cameroon

[b] Steel and Composite Structures, University of Kassel, Kurt-Wolters-Strasse 3, Kassel 34125, Germany

ARTICLE INFO

Article history:
Received 26 September 2015
Received in revised form
10 May 2016
Accepted 6 June 2016
Available online 8 June 2016

Keywords:
Horseshoes chaos
Random Melnikov theory
Cable-stayed bridge
Moving loads
Stochastic velocity

ABSTRACT

In this paper, the dynamic response of cable-stayed bridge loaded by a train of moving forces with stochastic velocity is investigated. The cable-stayed bridge is modelled by Rayleigh beam with linear elastic supports. The stochastic Melnikov method is derived and the mean-square criterion is used to determine the effects of stochastic velocity and cables number on the threshold condition for the inhibition of smale horseshoes chaos in the system. The results indicate that the intensity of the random component of the loads velocity can be contributed to the enlargement of the possible chaotic domain of the system, and/or increases the chances to have a regular behavior of the system. On the other hand, the presence of cables in cable-stayed bridges system increases it degree of safety and paradoxically can be contributed to its destabilization. Numerical simulations of the governing equations are carried out to confirm the analytical prediction. The effect of loads number on the system response is also investigated.

1. Introduction

Cable-stayed bridges have become very popular over the last three decades because of their aesthetic appeal, structural efficiency, enhanced stiffness compared with suspension bridges, ease of construction and comparatively small size of structures. Response prediction of this type of bridges subjected to randomly moving excitations is important for engineering practice [1,2].

The vibrations of a suspension bridge under a random train of moving loads are discussed in detail by Bryja and Śniady [3–5]. Generally, a very important parameter in the study of the vibration of bridges caused by moving loads is the velocity. Although there is scarcity of publications on this subject, one can mention the work of Zibdeh [6] who included the effect of random velocities on the dynamic response of a bridge traversed by a concentrated load. Chang et al. [7] investigated the dynamic response of a fixed–fixed beam with an internal hinge on an elastic foundation, which is subjected to a moving mass oscillator with uncertain parameters such as random mass, stiffness, damping, velocity and acceleration. In the same impetus, Śniady et al. [8,9] and Rystwej et al. [10] investigated on the problem of a dynamic response of a beam and a plate to the passage of a train of random forces. In this study they assumed that the random train of forces idealizes the flow of vehicles having random weights and travelling at the stochastic velocity. They show the effect of these stochastic quantities on the mean deflection of the beam.

On one hand, in all of the above-mentioned research, only the effect of stochastic parameters of the moving loads on the probabilistic features of the beam response namely the mean square amplitude and the probability density function is carried out. To the best knowledge of the authors, the effects of stochastic fluctuations of the load velocity and the number of cables on the possible appearance of horseshoes chaos in the cable-stayed bridge system have not been explored by the researchers yet. Thus in this paper, based on the Melnikov approach, which is widely used by most researchers [11–15], all these effects on the appearance of transverse intersection of perturbed and unperturbed heteroclinic orbits and the route to chaos are investigated.

Following this introduction, the effective model of cable-stayed bridge is presented in Section 2. Also, the random Melnikov analysis for the examination of the effect of a noisy part of velocity of moving loads and cables effects on the threshold condition for the inhibition of chaos is extended. Section 3 presents some numerical simulations to validate the theoretical predictions. Finally, Section 4 is devoted to the conclusion.

* Corresponding author at: Laboratory of Modelling and Simulation in Engineering, Biomimetics and Prototypes, Faculty of Science, University of Yaounde I, P.O. Box 812, Yaounde, Cameroon.
E-mail address: rnana@uy1.uninet.cm (B.R. Nana Nbendjo).

http://dx.doi.org/10.1016/j.ijnonlinmec.2016.06.002
0020-7462/